2018

Regulation of Local Auxin Metabolism during Soybean Nodule Development

Suresh Damodaran
South Dakota State University

REGULATION OF LOCAL AUXIN METABOLISM DURING SOYBEAN NODULE DEVELOPMENT

BY

SURESH DAMODARAN

A dissertation submitted in partial fulfillment of the requirements for the

Doctor of Philosophy

Major in Plant Science

South Dakota State University

2018

REGULATION OF LOCAL AUXIN METABOLISM DURING SOYBEAN NODULE DEVELOPMENT

SURESH DAMODARAN

This dissertation is approved as a creditable and independent investigation by a candidate for the Doctor of Philosophy in Plant Science degree and is acceptable for meeting the dissertation requirements for this degree. Acceptance of this dissertation does not imply that the conclusions reached by the candidate are necessarily the conclusions of the major department.

Senthil Subramanian, PhD
Dissertation Advisor Date

David Wright, PhD
Head, Department of Agronomy, Horticulture and Plant Science Date

Dean, Graduate School Date

TABLE OF CONTENTS

CONTENTS

LIST OF FIGURES

ABSTRACT

REGULATION OF LOCAL AUXIN METABOLISM DURING SOYBEAN NODULE DEVELOPMENT

SURESH DAMODARAN

2018

Legume-rhizobia symbiosis leads to the development of secondary root organs called nodules. Rhizobia bacteria housed inside nodules assimilate atmospheric nitrogen and convert them into plant usable forms thereby reducing the need for fertilizer application in crop legumes like soybean. Nodule development is a coordinated process orchestrated by multiple plant hormones. In soybean, the auxin responsive gene expression was detected in nodule primordia and in the periphery of mature nodules, primarily in nodule vasculature. Auxin hypersensitivity reduces nodule formation in soybean and also polar auxin transport inhibition at the site of nodule development is not crucial for determinate nodule formation. Therefore, auxin distribution and sensitivity appear to be crucial for proper nodule development. However, the role of auxin metabolism in nodule development is unclear. Using global gene expression analysis, we have identified genes involved in the auxin metabolism that are specifically expressed in nodule tissues at early and mature stages. A cytochrome P450 oxidase gene, GmCYP83B1 was preferentially enriched in mature nodules and it was also identified to be a close ortholog of AtCYP83B1. Suppression of GmCYP83B1 expression through RNA interference (GmCYP83B1-RNAi) in soybean roots led to a significant reduction in nodule number and altered mature nodule morphology. Auxin accumulation was

significantly higher in GmCYP83B1-RNAi nodules compared to vector control which suggested that suppression of GmCYP83B1 led to auxin accumulation which might have led to reduced nodule organogenesis and altered nodule development. Using the global gene expression data, we also identified three nodule-enriched genes encoding GRETCHEN HAGEN 3 (GH3) enzymes. Biochemical assays showed that the three GmGH3 enzymes can conjugate IAA with Asp for inactivation of free auxin levels. *GmGH3-15* showed a broad substrate preference, especially with different forms of auxin. We hypothesized that these GH3s might maintain auxin homeostasis in soybean nodules. Promoter:GUS expression analysis indicated that *GmGH3-14* acts primarily in the root epidermis and the nodule primordium where as *GmGH3-15* might act in the vasculature. Silencing the expression of these *GH3* genes in soybean composite plants led to altered nodule numbers, maturity, and size. Our results indicate that these GH3s are needed for proper nodule maturation in soybean, but the precise mechanism by which they regulate nodule development remains to be explained. Overall the results suggest that GmCYP83B1 and GmGH3 might act to regulate local auxin levels to direct proper soybean nodule development.

Chapter 1

1. INTRODUCTION

1.1. Legumes and Biological Nitrogen Fixation

Soybean (*Glycine max* L. Merr.) is an agriculturally important leguminous crop, which can convert atmospheric nitrogen in to plant usable form through symbiotic nitrogen fixing bacteria in specialized root structures called nodules. The high protein content of soybean seeds meets the dietary requirement of both ruminants and humans. The United States is the leading producer and exporter of soybean globally (www.ers.usda.gov/topics/crops/soybeans-oil-crops/). Current scientific research is aimed at developing biotic and abiotic stress-tolerant soybean plants in addition to devising best agricultural practices (www.sdsoybean.org/)(Mutava *et al.*, 2015). One of the major research areas is how the plant satisfies its nutrient demand, with specific focus on nitrogen status. Legumes like soybean have the ability to form a symbiotic relationship with nitrogen-fixing bacteria named rhizobia. This symbiosis leads to the development of nodules, secondary organs in the roots. Rhizobia bacteria within these nodules convert atmospheric nitrogen into plant-usable forms that are available to meet at least part of the plant's nitrogen requirement. This process, called biological nitrogen fixation, reduces the need for chemical fertilizers (Peoples *et al.*, 2009). Although biological nitrogen fixation is more sustainable and economically beneficial, the efficiency of nitrogen fixation is not sufficient to meet the plant demands, requiring supplementary fertilizer application (Harper, 1974). This issue can be circumvented by enhancing the nitrogen fixation capacity of soybean plants. However, this requires a clear understanding of the plant mechanisms that contribute

to the symbiosis and, specifically, to organogenesis of the nodules. Knowledge of these mechanisms will enable scientists to develop strategies to not only improve legume crops but to also engineer through synthetic biology other commercial crops with this symbiosis in an effort to contribute to a sustainable agriculture system (Mus *et al.*, 2016).

1.2. Nodule development

The root nodule is a secondary organ that arises through the symbiosis between leguminous plants and compatible rhizobia species. In this mutual relationship, the host plant supplies the bacteria with necessary carbon sources for bacterial growth and the bacteria repays the plant with ammonia synthesized from atmospheric nitrogen (Desbrosses and Stougaard, 2011). The symbiotic relationship between a diazotropic rhizobia bacteria and a legume begins with the exchange of specific chemical cues that initiate nodule development (Brewin, 1991, Hirsch, 1992). Under nitrogen starvation, the legume (e.g. soybean) secretes specific flavonoids (secondary metabolites which are biosynthesized via the phenylpropanoid pathway) into the soil that are recognized by compatible rhizobia bacteria (e.g. *Bradyrhizobium japonicum*). Signal perception by the bacteria leads to the release of nod factors (lipochitooligosaccharide molecules) that bind to lysine rich receptor kinase (LysM receptor like kinase) proteins in the plant root, triggering the signaling cascade referred to as the sym-pathway (Geurts and Bisseling, 2002). Activation of LysM receptor in the root epidermis and root hair causes a spike in the Ca^{2+} levels, which is perceived by the *CALCIUM CALMODULIN KINASE* protein (CCaMK). Activation of CCaMK leads to upregulation of multiple downstream genes, such as *NODULE*

INCEPTION 1 (NIN) and *NODULATION SIGNALING PATHWAY 1 & 2* (*NSP1 & NSP2*). The rhizobium attaches itself to the root hair and leads to deformation of the root hair through rearrangement of the microtubules (Hirsch, 1992). The rhizobium is released into the plant cortical cells through invagination of the plant cell wall via formation of a tubular structure referred to as the infection thread. Subsequently, the invading bacteria are released in to actively dividing cortical cells through mitotic activation. These diving cortical cells undergo redifferentiation that eventually leads to the development of the nodule primordium (Ferguson *et al.*, 2010).

Through the action of plant hormones and nodule-specific gene expression, nodule development progresses until specialized and functionally active mature nodule tissues are formed (F Sanchez *et al.*, 1991, Schultze and Kondorosi, 1998). As the infection progresses, cell division is reduced, and differentiation begins to form specialized nodule tissue for maturation. In the mature nodules, two major nodule zones are formed, namely the central infection zone and the peripheral parenchyma.

The central tissue consists of both uninfected and infected cells containing rhizobia bacteria and is referred to as the infection zone. The bacteria are enclosed in a plant-derived membrane called the peribacteroid membrane, which supports nutrient exchange in the infection zone (Newcomb, 1976, Newcomb *et al.*, 1979, Udvardi and Day, 1997). The membrane-encapsulated bacteria divide within the host cells and later differentiate into bacteriods that fix atmospheric nitrogen. The nodulin gene GmENOD40 has been shown to be expressed early in this development, initially in the nodule primordia and later in the infection zone of the mature soybean nodules in the uninfected cells (Yang *et al.*, 1993).

In the peripheral zone, the parenchyma tissue is separated into two layers [formerly referred to as the nodule cortex (outer most layer) and inner cortex (or nodule parenchyma)] by the nodule endodermis or the sclerid layer made of highly lignified tissues (Brown and Walsh, 1994). The nodule parenchyma tissue external to the sclerid layer is highly vacuolated with intercellular spaces between the cells. These cells are developed through cell enlargement as well as division of root-derived cortical cells. The tissue at the base of the nodule is derived from the dividing root pericycle cells and its surrounding tissue (Bond, 1948). The nodule parenchyma tissue surrounds the infection zone, which is traversed by the nodule vascular strands. The nodule vascular strands are differentiated from small and cytoplasmically dense nodule primordia cells, yet the exact developmental pattern is still undiscovered (Newcomb *et al.*, 1979, Calvert *et al.*, 1984). The nodule vasculature transports nutrients between the root and nodule, necessary for bacteroid survival and transfer of nitrogen to the plant.

Among the land plants that form symbiotic relationships with rhizobia, two morphologically distinct nodules have been identified, namely determinate and indeterminate nodules (Hirsch 1992, Ferguson *et al.*, 2010). Determinate nodules are found in temperate legumes such as soybean and *Lotus japonicus*, and indeterminate nodules are found in clovers, peas and *Medicago truncatula*. The type of nodule that is formed is dependent of the host plant (Hirsch, 1992, Ferguson *et al.*, 2010). The major morphological difference involves the continuous renewal of meristematic tissue in an indeterminate nodule, which is absent in a determinate nodule upon maturation.

During determinate nodule development, initial cell division occurs anticlinally in the outer root cortex cells and subsequently in the root pericycle and its adjacent inner cortex tissue (nodule parenchyma) (Hirsch, 1992, Ferguson *et al.*, 2010). The cells dividing in the root outer cortex differentiate into the central tissue, while the dividing pericycle and inner cortex give rise to the parenchyma tissue that surrounds the central zone. The nodule vascular tissues traverse the parenchyma tissue in the periphery of the mature nodule. Since the nodule lacks a persistent meristem, maturation consists primarily of cell elongation rather than division, leading to a spherical shape for the mature nodule. Inside the infection zone/central tissue, the bacteria convert the atmospheric nitrogen and transfers the assimilated nutrient via the uninfected cells and through the nodule vasculature.

In a indeterminate nodule, the primary cell division occurs in the inner cortex through anticlinal division and is followed by cell division in the pericycle (Bond, 1948, Ferguson *et al.*, 2010). The cell division in the nodule primordia is continuous, although it is restricted to the meristematic zone upon nodule maturation. This continuous meristematic activity results in a nodule with an elongated oblong structure with multiple functional zones. The nodule meristem in Zone I consists of the continuously dividing cells. Zone II is referred to as the infection zone. Zone III is the nitrogen fixation zone. Finally, Zone IV is the senescence zone (Gage, 2004, Ferguson *et al.*, 2010). All of these zones in the central tissue are covered at the periphery by the nodule parenchyma tissue, with vascular bundles traversing it.

In addition to the morphological differences between the two types of nodules, there are variations in the effects that the phytohormone auxin has on the development of

determinate and indeterminate nodules (Mathesius, 2008, Ferguson *et al.*, 2010, Ferguson and Mathesius, 2014a). Determinate and indeterminate nodules also regulate auxin expression and transport differently (discussed in detail in section 1.3). Understanding the influence of auxin in nodule development is crucial to understanding this process and developing ways to modify or enhance it.

1.3. Auxin in nodule development

The importance of auxin in nodule development came to light when synthetic auxin transport inhibitors were able to induce nodule-like structures expressing early nodulin genes in alfalfa (Hirsch *et al.*, 1989). Mathesius *et al.*, 1998 showed inhibition of auxin transport at the sites of nodule initiation, prior to nodule primordia formation, using auxin-inducible marker expression (GH3). In the determinate nodule of *Lotus japonicus*, the auxin-inducible marker was expressed in the outer cortex cells at the site of nodule development (Pacios-Bras *et al.*, 2003). This increased auxin output at the site of nodule development was hypothesized to induce the cell division necessary for nodule organogenesis and, this accumulation could have arisen from the inhibition of auxin transport.

Flavonoids act as auxin transport inhibitors (Peer and Murphy, 2007). Flavonoids are produced in most higher plants. The inhibition of auxin transport, mediated by flavonoids, increases auxin accumulation, which is crucial during indeterminate nodule development (Wasson *et al.*, 2006, Mathesius, 2008). On the contrary, flavonoid-mediated auxin inhibition is not crucial for determinate nodule development (Subramanian *et al.*, 2006). These results indicated the likely difference in the role of auxin regulation in the development of determinate and indeterminate

nodules. Recently our lab has shown that the auxin-inducible marker DR5 is expressed in the early divisions of the cortical cells in soybean nodule primordia, indicating the importance of auxin in nodule initiation (Turner *et al.*, 2013b). In mature determinate nodules, the auxin response is primarily limited to the nodule parenchyma in the periphery of the infection zone, specifically in the nodule vasculature (Suzaki *et al.*, 2012a, Suzaki *et al.*, 2013, Turner *et al.*, 2013b, Nizampatnam *et al.*, 2015). In indeterminate nodules such as in Medicago, a high auxin maxima is observed at an earlier phase of cortical cell division, but, similar to determinate nodules, the auxin response is observed only in the nodule parenchyma, specifically in the vasculature tissue (Mathesius, 2001b, Mathesius, 2008). Apart from this, an auxin response is also observed in the nodule meristem of the indeterminate nodule (Guan *et al.*, 2013, Breakspear *et al.*, 2014b). This spatio-temporal auxin response pattern is crucial for proper nodule development.

As mentioned, auxin transport inhibition by flavonoids is crucial for indeterminate nodule development, but not for determinate nodule. Experiments using small regulatory RNA molecules, like miRNA, have further demonstrated the importance of auxin signaling in nodule development. Recently our lab has shown that when overexpression of miR160 suppresses the expression of its targets, namely the repressor AUXIN RESPONSE FACTORs ARF10/16/17, there is reduced nodule formation, indicating the significance of maintaining spatio-temporal auxin regulation (Turner *et al.*, 2013b, Nizampatnam *et al.*, 2015). The importance of precise auxin localization during nodule development is shown by enhanced auxin sensitivity in the nodule primordium, resulting in reduced nodule formation. Additionally, when the

levels of miR160 were suppressed, there was increased formation of emerging nodules, but a delay in nodule maturation, indicating that high miR160 levels are required to regulate auxin output during nodule maturation. This was further validated by addition of exogenous auxin in the miR160-suppressed roots, which partially rescued the increased nodule phenotype. When miR160 was expressed ectopically using the ENOD40 promoter, which is known to be expressed in the nodule primordium/infection zone, there was an increase in emerging nodules but no change in the number of mature nodules. This further indicated that miR160 activity might be crucial in the nodule parenchyma region and may not be essential in the development of the infection zone during maturation. Collectively these data show that proper maintenance of the spatio-temporal activity of auxin is crucial for proper nodule development.

Nodule vascular tissue forms in the nodule periphery, primarily in the parenchyma tissue. Auxin plays an important role in the development of vascular bundles in multiple organs of the plant, and likewise has been shown to be important in nodule vascular development. Auxin response markers are expressed in the nodule vascular tissues of both determinate and indeterminate nodules, indicating a possible role of auxin. The change in the auxin response during nodule development has been observed to alter vasculature development. In both determinate and indeterminate nodules, perturbation of auxin responses lead to aberrant vascular patterning (Guan *et al.*, 2013, Nizampatnam *et al.*, 2015). As mentioned, the source of auxin for such programmed development in the indeterminate nodule occurs through inhibition of auxin transport by flavonoids, creating increased auxin levels at the site of nodule

initiation (Mathesius *et al.*, 1998, Wasson *et al.*, 2006, Mathesius, 2008). But such inhibition is not crucial for determinate nodule development. Neither of these observances address the detection of high auxin accumulation at the site of determinate nodule initiation (Subramanian *et al.*, 2006). One possible hypothesis is that local auxin production at the nodule initial cells or in the dividing outer cortex tissue might function in relation to coordinated auxin transport. Evidence to support this hypothesis is the increased expression of the auxin biosynthesis enzyme LjTAR1 (TRYPTOPHAN AMINOTRANSFERASE RELATED 1) in young nodule primordia of *L. japonicus* 3 days post-inoculation with rhizobia (Suzaki *et al.*, 2012a). Apart from local auxin biosynthesis, there is a possibility of active Indole 3-Acetic Acid (IAA) production at the site of nodule initiation through hydrolysis of auxin conjugates. In white clover it has been shown that flavonoids along with peroxidases could modulate local auxin metabolism during nodule primordia development (Mathesius, 2001b). There are multiple other auxin metabolism-related mechanisms which could contribute to the active IAA pool during nodule development, which need further investigation. It is also important to consider the auxin synthesized by rhizobia itself as a contributor to the local auxin pool. In Medicago, plants inoculated with the IAA-overproducing *Sinorhizobium meliloti*, an increased rate of nodule formation was observed (Pii *et al.*, 2007). However, it is unlikely that this auxin contributes to the auxin maxima in the inner cortex tissue at the earliest time points of rhizobia infection.

Autoregulation of nodule development (AON) is a negative regulatory mechanism present in legumes which controls nodule development (Ferguson *et al.*, 2010,

Kouchi *et al.*, 2010, Ferguson and Mathesius, 2014a). In the AON mechanism, nitrate levels in coordination with NOD factors determine the number of nodules developing in the roots. The CLAVATA3 (CLE) peptide acts as a systemic signal of nodule initiation from the root to the shoot, where it binds to leucine rich receptor kinases (LRR-RLKs) which then transfer a signal from the shoot, resulting in the inhibition of nodule development. Each CLE peptide, identified in legumes like Medicago (MtCLE12 and MtCLE13), soybean (GmNIC1) and *L. japonicus* (CLE-RS), binds to its respective receptor, such as MtSUNN1, GmNARK, and LjHAR1, to trigger AON (Nishimura *et al.*, 2002, Schnabel *et al.*, 2005, Ferguson *et al.*, 2010, Reid *et al.*, 2011). The shoot-derived signal was identified to be the phytohormone cytokinin, which acts as the signal for AON in *L. japonicus* (Sasaki *et al.*, 2014). A significant increase in the amount of auxin was observed in the MtSUNN1 loss-of-function mutant, *Mtsunn* (van Noorden *et al.*, 2016). Additionally, application of an auxin transport inhibitors at the root-shoot junction reduced the number of nodules in the super-nodulating *Mtsunn* mutant (van Noorden *et al.*, 2016). In the determinate nodule of soybean, a spike in the auxin levels is not observed in the rhizobia-inoculated super-nodulating mutant *nts382* (Caba *et al.*, 2000). In the *Ljhar1* mutant, there was an increase in the auxin response zone, with a much dispersed auxin activity in the cortical region of the rhizobia-inoculated root region, similar to that of the *Mtsunn* mutant (Suzaki *et al.*, 2012a, van Noorden *et al.*, 2016). Overall these show that auxin plays a crucial role in AON and proper nodule organogenesis. But the mechanism(s) involved in this still needs to be elaborated.

Most of the information regarding auxin functions and their underlying mechanisms is based on knowledge from the model plant species *Arabidopsis thaliana.* Even though the importance of auxin as a growth regulator was known since the early days of plant science, the precise functions of auxin in these developmental pathways were only more recently demonstrated using genetic mutants in the biosynthesis, transport, and signaling pathways of auxin (Cheng *et al.*, 2006, Abel and Theologis, 2010, Enders and Strader, 2015). The most common chemical form of auxin present in a plant is indole acetic acid, although other auxins like indole butyric acid (IBA) and phenyl acetic acid (PAA) have been detected in plants. Apart from the naturally synthesized auxin molecules, there are synthetically derived auxin molecules like naphthalene acetic acid (NAA), and 2,4-dichloro phenoxy acetic acid (2, 4-D). Auxin influences diverse plant development processes, including embryo development, post-embryonic meristematic maintenance and cell proliferation, and vasculature, leaf and flower development (Cheng *et al.*, 2006, Tao *et al.*, 2008, Overvoorde *et al.*, 2010a). Recently this hormone has been demonstrated to be crucial in the development of root nodules. To understand the role of auxin metabolism in these developmental processes it is necessary to understand auxin biosynthesis and catabolism in plants.

1.4. Auxin biosynthesis

Indole-3-acetic acid (IAA), the most predominantly found form of auxin in a plant, is derived from two pathways, namely the tryptophan- (Trp) dependent and the tryptophan-independent pathways (Zhao, 2010, Zhao, 2014). Active IAA, or free IAA, can also be synthesized through conversion of conjugated IAA molecules, such as IAA-ester, IAA-sugar and a few amino acid conjugates (IAA-aa). IAA has been

shown to be converted from IBA through β-oxidation (reviewed by (Woodward and Bartel, 2005a)).

Genetic analysis has shown that conversion of tryptophan to IAA through the two-step IPA pathway is the primary source of auxin in Arabidopsis (Zhao, 2012b). The IPA pathway involves transamination of tryptophan by the *TRYPTOPHAN AMINOTRANSFERASE OF ARABIDOPSIS* (TAA1) to produce indole pyruvic acid (IPA) (Stepanova *et al.*, 2008). *YUCCA*, a flavin monoxygenase, converts IPA into IAA (Zhao *et al.*, 2001). Apart from the metabolites in the IPA pathway, there were multiple other metabolites, such as indole 3-acetonitrile and indole 3-acetamide, that were identified as intermediates in the auxin biosynthesis pathway, but they may not be major contributors to IAA biosynthesis. The tryptophan-mediated IPA pathway is the major auxin biosynthetic pathway (Figure 1.4-1). In a parallel pathway, tryptophan is also used as a substrate by CYP79B2, which converts Trp to indole acetaldoxime (IAOx) for indole glucosinolate production. Loss-of-function mutations in the *SUR2* gene, which encodes a cytochrome P450 oxidase enzyme, CYP83B1 lead to increased auxin accumulation, causing increased hypocotyl length. This CYP83B1 enzyme catalyzes the conversion of IAOx to indole thiohydroximate (Bak *et al.*, 2001). The first investigation into auxin over production in plants was inititated through screening of genetic mutants, which led to identification of the *sur1* and *sur2* mutants (Delarue *et al.*, 1998). The reason for increased auxin accumulation in *sur2* was hypothesized to be due to the change in the metabolic flux in the conversion of IAOx (Bak and Feyereisen, 2001) and the strong preference of CYP83B1 to bind to aromatic oximes derived from aromatic amino acids (Naur *et al.*, 2003). When the

loss-of-function mutants in Arabidopsis CYP83B1 led to reduced accumulation of indole glucosinolate, it also led to reduced phenylpropanoid content (Kim *et al.*, 2015). The dramatic effects caused by a mutation of a single gene were also highlighted by the identification of mutants such as *ref5, rnt1-1*, and *gul1* (Bak *et al*. 2001, Kim *et al*. 2015, (Maharjan *et al.*, 2014). Light-grown *sur2* mutant lines exhibited increased hypocotyl length 6 days after germination, but the mutant phenotype became variable and undistinguishable in some lines compared to wildtype. The variation in phenotypes of *sur2* mutants could possibly be due to the influence of multiple signals, like hormones such as abscisic acid, ethylene and other stress responses such as drought (Morant *et al.*, 2010).

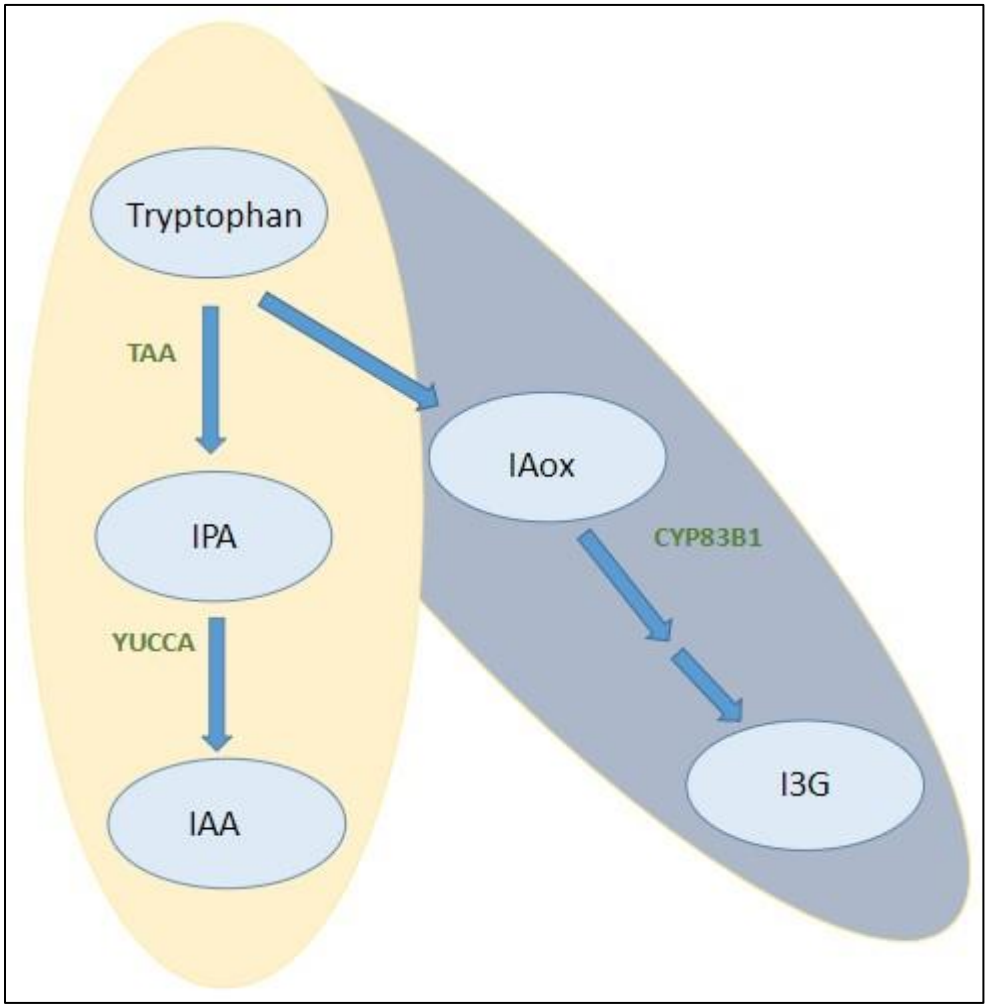

Figure 1.4-1 : **Schematic representation of auxin and Indole glucosinolate biosynthesis pathway.**

A schematic picture depicting the two step Arabidopsis auxin biosynthesis pathway. The substrates in the pathway are mentioned in the oval shapes and the catalyzing enzymes are mentioned along with the blue arrows. IPA-Indole pyruvic acid, IAA-Indole acetic acid, IAOx-Indole acetaldoxime, I3G-Indole 3 glucosinolate. The figure is modified from Zhao et al., 2012.

Auxin biosynthesis in Arabidopsis has been shown to primarily occur in the young leaf primordia tissue, from where it is transported to other tissues for proper organ development (Zhao, 2014). Apart from the auxin arriving through polar auxin transport (PAT), endogenous tissue-specific auxin biosynthesis has been recently demonstrated to be crucial for organ development (Chandler, 2009, Zhao, 2010, Guo *et al.*, 2014). The roles in secondary organ formation of auxin biosynthetic genes were shown in Arabidopsis and petunia by overexpressing the flavin monooxygenase gene (YUC & FLZ, respectively), which causes overproduction of auxin (Tobena-Santamaria *et al.*, 2002, Zhao, 2012a). Such overproduction of auxin through over-expression of YUCCA in certain tissues indicates the possibility of local auxin production (Cheng *et al.*, 2006, Kim *et al.*, 2007). A single loss-of-function YUCCA mutant failed to show any visible phenotype, but triple and quadruple mutants in Arabidopsis showed more prominent alterations, indicating the significance of the genes in altering the local auxin gradient necessary for flower and vascular development (Zhao *et al*. 2001). Genes involved in auxin biosynthesis were also found to be highly enriched in the root apical meristem, which, in combination with polar auxin transport, is necessary to establish the auxin gradient in the root apex (Ljung *et al.*, 2005). The significance of local auxin biosynthesis in primary root development and lateral root organogenesis is reviewed in detail by (Overvoorde *et al.*, 2010b), and its influence on cell division, differentiation, and elongation in organ development is reviewed by (Marhavy *et al.*, 2013).

Understanding any cell-specific expression of these auxin biosynthesis-related genes will help us in understanding the action of local auxin biosynthesis on auxin activity

during nodule development. In legumes, Trp-derived IAA production was identified through labeling assays that indicated a possibility of the IPA pathway in this plant family, even though it has not been clearly demonstrated (Bialek *et al.*, 1992, Quittenden *et al.*, 2009). In addition, transcriptomics data in multiple legumes at different developmental stages, including nodule development, provides an insight into the tissue-specific expression of auxin biosynthesis genes (Libault *et al.*, 2010a, Larrainzar *et al.*, 2015). This suggest that understanding the roles of auxin biosynthesis-related genes in soybean root nodule development could assist in revealing their role in overall auxin activity.

1.5. Auxin inactivation

The significance of auxin biosynthesis has been discussed, but more important to plant development and specifically to nodule development is auxin inactivation, which includes both auxin conjugation and degradation, as reviewed by (Ljung, 2013b, Kramer and Ackelsberg, 2015). With the aid of genetics, several genes involved in the maintenance of auxin and auxin-conjugate levels were identified in recent years, such as GH3, UGT, and DAO1 (Liu *et al.*, 1994, Ludwig-Müller, 2011, Zhang *et al.*, 2016a). Plants have the ability to control the levels of free IAA and active IAA through conjugation of excess IAA for either degradation or storage. GH3 is an acyl amido transferase that has the ability to conjugate an acyl substrate like IAA with an amino acid. This conjugation with an amino acid assigns it for either degradation, such as IAA-Asp, or for storage, like IAA-Leu (Ludwig-Müller, 2011). The GH3 enzyme was first identified in soybean through a screen for auxin-induced cDNA expression. GH3 expression can be induced by free IAA or through exogenous

IAA treatment due to the presence of an auxin response element (AuxRE)(Liu *et al*. 1994). Due to gene redundancy in Arabidopsis, the effect of a single GH3 enzyme could not be identified through loss-of-function mutants. Whereas overexpression of a GH3 enzyme, such as *ydk1-D* and *dfl1-D* in Arabidopsis, resulted in strong auxin deficiency-related phenotypes, such as reduced hypocotyl length (Nakazawa *et al.*, 2001, Takase *et al.*, 2004). Enzymatic studies in both Arabidopsis and rice have shown the specificity of GH3 in conjugating IAA, as the acyl substrate, and Asp, as the amino acid conjugate (Westfall et al. 2012; Chen et al. 2010). Apart from amino acid conjugation, auxin can be conjugated to low molecular weight sugar molecules, such as through an ester bond to glucose (glc) by the enzyme UGT. DAO1 catalyzes the oxidation of auxin to form 2-oxindole-3-acetic acid (oxIAA) , which can be further conjugated by UDP glucosyltransferase UGT74D1 to glycosylate oxIAA to form oxIAA-glc (Pěnčík *et al.*, 2013a, Tanaka *et al.*, 2014, Zhang *et al.*, 2016b). In Arabidopsis it has been clearly shown that oxIAA is the major catabolite that the plant produces to maintain auxin homeostasis. The conjugation of oxIAA to glc is irreversible. oxIAA-glc is the major product of this catabolic process, rather than IAA-Asp or IAA-Glu (Kowalczyk and Sandberg, 2001). All these catabolic mechanisms have been identified in Arabidopsis and seem to primarily contribute to auxin homeostasis. It remains unknown if these enzymes, specifically GH3, have roles in nodule development and what conjugates are catabolically generated over the course of nodule development to maintain proper auxin balance in the nodule tissue.

1.6. Functional analysis of soybean genes using hairy root composite plants

The determination of gene function and expression pattern has been made simpler in model plant species like Arabidopsis through stable whole-plant transformation. This is primarily due to simple, but effective transformation methods e.g. the floral dip method (Clough and Bent, 1998). In what has become the most efficient transformation procedure, the disarmed plant pathogenic bacteria *Agrobacterium tumifaciens* is used. This approach has enabled identification of gene function through loss- or gain-of-function mutations, localization of signaling molecules, evaluation of markers like DR5, and several other genetic techniques. But this transformation procedure is compatible only with a selected set of species. Transformation of other plant species is lengthy and cumbersome and met with technical difficulties owing to the necessitation of tissue culture. The use of hairy root composite plants is another effective transformation procedure for gene functional analysis. In this approach, disarmed *Agrobacterium rhizogenes*, a close relative of *A. tumefaciens*, is used to generate roots carrying the transgene of interest without the need for an entirely transgenic whole plant, yielding a composite plant (Collier *et al.*, 2005a). The foreign gene of interest is cloned into the T-DNA region of the binary vector system before integration into the plant genome, where the *A. rhizogenes* genes promote “hairy root” generation (Bevan and Chilton, 1982). This transformation system has proven ideal for studying plant-microbe interactions, primarily in nodule development. The major advantages with this approach are the fast generation of hairy roots and the easier maintenance compared to tissue culture. The use of the composite hairy root system has been exploited to determine gene

expression using promoter:marker fusions, such as for the key marker gene in nodulation, ENOD40 (Gronlund *et al.*, 2005, Nizampatnam *et al.*, 2015). Transformed hairy roots are being used to understand the function of genes and small RNAs involved in root nodulation, such as FWL1 (Libault *et al.*, 2010b) and the miRNA gma-miR160 (Turner *et al.*, 2013b, Nizampatnam *et al.*, 2015). Hairy roots have also been used to investigate the activation of signaling pathways, changes in root metabolites, and microbial diversity. For example, this approach was used to generate flavonoid-deficient roots in legumes to study plant microbe interaction that generate either indeterminate nodule in *Medicago truncatula* (Wasson *et al.*, 2006) or determinate nodules in soybean (Subramanian *et al.*, 2006). Suppression of flavonoid biosynthesis genes using RNAi in hairy roots had shown that auxin accumulation at the site of nodule development is crucial for the formation of indeterminate nodules. Numerous studies have shown that hairy root transformation is ideal for studying gene function related to plant metabolites, including plant hormones. Hormone-inducible marker constructs, like DR5, in the root tip of transgenic hairy roots show similar expression patterns to the stable transgenic roots in Arabidopsis (Mathesius, 2008, Turner *et al.*, 2013b). Such promoter:marker studies have enabled valid interpretation of the role of hormones in nodule development (Suzaki *et al.*, 2012a, Turner *et al.*, 2013a). Although the hairy root transformation system has multiple advantages, it is important to understand the caveats behind this approach. Since the root generated from this technique is transformed, it may not be appropriate for the study of systemic signaling, since the shoot will be non-transgenic. Hairy roots may also not be suitable for determining the function of genes involved in the

autoregulation of nodule (AON). Hairy root composite transformation is an effective approach for reverse genetics when there is expression data available for a specific gene of interest (Libault *et al.*, 2010a, Libault *et al.*, 2010b, Turner *et al.*, 2013b).

1.7. Objective of this study

Auxin plays a major role in multiple plant developmental processes, including the development of nodules during the symbiotic interactions between nitrogen-fixing *Rhizobia* bacteria and leguminous plants. Unfortunately, the mechanisms regulating auxin levels and activity during the stages of nodule initiation and development remain unclear. The objectives in this research were to determine (i) if and what role does CYP83B1, a gene specifically expressed in nodules, and (ii) a set of three nodule-enriched GH3 enzymes, play in regulating auxin production levels and/or nodule development in soybean. The results were expected to help reveal novel mechanisms that dictate auxin homeostasis for proper nodule development.

1.8. References

Abel S, Theologis A (2010) Odyssey of Auxin. Cold Spring Harbor Perspectives in Biology 2 (10). doi:10.1101/cshperspect.a004572

Bak S, Feyereisen R (2001) The Involvement of Two P450 Enzymes, CYP83B1 and CYP83A1, in Auxin Homeostasis and Glucosinolate Biosynthesis. Plant Physiology 127 (1):108-118

Bak S, Tax FE, Feldmann KA, Galbraith DW, Feyereisen R (2001) CYP83B1, a cytochrome P450 at the metabolic branch point in auxin and indole glucosinolate biosynthesis in Arabidopsis. Plant Cell 13 (1):101-111

Bialek K, Michalczuk L, Cohen JD (1992) Auxin Biosynthesis during Seed Germination in Phaseolus vulgaris. Plant Physiology 100 (1):509-517

Calvert HE, Pence MK, Pierce M, Malik NSA, Bauer WD (1984) Anatomical analysis of the development and distribution of Rhizobium infections in soybean roots. Canadian Journal of Botany 62 (11):2375-2384. doi:10.1139/b84-324

Chandler JW (2009) Local auxin production: a small contribution to a big field. BioEssays : news and reviews in molecular, cellular and developmental biology 31 (1):60-70. doi:10.1002/bies.080146

Cheng Y, Dai X, Zhao Y (2006) Auxin biosynthesis by the YUCCA flavin monooxygenases controls the formation of floral organs and vascular tissues in Arabidopsis. Genes Dev 20 (13):1790-1799. doi:10.1101/gad.1415106

Delarue M, Prinsen E, Onckelen HV, Caboche M, Bellini C (1998) Sur2 mutations of Arabidopsis thaliana define a new locus involved in the control of auxin homeostasis. The Plant journal : for cell and molecular biology 14 (5):603-611

Enders TA, Strader LC (2015) Auxin activity: Past, present, and future. American journal of botany 102 (2):180-196. doi:10.3732/ajb.1400285

F Sanchez, J E Padilla, H Perez a, Lara M (1991) Control of Nodulin Genes in Root-Nodule Development and Metabolism. Annual review of plant physiology and plant molecular biology 42 (1):507-528. doi:10.1146/annurev.pp.42.060191.002451

Geurts R, Bisseling T (2002) Rhizobium Nod Factor Perception and Signalling. The Plant Cell 14 (Suppl):s239-s249. doi:10.1105/tpc.002451

Guo J, Wei J, Xu J, Sun M-X (2014) Inducible knock-down of GNOM during root formation reveals tissue-specific response to auxin transport and its modulation of local auxin biosynthesis. Journal of Experimental Botany. doi:10.1093/jxb/ert475

Harper JE (1974) Soil and Symbiotic Nitrogen Requirements for Optimum Soybean Production1. Crop Science 14:255-260. doi:10.2135/cropsci1974.0011183X001400020026x

Hirsch AM (1992) Developmental biology of legume nodulation. New Phytologist 122 (2):211-237. doi:10.1111/j.1469-8137.1992.tb04227.x

Hirsch AM, Bhuvaneswari TV, Torrey JG, Bisseling T (1989) Early nodulin genes are induced in alfalfa root outgrowths elicited by auxin transport inhibitors. Proc Natl Acad Sci U S A 86 (4):1244-1248

Kim JI, Dolan WL, Anderson NA, Chapple C (2015) Indole Glucosinolate Biosynthesis Limits Phenylpropanoid Accumulation in Arabidopsis thaliana. Plant Cell. doi:10.1105/tpc.15.00127

Kim JI, Sharkhuu A, Jin JB, Li P, Jeong JC, Baek D, Lee SY, Blakeslee JJ, Murphy AS, Bohnert HJ, Hasegawa PM, Yun DJ, Bressan RA (2007) yucca6, a dominant mutation in Arabidopsis, affects auxin accumulation and auxin-related phenotypes. Plant Physiol 145 (3):722-735. doi:10.1104/pp.107.104935

Kramer EM, Ackelsberg EM (2015) Auxin metabolism rates and implications for plant development. Frontiers in Plant Science 6:150. doi:10.3389/fpls.2015.00150

Larrainzar E, Riely BK, Kim SC, Carrasquilla-Garcia N, Yu H-J, Hwang H-J, Oh M, Kim GB, Surendrarao AK, Chasman D, Siahpirani AF, Penmetsa RV, Lee G-S, Kim N, Roy S, Mun J-H, Cook DR (2015) Deep Sequencing of the Medicago truncatula Root Transcriptome Reveals a Massive and Early Interaction between Nodulation Factor and Ethylene Signals. Plant Physiology 169 (1):233-265. doi:10.1104/pp.15.00350

Libault M, Farmer A, Joshi T, Takahashi K, Langley RJ, Franklin LD, He J, Xu D, May G, Stacey G (2010) An integrated transcriptome atlas of the crop model Glycine

max, and its use in comparative analyses in plants. The Plant journal : for cell and molecular biology 63 (1):86-99. doi:10.1111/j.1365-313X.2010.04222.x

Liu ZB, Ulmasov T, Shi X, Hagen G, Guilfoyle TJ (1994) Soybean GH3 promoter contains multiple auxin-inducible elements. The Plant Cell 6 (5):645-657. doi:10.1105/tpc.6.5.645

Ljung K (2013) Auxin metabolism and homeostasis during plant development. Development (Cambridge, England) 140 (5):943-950. doi:10.1242/dev.086363

Ljung K, Hull AK, Celenza J, Yamada M, Estelle M, Normanly J, Sandberg G (2005) Sites and regulation of auxin biosynthesis in Arabidopsis roots. Plant Cell 17 (4):1090-1104. doi:10.1105/tpc.104.029272

Ludwig-Müller J (2011) Auxin conjugates: their role for plant development and in the evolution of land plants. Journal of Experimental Botany 62 (6):1757-1773. doi:10.1093/jxb/erq412

Maharjan PM, Dilkes BP, Fujioka S, Pencik A, Ljung K, Burow M, Halkier BA, Choe S (2014) Arabidopsis gulliver1/SUPERROOT2-7 identifies a metabolic basis for auxin and brassinosteroid synergy. The Plant journal : for cell and molecular biology 80 (5):797-808. doi:10.1111/tpj.12678

Marhavy P, Vanstraelen M, De Rybel B, Zhaojun D, Bennett MJ, Beeckman T, Benkova E (2013) Auxin reflux between the endodermis and pericycle promotes lateral root initiation. Embo j 32 (1):149-158. doi:10.1038/emboj.2012.303

Mathesius U (2008) Goldacre paper: Auxin: at the root of nodule development? Functional Plant Biology 35 (8):651-668. doi:http://dx.doi.org/10.1071/FP08177

Morant M, Ekstrom C, Ulvskov P, Kristensen C, Rudemo M, Olsen CE, Hansen J, Jorgensen K, Jorgensen B, Moller BL, Bak S (2010) Metabolomic, transcriptional, hormonal, and signaling cross-talk in superroot2. Molecular plant 3 (1):192-211. doi:10.1093/mp/ssp098

Mus F, Crook MB, Garcia K, Garcia Costas A, Geddes BA, Kouri ED, Paramasivan P, Ryu MH, Oldroyd GE, Poole PS, Udvardi MK, Voigt CA, Ane JM, Peters JW (2016) Symbiotic Nitrogen Fixation and the Challenges to Its Extension to Nonlegumes. Applied and environmental microbiology 82 (13):3698-3710. doi:10.1128/aem.01055-16

Mutava RN, Prince SJ, Syed NH, Song L, Valliyodan B, Chen W, Nguyen HT (2015) Understanding abiotic stress tolerance mechanisms in soybean: a comparative evaluation of soybean response to drought and flooding stress. Plant physiology and biochemistry : PPB 86:109-120. doi:10.1016/j.plaphy.2014.11.010

Nakazawa M, Yabe N, Ichikawa T, Yamamoto YY, Yoshizumi T, Hasunuma K, Matsui M (2001) DFL1, an auxin-responsive GH3 gene homologue, negatively regulates shoot cell elongation and lateral root formation, and positively regulates the light response of hypocotyl length. The Plant journal : for cell and molecular biology 25 (2):213-221

Naur P, Petersen BL, Mikkelsen MD, Bak S, Rasmussen H, Olsen CE, Halkier BA (2003) CYP83A1 and CYP83B1, two nonredundant cytochrome P450 enzymes metabolizing oximes in the biosynthesis of glucosinolates in Arabidopsis. Plant Physiol 133 (1):63-72

Newcomb W, Sippell D, Peterson RL (1979) The early morphogenesis of Glycine max and Pisum sativum root nodules. Canadian Journal of Botany 57 (23):2603-2616. doi:10.1139/b79-309

Overvoorde P, Fukaki H, Beeckman T (2010a) Auxin Control of Root Development. Cold Spring Harbor Perspectives in Biology 2 (6):a001537. doi:10.1101/cshperspect.a001537

Overvoorde P, Fukaki H, Beeckman T (2010b) Auxin Control of Root Development. Cold Spring Harbor Perspectives in Biology 2 (6). doi:10.1101/cshperspect.a001537

Pacios-Bras C, Schlaman HRM, Boot K, Admiraal P, Mateos Langerak J, Stougaard J, Spaink HP (2003) Auxin distribution in Lotus japonicus during root nodule development. Plant Mol Biol 52 (6):1169-1180. doi:10.1023/B:PLAN.0000004308.78057.f5

Peer WA, Murphy AS (2007) Flavonoids and auxin transport: modulators or regulators? Trends in plant science 12 (12):556-563

Peoples MB, Brockwell J, Herridge DF, Rochester IJ, Alves BJR, Urquiaga S, Boddey RM, Dakora FD, Bhattarai S, Maskey SL, Sampet C, Rerkasem B, Khan DF, Hauggaard-Nielsen H, Jensen ES (2009) The contributions of nitrogen-fixing crop

legumes to the productivity of agricultural systems. Symbiosis 48 (1):1-17. doi:10.1007/bf03179980

Quittenden LJ, Davies NW, Smith JA, Molesworth PP, Tivendale ND, Ross JJ (2009) Auxin Biosynthesis in Pea: Characterization of the Tryptamine Pathway. Plant Physiology 151 (3):1130-1138. doi:10.1104/pp.109.141507

Schultze M, Kondorosi A (1998) Regulation of symbiotic root nodule development. Annual review of genetics 32:33-57. doi:10.1146/annurev.genet.32.1.33

Stepanova AN, Robertson-Hoyt J, Yun J, Benavente LM, Xie DY, Dolezal K, Schlereth A, Jurgens G, Alonso JM (2008) TAA1-mediated auxin biosynthesis is essential for hormone crosstalk and plant development. Cell 133 (1):177-191. doi:10.1016/j.cell.2008.01.047

Subramanian S, Stacey G, Yu O (2006) Endogenous isoflavones are essential for the establishment of symbiosis between soybean and Bradyrhizobium japonicum. The Plant journal : for cell and molecular biology 48 (2):261-273. doi:10.1111/j.1365-313X.2006.02874.x

Takanashi K, Sugiyama A, Yazaki K (2011) Involvement of auxin distribution in root nodule development of Lotus japonicus. Planta 234 (1):73-81. doi:10.1007/s00425-011-1385-0

Takase T, Nakazawa M, Ishikawa A, Kawashima M, Ichikawa T, Takahashi N, Shimada H, Manabe K, Matsui M (2004) ydk1-D, an auxin-responsive GH3 mutant

that is involved in hypocotyl and root elongation. The Plant journal : for cell and molecular biology 37 (4):471-483

Tao Y, Ferrer JL, Ljung K, Pojer F, Hong F, Long JA, Li L, Moreno JE, Bowman ME, Ivans LJ, Cheng Y, Lim J, Zhao Y, Ballare CL, Sandberg G, Noel JP, Chory J (2008) Rapid synthesis of auxin via a new tryptophan-dependent pathway is required for shade avoidance in plants. Cell 133 (1):164-176. doi:10.1016/j.cell.2008.01.049

Tobena-Santamaria R, Bliek M, Ljung K, Sandberg G, Mol JN, Souer E, Koes R (2002) FLOOZY of petunia is a flavin mono-oxygenase-like protein required for the specification of leaf and flower architecture. Genes & development 16 (6):753-763. doi:10.1101/gad.219502

Udvardi MK, Day DA (1997) Metabolite transport across symbiotic membranes of legume nodules. Annual review of plant physiology and plant molecular biology 48:493-523. doi:10.1146/annurev.arplant.48.1.493

Wasson AP, Pellerone FI, Mathesius U (2006) Silencing the flavonoid pathway in Medicago truncatula inhibits root nodule formation and prevents auxin transport regulation by rhizobia. Plant Cell 18 (7):1617-1629. doi:10.1105/tpc.105.038232

Woodward AW, Bartel B (2005) Auxin: regulation, action, and interaction. Annals of botany 95 (5):707-735. doi:10.1093/aob/mci083

Zhang J, Lin JE, Harris C, Campos Mastrotti Pereira F, Wu F, Blakeslee JJ, Peer WA (2016) DAO1 catalyzes temporal and tissue-specific oxidative inactivation of auxin

in Arabidopsis thaliana. Proceedings of the National Academy of Sciences 113 (39):11010-11015. doi:10.1073/pnas.1604769113

Zhao Y (2010) Auxin biosynthesis and its role in plant development. Annual review of plant biology 61:49-64. doi:10.1146/annurev-arplant-042809-112308

Zhao Y (2012a) Auxin biosynthesis: a simple two-step pathway converts tryptophan to indole-3-acetic acid in plants. Molecular plant 5 (2):334-338. doi:10.1093/mp/ssr104

Zhao Y (2012b) Auxin Biosynthesis: A Simple Two-Step Pathway Converts Tryptophan to Indole-3-Acetic Acid in Plants. Molecular plant 5 (2):334-338. doi:https://doi.org/10.1093/mp/ssr104

Zhao Y (2014) Auxin Biosynthesis. The Arabidopsis Book:e0173. doi:10.1199/tab.0173

Zhao Y, Christensen SK, Fankhauser C, Cashman JR, Cohen JD, Weigel D, Chory J (2001) A role for flavin monooxygenase-like enzymes in auxin biosynthesis. Science (New York, NY) 291 (5502):306-309. doi:10.1126/science.291.5502.306

Chapter 2

2. REGULATION OF AUXIN HOMEOSTASIS BY CYP83B1 IN SOYBEAN NODULE

2.1. Abstract

Developmental stage-specific auxin output dictates proper symbiotic nodule development in legumes. While some signaling modules that regulate auxin sensitivity during nodule development are known, the role of auxin biosynthesis and metabolism in nodule development are unclear. We identified genes enriched in emerging nodules, mature nodules, emerging lateral roots, and young lateral roots in soybean by comparing global gene expression profiles between each of these organs and adjacent root segments. The use of adjacent root tissues as controls, and comparison to expression in lateral roots helped us identify an accurate set of nodule-enriched genes in soybean. Genes associated with auxin biosynthesis appeared to be active in both nodules and lateral roots except for a CYP83B1 ortholog that had nodule-specific enrichment. Based on observations in Arabidopsis and the expression pattern of this gene, we hypothesized that GmCYP83B1 might regulate auxin homeostasis acting in parallel to the indole pyruvate pathway. Indeed, suppression of GmCYP83B1 led to high auxin levels in nodules, a reduction in nodule numbers and size, and defective nodule vascular development suggesting that regulation of auxin homeostasis by GmCYP83B1 is crucial for proper nodule numbers and maturity. Inhibition of auxin biosynthesis in GmCYP83B1 silenced roots using yucasin rescued nodule numbers, but not maturity. We have discovered a key role for GmCYP83B1 in regulating auxin homeostasis during soybean nodule development.

2.2. Introduction

Many leguminous plants develop symbiotic root nodules through well-coordinated interactions with nitrogen-fixing soil bacteria collectively termed rhizobia. Nodule development can be broadly classified in to three major temporally overlapping stages: (i) host-symbiont signal exchange for compatibility which primarily occurs in the root hair and epidermal cells; (ii) nodule organogenesis and rhizobial colonization involving a number of intrinsic plant hormonal and developmental pathways which occurs in the root cortex; and (iii) biological nitrogen fixation involving bacterial differentiation, nitrogen metabolism pathways, and nutrient exchange which occurs in the differentiated nodule tissues. Genetic and functional genomic studies have revealed a number of genes associated with these different processes in particular root hair and cortical responses [reviewed by (Crespi and Frugier, 2008, Oldroyd *et al.*, 2011)].

There are two major types of nodules formed in legume roots: indeterminate and determinate (reviewed in (Hirsch, 1992, Mathesius, 2003)). Indeterminate nodules are oblong and are characterized by the presence of a persistent nodule meristem analogous to lateral roots (LRs). Examples of plants that form indeterminate nodules include temperate legumes viz. *Pisum sativum* (pea), *M. truncatula* (Barrel Medic) and *Trifolium* species (clover). In contrast, determinate nodules are spherical and lack a persistent nodule meristem. Examples of plants producing determinate nodules include tropical/subtropical legumes viz. *Glycine max* (soybean), *Vicia faba* (common bean), and *Lotus japonicus*. Additionally, indeterminate nodules arise from inner cortical cell layers whereas determinate nodules arise from outer cortical cell layers.

Nearly all plant hormones play a key role in the development of both these types of nodules (reviewed by (Ding and Oldroyd, 2009, Ferguson and Mathesius, 2014b). Auxin has been associated with the development of both these types of nodules and appears to play a role in both root hair and cortical responses. For example, auxin perception and signaling mechanisms regulate rhizobial infection and root hair responses in soybean and *M. truncatula* (Breakspear *et al.*, 2014a, Cai *et al.*, 2017). While auxin response gene expression is observed during nodule initiation, there is relatively low auxin output during nodule initiation vs. LR initiation. In fact, increased auxin output generally inhibits nodule formation in both determinate and indeterminate legume nodules (Suzaki *et al.*, 2012b, Turner *et al.*, 2013b, Champion *et al.*, 2015, Wang *et al.*, 2015, Hobecker *et al.*, 2017). We and others have reported that precise spatio-temporal regulation of auxin output might be crucial for proper nodule development (Breakspear *et al.*, 2014a, Li *et al.*, 2014, Nizampatnam *et al.*, 2015, Wang *et al.*, 2015, Cai *et al.*, 2017, Hobecker *et al.*, 2017). Therefore, a tight spatio-temporal control of auxin homeostasis, transport, and/or signaling is required to achieve properly balanced and precisely distributed auxin output during nodule development (Kohlen *et al.*, 2017). However, deregulation of auxin transport does not affect nodule development in soybean (Subramanian *et al.*, 2006, Subramanian *et al.*, 2007). Therefore, it is likely that precisely regulated auxin metabolism and signaling specify domains of auxin output especially during determinate nodule development. Different mechanisms primarily involving miRNA modules that regulate auxin signaling during the infection as well as organogenesis stages of both determinate and

indeterminate nodules have been discovered (Breakspear *et al.*, 2014a, Li *et al.*, 2014, Nizampatnam *et al.*, 2015, Wang *et al.*, 2015, Cai *et al.*, 2017, Hobecker *et al.*, 2017). However, the role of auxin homeostasis in dictating auxin output during nodule development is poorly understood. While some of genes associated with auxin metabolism are induced in response to rhizobium inoculation (Campanella *et al.*, 2008, Suzaki *et al.*, 2012b), there is no functional evidence for the role of auxin metabolism genes during nodule development.

Indole-3-acetic acid (IAA) is the major form of auxin in many plant species. In most dicots, the primary biosynthetic pathway for IAA appears to be the tryptophan-dependent indole-3-pyruvic acid (IPA) pathway (Zhao, 2012c). In this simple two-step pathway, tryptophan (Trp) is converted to IPA by TAA aminotransferase family of enzymes; Subsequently, IPA is converted to IAA by YUCCA family of flavin monooxygenase enzymes (Mashiguchi *et al.*, 2011, Won *et al.*, 2011, Dai *et al.*, 2013). Another parallel pathway with indole-3-acetaldoxime (IAOx) as the key intermediate was previously proposed as the major auxin biosynthesis pathway; but recent evidence suggests otherwise. For example, plants defective in IAOx biosynthesis have only subtle phenotypes compared to IPA deficient multi-order *taa* mutants (Sugawara *et al.*, 2009). However, mutations in SUR2, a CYP83B1 enzyme that acts directly downstream of IAOx led to high auxin levels in Arabidopsis (Barlier *et al.*, 2000). Similarly, over-expression of *SUR2* led to auxin-deficient phenotypes. These observations suggested that SUR2 might regulate auxin homeostasis by competing with the primary auxin biosynthesis pathway for substrates(Bak *et al.*, 2001). Auxin catabolism also plays a key role in maintaining free auxin levels and

thus auxin output. GH3 enzymes conjugate auxin to amino acids (*e.g.* IAA-Asp) leading to inactivation and in most cases catabolism of auxin (Staswick *et al.*, 2005a). Reversible inactivation mechanisms such as conjugation to Leu or Ala, methylation, glucosylation, and conversion to IBA are also known (Woodward and Bartel, 2005b). It was recently revealed that 2-oxoindole-3-acetic acid (oxIAA) is the major catabolite of auxin in Arabidopsis and rice (Peer *et al.*, 2013, Pěnčík *et al.*, 2013b).A dioxygenase enzyme that catabolizes IAA to oxIAA has also been identified(Pěnčík *et al.*, 2013b, Zhao *et al.*, 2013, Porco *et al.*, 2016, Zhang *et al.*, 2016b). Controlled biosynthesis, inactivation, and catabolism establish optimal auxin levels, and thus auxin output to regulate various plant development processes.

To determine key nodule-specific hormonal pathways, in particular those related to auxin homeostasis, we compared transcriptomic profiles of nodules and lateral roots at two different stages of development in soybean. Further evaluation revealed organ-specific expression patterns of key auxin homeostasis-associated genes, in particular a nodule-specific CYP83B1. Results from genetic, molecular, biochemical and microscopy experiments demonstrated a crucial role for this nodule-specific CYP83B1 in regulating auxin homeostasis to enable proper nodule development in soybean.

2.3. Results

2.3.1. GmCYP83B1 expression is enriched in nodule parenchyma, but is absent in nodule vasculature.

Comparative transcriptomics indicated enrichment of auxin biosynthesis related genes in nodules, yet the role of auxin homeostasis in regulating auxin output during nodule development is poorly understood. Among the different genes associated with auxin homeostasis, a CYP83B1 family member (Glyma01g17330.1 (a1.v1.1)/ Glyma.01G078300.1 (a2.v1.1)) with high sequence similarity to Arabidopsis *SUR2* (Figure S2-1A;(Barlier *et al.*, 2000, Bak *et al.*, 2001)) was specifically enriched in mature nodules (Figure 2.3-1A) while no other gene from that family was enriched in any of the tissues evaluated. We refer to this gene as GmCYP83B1 from this point onwards. The nodule-specific nature of GmCYP83B1 expression was further supported by the soybean transcriptomic atlas data (Libault *et al.*, 2010a) (Figure S2-1B).

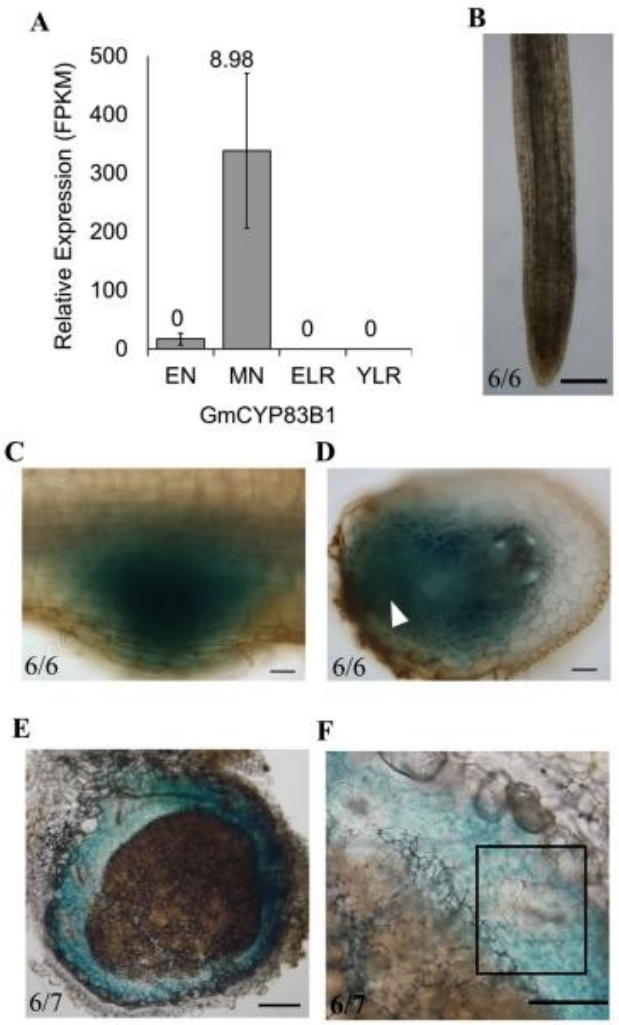

Figure 2.3-1: **Nodule enriched expression pattern of GmCYP83B1.**

(A) Expression levels of GmCYP83B1 in EN, MN, ELR, YLR tissues from the transcriptome dataset. Data shown are average expression values ± SD from three biological replicates. Statistically significant fold change vs. respective control root segments are indicated above each bar; (**B-F**) Expression of GmCYP83B1p:GUS (**B**) at 0 dpi in mock inoculated roots, (**C**) whole mount and (**D**) transverse section of an emerging nodule at 7 dpi, and (**E**) transverse section of a mature nodule at 14 dpi. **(F**) A magnified section showing nodule vasculature excluded expression of GmCYP83B1p:GUS in mature nodules. Arrow head in D indicates the nodule primordium. The number of independent transgenic roots showing the representative staining pattern out of the number of roots examined is indicated in each panel. Scale bars: B, F – 100µm; C,D – 50µm, E - 200µm.

To identify the potential role of this nodule enriched GmCYP83B1, its full-length peptide sequence was obtained and corresponding orthologs of *Arabidopsis thaliana, Medicago truncatula, Populus trichocarpa, Brachypodium distachyon, Solanum lycopersicum, Vitis vinifera and Lotus japonicus* were obtained. Phylogenetic analysis indicated that the soybean CYP83B1 gene is in the same clade as the Arabidopsis CYP83B1 (Figure S2-2A). High sequence similarity indicated the possibility of GmCYP83B1 to be functionally similar to AtCYP83B1 (Figure S2-2A). We also analyzed for the presence of any signal peptide using signalP tool and GmCYP83B1 peptide possesses a membrane binding domain which might enable ER localization common for P450 enzymatic function. The GmCYP83B1 peptide sequence was identified to possess a signal peptide sequence but the Arabidopsis sequence does not possess any (Figure S2-2B and C). Although they possess high sequence similarity such variation with signal peptide sequence suggests that mechanism or activity of both the P450 oxidase enzyme could possibly have some variations. Based on the high expression and enrichment of GmCYP83B1 in nodules, and its high sequence similarity to Arabidopsis *SUR2*, we suspected that it might regulate nodule auxin levels during soybean nodule development.

To evaluate the spatio-temporal patterns of GmCYP83B1 expression in roots and nodules, a transcriptional fusion of its promoter region (~1900bp upstream of start codon) to GUS (GmCYP83B1p:GUS) was constructed and transformed in to composite transgenic soybean plants. The expression of GmCYP83B1p:GUS was not detectable in uninoculated roots (Figure 2.3-1B), but was prominently

detected in the nodule primordia and periphery of emerging nodules at 7dpi (Figure 2.3-1C and D). In mature nodules, GmCYP83B1p:GUS was localized specifically to the nodule parenchyma, particularly the inner nodule cortex (Figure 2.3-1E) in agreement with our nodule zone-specific expression data. Upon closer examination, GmCYP83B1p:GUS expression was not detectable in the vascular bundles of mature nodules (Figure 2.3-1F). Interestingly, the absence of GmCYP83B1 expression in nodule vasculature was in contrast to that of auxin reporter expression localized primarily in the nodule vasculature in the determinate nodules of soybean and *Lotus japonicus* (Suzaki *et al.*, 2012a, Turner *et al.*, 2013b). The apparent complementary expression pattern between GmCYP83B1 and auxin response markers further supported a hypothesized role for GmCYP83B1 in regulating auxin homeostasis in soybean nodules.

2.3.2. GmCYP83B1 expression is crucial for proper nodule numbers and maturity.

To determine the function of GmCYP83B1, we silenced its expression using RNAi in soybean composite plant roots. Since the gene was poorly expressed in uninoculated roots, silencing was evaluated in rhizobium-inoculated roots using RT-qPCR. In agreement with our transcriptome data, we observed induction of the gene in response to rhizobium inoculation in vector control roots when evaluated at 5 and 10 dpi (Figure 2.3-2A). However, the induction was significantly suppressed (~ 7 to 10 fold) in GmCYP83B1-RNAi roots at both time points (Figure 2.3-2A). The expression of two closely related homologs (Glyma18g11820 and Glyma03g03670) were slightly but significantly silenced

(Figure S2-3A & B). However, any impact of GmCYP83B1-RNAi in nodule development is most likely due to the suppression of GmCYP83B1 since the expression levels of these off targets were minimal, and neither were they enriched in nodule tissues (Figure S2-1B and Figure S2-3). In conclusion, our RNAi construct successfully silenced the expression of GmCYP83B1.

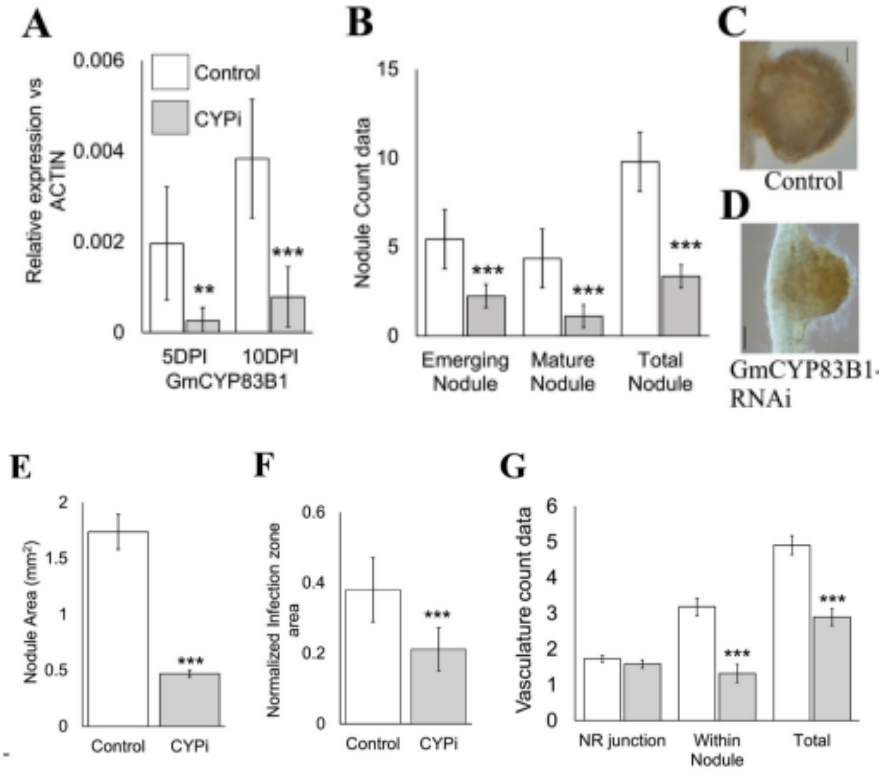

Figure 2.3-2: **Suppression of GmCYP83B1 leads to impaired nodule development.**

(A) Expression levels of GmCYP83B1 in vector control and GmCYP83B1-RNAi roots at 5 and 10 dpi assayed by RT-qPCR. Data shown are the average of three biological replicates and error bars indicate SD. *** - P<0.001 and **-P<0.01 – WilcoxonMann-Whitney test. (B) Numbers of emerging, mature, and total nodules in vector control and CYP83B1-RNAi roots at 17 dpi. Data shown are the average of at least 105 roots from three independent experiments. Error bars indicate SE. *** - P<0.001 –Poisson distribution test. (C & D) Images of representative mature nodules from (C) vector control and (D) CYP83B1-RNAi roots. (E and F) Nodule area and normalized infection zone size of mature nodules from vector control and CYP83B1-RNAi roots. Data shown are average of at least 15 nodules each from three biological replicates. Error bars indicate SE. *** - P<0.001–Wilcoxon-Mann-Whitney test. (G) Number of vasculature branches detectable at the nodule-root junction and within the nodule of transverse sections of mature nodules from vector control and CYP83B1-RNAi roots. Data shown are average of at least 18 nodules each from three biological replicates. Error bars indicate SE. *** - P<0.001– Student's t-test. Scale bars in C, D - 100µm.

When nodule numbers were evaluated at 14-17 dpi, GmCYP83B1-RNAi roots had a significant reduction in the number of both emerging and mature nodules compared to the vector control leading to a ~66% reduction in total nodule numbers (Figure 2.3-2B). In addition, the mature nodules that formed on GmCYP83B1-RNAi roots were visibly smaller and had a striking "dome" shaped morphology compared to the typical mushroom shaped mature nodules on vector control roots (Figure 2.3-2C & D). We measured the nodule area using median transverse sections of nodules and observed that the majority of mature nodules that formed on GmCYP83B1-RNAi roots were indeed significantly smaller in size compared to those on control roots (1.74 vs 0.47 mm^2; Figure 2.3-2E). We also observed a significant reduction in the relative size of the infection zone in GmCYP83B1-RNAi nodules compared to vector control (Figure 2.3-2F). While the infection zone occupied ~38% of the nodule in vector control roots, it occupied only 21% of the GmCYP83B1-RNAi nodules.

Given the vasculature-excluded expression pattern of GmCYP83B1, we evaluated nodule vasculature organization by counting the number of vasculature branches near the root-nodule junction and within the nodule parenchyma in transverse sections of mature nodules (Figure 2.3-2G). There was a significant reduction in the number of vasculature traces/branches observable within the nodule parenchyma of GmCYP83B1-RNAi roots compared to vector control, but there was no difference in the number of branches at the root-nodule junction (Figure 2.3-2F). Overall, impaired nodule development in GmCYP83B1-RNAi roots

indicated that GmCYP83B1 expression is crucial not only for proper nodule numbers, but also maturation and vasculature branching.

2.3.3. Suppression of GmCYP83B1 leads to increased auxin levels in nodule

In Arabidopsis, the CYP83B1 loss of function mutant *rnt1-1* (allelic to *sur2*) had increased auxin levels (Bak *et al.*, 2001); and in soybean, auxin hypersensitivity caused a reduction in nodule numbers (Turner *et al.*, 2013b, Nizampatnam *et al.*, 2015). Therefore, we hypothesized that the reduced nodule numbers in GmCYP83B1-RNAi roots might potentially be due to increased auxin levels. As an initial evaluation of the hypothesis, we assayed the expression of auxin responsive marker genes in *B. japonicum*-inoculated GmCYP83B1-RNAi roots as a proxy for increased auxin output. At 10dpi when the GmCYP83B1 expression levels were significantly down-regulated in GmCYP83B1-RNAi roots (Figure 2.3-3A & B), the expression levels of the auxin response markers GmGH3 and GmIAA1 (Nizampatnam *et al.*, 2015) were respectively 8.6 fold and 1.8 fold higher vs. vector control roots (Figure 2.3-3A & B). This suggested that silencing of GmCYP83B1 might have indeed led to increased auxin levels as reported in Arabidopsis CYP83B1 loss of function mutants (Barlier *et al.*, 2000).

Encouraged by this observation, we measured the levels of tryptophan (Trp) and IAA using LC-MS/MS (Liquid Chromatography –Mass Spectrometry) in emerging and mature nodule tissues harvested from vector control and CYP83B1-RNAi roots. Root segments adjacent to these nodule tissues devoid of any root lateral organs were used as age-appropriate control tissues to evaluate if any observed changes are specific to nodule tissues. In vector control roots, emerging

nodules (EN) had a significantly higher level of both Trp and IAA compared to the adjacent control root tissues (ABEN) strongly suggesting local auxin biosynthesis via IPA pathway might occur early during nodule development (Figure 2.3-3C & D; ABEN-VC vs. EN-VC). Interestingly, mature nodule (MN) tissues had much lower levels of Trp compared to EN tissues, but the levels of IAA were not different between the two tissues (Figure 2.3-3C & D; EN-VC vs MN-VC). This suggested that Trp and/or its shikimic acid precursors might be routed into the production of other indolic or phenolic metabolites during nodule maturation. Alternate possibilities include the utilization of Trp by the rhizobia or reduced Trp biosynthesis in MN. The levels of neither Trp nor IAA were different between control root segments of EN or MN tissues (ABEN and ABMN respectively) suggesting that changes in Trp metabolism and auxin biosynthesis are localized to nodule tissues during early nodule development and nodule maturation (Figure 2.3-3C & D).

Mature nodules of CYP83B1-RNAi roots had significantly higher levels of both Trp and IAA compared to that of vector control mature nodules (Figure 2.3-3C & D; MN-CYPi vs. MN-VC). Therefore, suppression of GmCYP83B1 indeed led to increased auxin accumulation during nodule development likely due to increased accumulation of Trp. The increase in Trp and IAA in GmCYP83B1-RNAi roots was limited to MN tissues where CYP83B1 is highly expressed. There was no difference in either Trp or IAA levels in other tissue types between vector control and GmCYP83B1-RNAi roots. Unlike in vector control roots, there was no significant reduction in Trp levels in MN compared to EN in GmCYP83B1-RNAi

roots suggesting that there was reduced utilization of Trp when the expression of GmCYP83B1 is silenced. The increased Trp availability is likely to have resulted in over production of IAA in GmCYP83B1-RNAi mature nodules. Therefore, a change in metabolic flux from the IAOx (or other pathway involving GmCYP83B1) to the IPA pathway might have occurred when GmCYP83B1 was silenced resulting in IAA overproduction via the IPA pathway.

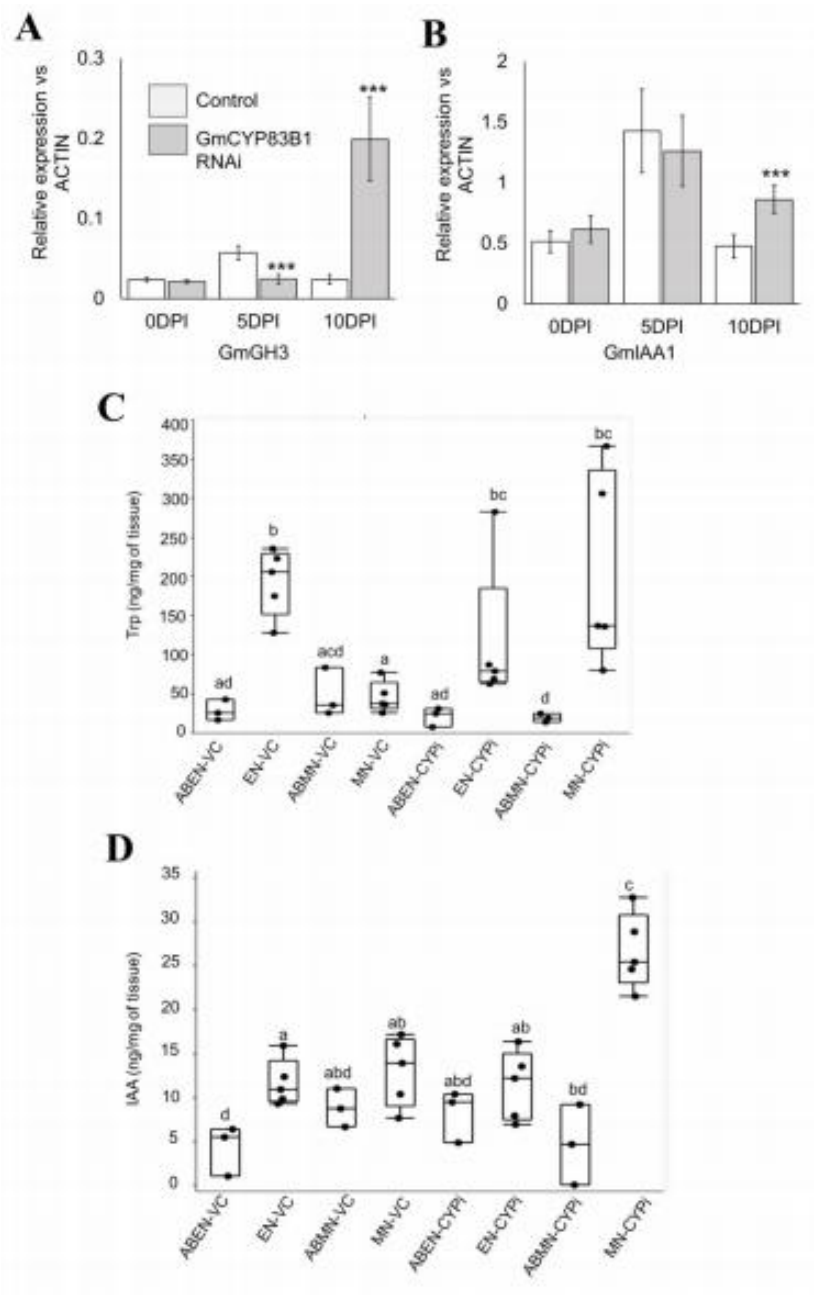

Figure 2.3-3: **Suppression of GmCYP83B1 leads to increased nodule auxin levels.**

(A & B) Expression levels of auxin response marker genes, (A) GH3 and (B) IAA1 in vector control and GmCYP83B1-RNAi roots at 0, 5 and 10 dpi assayed by RT-qPCR. Data shown are the average of three biological replicates and error bars indicate SD. ***-P<0.001 – Wilcoxon-Mann-Whitney test. (C & D) Levels of (C) Tryptophan and (D) IAA in emerging (EN) and mature (MN) nodule tissues, and respective control root segments (ABEN and ABMN) harvested from vector control (VC) and CYP83B1-RNAi roots (CYPi) assayed using LC- MS/MS. Boxplots show data from 5 biological replicates for nodule tissues and 3 biological replicates for control root segments. Each replicate sample was harvested from approx. 5-20 independent transgenic roots. Samples marked with different letters are significantly different from each other based on Wilcoxon-Mann-Whitney test. (P<0.05).

2.3.4. Chemical Inhibition of IAA biosynthesis restored nodule numbers, but not maturity in GmCYP83B1-RNAi roots

To determine if the nodulation phenotypes and increased auxin output in CYP83B1-RNAi nodules were indeed due to IAA over production via the IPA pathway, we sought to inhibit YUCCA activity using the inhibitor yucasin (5-(4-chlorophenyl)-4H-1,2,4-triazole-3-thiol) (Nishimura *et al.*, 2014). If reduced nodule numbers and abnormal nodule development in CYP83B1-RNAi roots were due to increased auxin produced via the IPA pathway, one can expect yucasin to rescue nodulation phenotypes of CYP83B1-RNAi roots. Based on the data from Arabidopsis three different concentrations of yucasin were used to treat wild type soybean plants (10, 20 and 50µM) along with a mock solvent control (0 µM). After treatment of plants with yucasin, their root length and lateral roots were measured as a proxy for potential reduction in endogenous auxin levels. Wild type seedlings treated with 10µM yucasin did not show any significant change in the root length or lateral root density; but, seedlings treated with 20µM or 50µM yucasin displayed a significant increase in root length and a significant reduction in lateral root density in a dose-dependent manner (Figure 2.3-4A & B). This suggested that 20 and 50 µM concentrations of yucasin likely reduced the levels of auxin. When the auxin output marker expression was analyzed in yucasin-treated wild type roots, seedlings treated with 20 µM yucasin had a consistent trend of reduced marker gene expression; in particular, there was a significant reduction in the expression of IAA1 and IAA9 in 20 µM yucasin treatment (Figure 2.3-4C). Seedlings treated with 10 and 50 µM yucasin treatment

showed varied responses (Figure 2.3-4C). This suggested that 20 µM yucasin treatment might consistently reduce auxin levels in soybean roots.

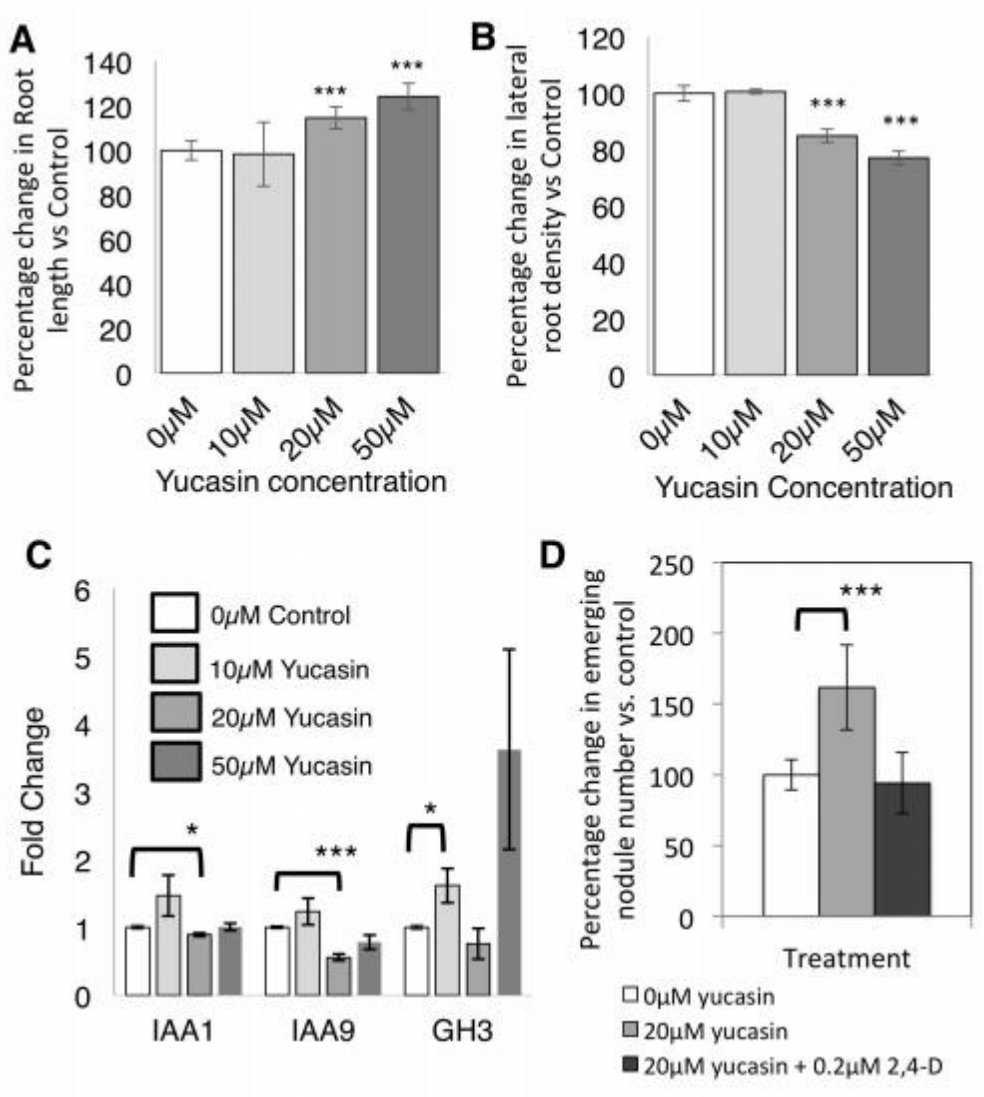

Figure 2.3-4: **Effect of yucasin on auxin response phenotype.**

(A & B) Root length (A) and lateral root density (B; number of lateral roots/ cm of root length) of wild type soybean plants treated with yucasin at 0μM, 10μM, 20μM, or 50μM concentration for 10 days. Data shown in A and B are average of 48 plants from three biological replicates expressed as percentage change vs. 0μM controls and error bars indicate SEM. *** -P<0.001, Wilcoxon-Mann-Whitney test, vs. 0μM. (C) Expression levels of auxin response marker genes, in wild type soybean plant roots treated with yucasin at 0μM, 10μM, 20μM, or 50μM concentration for 10 days. Data shown are the average fold change in gene expression compared to 0μM control and error bars indicate SEM. * -P<0.05, **-P<0.01, ***-P<0.001, Wilcoxon-MannWhitney test, vs 0μM. (D) Number of emerging nodules in wild type soybean seedlings plants treated with 0μM or 20μM yucasin, or 20μM yucasin + 0.2 μM 2,4-D. 50μM concentration for 10 days. Data shown are average of at least 45 plants from two independent experiments expressed as percentage change vs. 0μM controls and error bars indicate SEM. *** -P<0.001, Wilcoxon-Mann-Whitney test, vs. 0μM.

We treated vector control and CYP83B1-RNAi plants with 20µM yucasin to determine if inhibition of IAA biosynthesis can rescue nodulation defects. As expected, roots of mock-treated CYP83B1-RNAi plants (0µM yucasin), developed fewer nodules compared to those of vector control (Figure 2.3-5A). In vector control roots treated with 20µM yucasin, there was a significant increase in the number of emerging nodules, but no change in the number of mature nodules. This indicated that suppression of auxin biosynthesis by yucasin led to increased nodule organogenesis. This was consistent with our previous report of increased number of emerging nodules in miR160 suppressed soybean roots with reduced auxin sensitivity (Nizampatnam et al., 2015). GmCYP83B1-RNAi roots treated with 20µM yucasin also had a significant increase in the number of emerging nodules. The number of emerging nodules and total nodules in yucasin-treated vector control and GmCYP83B1-RNAi roots were comparable indicating a rescue of nodule number (organogenesis) by suppression of auxin biosynthesis (Figure 2.3-5A). However, neither the number of mature nodules, nor the defects in nodule vasculature branching, nodule area, and infection zone size of CYP83B1-RNAi roots were rescued by yucasin treatment (Figure 2.3-5A, B, C and D). Therefore, yucasin treatment was able to rescue the nodule number (organogenesis), but not nodule maturation in GmCYP83B1-RNAi roots. Rescue of nodule numbers by yucasin strongly suggested that reduced nodule numbers in GmCYP83B1-RNAi roots were indeed due to IAA over production via the IPA pathway.

Our results demonstrate that GmCYP83B1 plays a crucial role in soybean nodule development by regulating auxin homeostasis. Combined with previous observations that developmental stage specific regulation of auxin signaling is crucial for proper nodule development in soybean (Breakspear *et al.*, 2014a, Li *et al.*, 2014, Nizampatnam *et al.*, 2015, Wang *et al.*, 2015, Cai *et al.*, 2017, Hobecker *et al.*, 2017), we conclude that auxin output might be regulated at both metabolic and signaling levels to achieve proper nodule development in soybean.

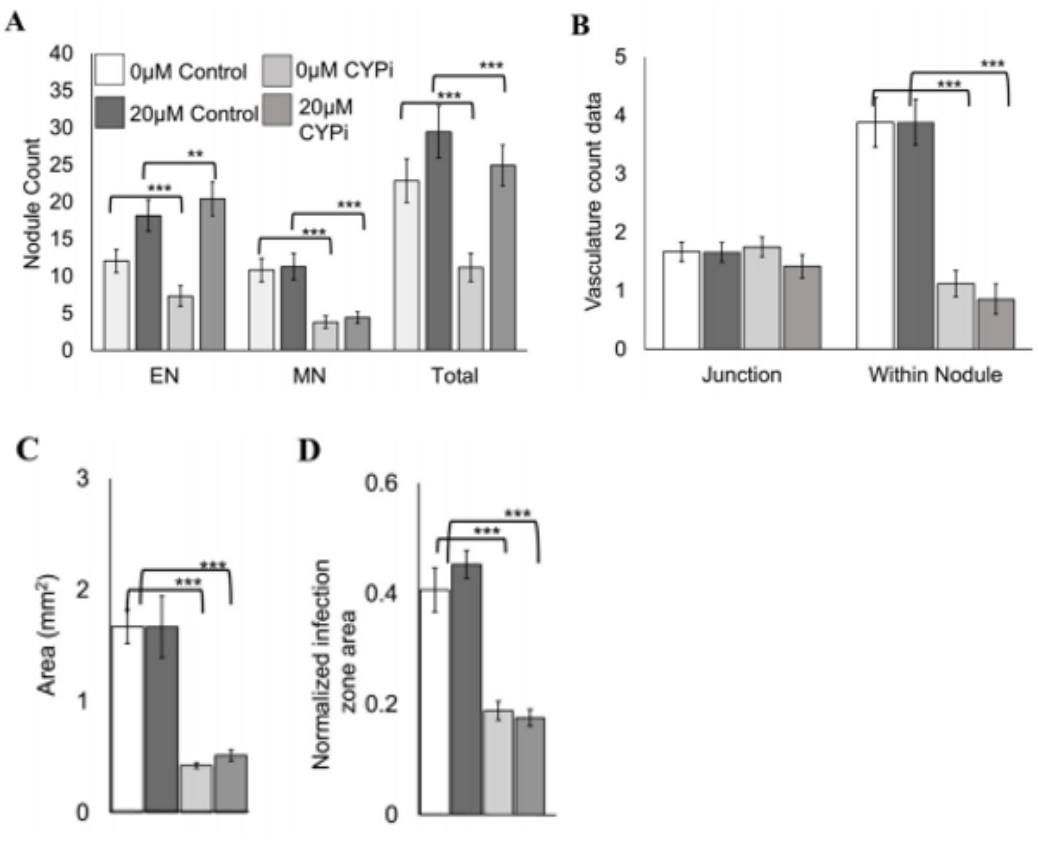

Figure 2.3-5: **Effect of yucasin on GmCYP83B1-RNAi nodule development**.

(A) Numbers of emerging, mature, and total nodules in vector control and CYP83B1-RNAi roots at 17 dpi. Plants were treated with yucasin at 0μM or 20μM. Data shown are average of count data from three biological replicates (N>70) and error bars indicate SEM.*- P<0.05, **-P<0.01 and *** -P<0.001, Poisson distribution test. (B) Number of vasculature branches detectable at the nodule-root junction and within the nodule of transverse sections of mature nodules from vector control and CYP83B1-RNAi roots treated with yucasin. Data shown are average of at least 9 nodules each, error bars indicate SD. ***P<0.001, Student's ttest. (C & D) Nodule area (C) and normalized infection zone size (D) of mature nodules from vector control and CYP83B1-RNAi roots. Data shown are average of at least 7 nodules each, error bars indicate SEM ***-P<0.001, Wilcoxon-Mann-Whitney test.

2.3.5. Over and mis-expression of GmCYP83B1

Suppression of GmCYP83B1 led to increased auxin production. We evaluated if over expression of GmCYP83B1 leads to reduced auxin levels in the root tissues. If the CYP83B1 uses the tryptophan-derived substrate for production of indole thiohydroximate, over expression of CYP83B1 should lead to reduced auxin production. The coding sequence of GmCYP83B1 was cloned under the constitutively expressing promoter CsVMV and along with the auxin reporter DR5:GUS construct. Gene expression of GmCYP83B1ox (over expression) roots showed a 100 fold increase in the CYP83B1 expression compared to the vector control (CsVMV:TdTomato-DR5:GUS) (Figure 2.3-6A). The levels of IAA and IAA-Aspartate conjugates (for degradation to maintain auxin homeostasis) in the root tips of over expressing plants were measured (Figure 2.3-6B). There was no significant difference in the levels of IAA or IAA-Asp observed in the over expressing root tips compared to vector control. In parallel using the DR5:GUS reporter construct the change in auxin levels were monitored microscopically in the roots of GmCYP83B1 over expression plants. There was a slight reduction in the GUS expression pattern observed in the GmCYP83B1 overexpressing roots (Figure 2.3-6C). The auxin marker gene expression (Figure 2.3-6A) and auxin quantification (Figure 2.3-6B) could not clearly reveal the reduced auxin levels in the GmCYP83B1 over expression.

Another objective with a similar question was to identify if ectopic mis-expression of GmCYP83B1 in the nodule primodium/infection zone leads to altered nodule development. Two-different nodule specific promoters FWL1 and

ENOD40 were used to mis-express GmCYP83B1 (Figure 2.3-7A and B). GmFWL1 promoter is actively expressed in the nodule primordia of emerging nodule and up on maturation the expression if restricted to nodule parenchyma region (Libault M *et al.*,2010). GmENOD40 promoter on the other hand is expressed in the nodule primordia of the emerging nodules and later in the uninfected cells of the infection zone in mature nodules (Yang WC *et al.,* 1993). The transgenic plants were treated with rhizobia and the nodule numbers were evaluated 14-17dpi. There was no significant change in nodule numbers in GmCYP83B1 mis-expressing roots (Figure 2.3-7A and B) compared to vector control. However, the effect of mis-expression on auxin production was not evaluated.

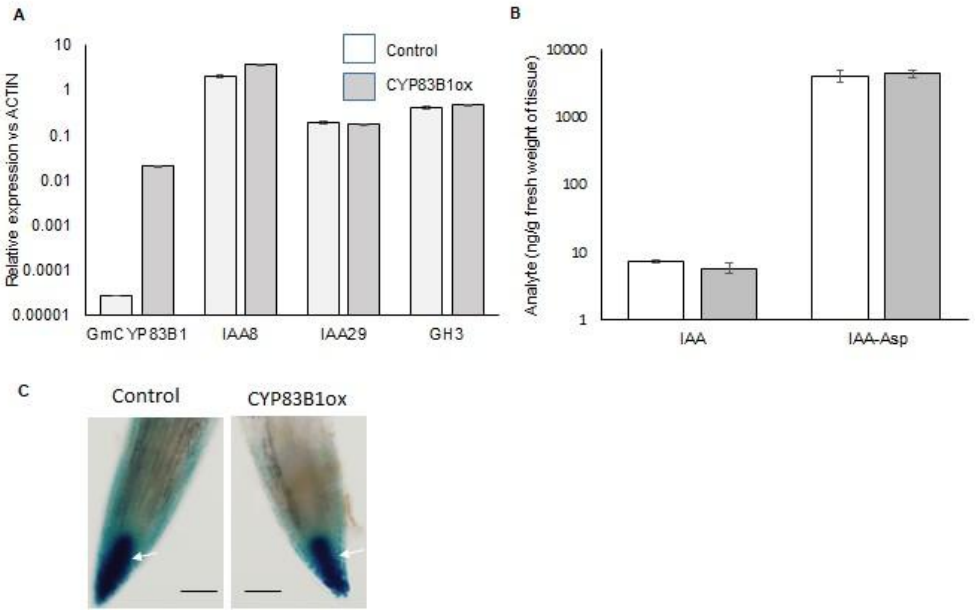

Figure 2.3-6: **Over expression of GmCYP83B1.**

A) Gene expression data showing over expression of GmCYP83B1 in GmCYP83B1ox roots compared to vector control. The data represents average gene expression from three biological replicates and error bars represent SE. B) Quantification of IAA and IAA-Asp levels in CYP83B1 over expressing root tips. Data represents average of three replicates and error bars indicate SEM C) DR5:GUS expression pattern in CYP83B1ox root tips (20/26) and control (15/18). Scale bar = 200μM.

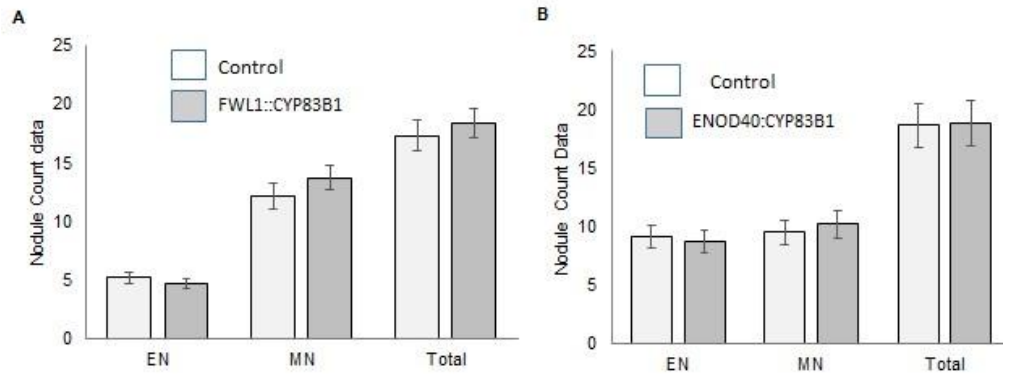

Figure 2.3-7: **Over and Mis-expression of GmCYP83B1.**

A) Nodule count data of mis-expression of GmCYP83B1 using GmFWL1 promoter. B) Nodule count data of mis-expression of GmCYP83B1 using GmENOD40 promoter. The data is average of three biological replicate (n>70) and error bars indicate SEM. Statistical significance was determined using zero inflated poisson distribution.

2.4. Discussion

While transport and signaling mechanisms that contribute to spatio-temporal auxin output during nodule development have been discovered, little was known about the role of auxin metabolism in this process. Flavonoids that inhibit peroxidases capable of degrading auxin accumulate at the sites of nodule initiation in white clover suggesting that this might be a mechanism for auxin accumulation in these tissues(Mathesius, 2001a). Auxin amidohydralases capable of hydrolyzing the ester bonds of IAA-glucose (and thus releasing free IAA) are induced upon rhizobium infection in *M. truncatula* (Campanella *et al.*, 2008). In *L. japonicus, TRYPTOPHAN AMINOTRANSFERASE RELATED1,* a paralog of TAA was transiently induced at 3 dpi, coinciding with the earliest auxin response marker gene expression at the site of rhizobial colonization. Our results also showed enrichment of YUC, GH3, and IAA oxidase gene family members in EN tissues (Damodaran S et al., in preparation). While these observations suggested that local auxin metabolism might contribute to auxin output during nodule initiation and development, no functional evidence existed for this hypothesis. The expression landscape of genes associated with auxin homeostasis provided key target genes for functional analysis. Because of the strikingly nodule-specific expression of GmCYP83B1, we evaluated its role in regulating auxin levels and nodule development in soybean. The complementary expression pattern of GmCYP83B1 and auxin-responsive marker gene expression in soybean nodules, and increased auxin levels in Arabidopsis CYP83B1 loss of function mutants prompted us to

hypothesize that GmCYP83B1 might regulate spatio-temporal auxin homeostasis in nodules. In agreement with results from Arabidopsis CYP83B1 loss of function mutants, we also observed increased auxin levels in soybean nodules when GmCYP83B1 expression was suppressed. This suggested that GmCYP83B1 might act in a parallel pathway to that of the primary auxin biosynthesis pathways. Since soybean root hair tissue accumulates indole glucosinolates (Brechenmacher *et al.*, 2010), it was tempting to speculate that GmCYP83B1 acts in a similar pathway to that in Arabidopsis (the IAOx pathway).

In soybean nodules with reduced expression of GmCYP83B1, we observed increased levels of Trp suggesting that the increased auxin might have come from the IPA pathway during nodule development. Metabolite profiling and enzymatic assays in Arabidopsis ruled out tryptophan derived IAA production as the cause of increased auxin in Arabidopsis CYP83B1 loss of function *sur2* mutants. IAOx was suggested to be the metabolic branching point for auxin and indole glucosinolate biosynthesis pathway in Arabidopsis, but this has yet to be experimentally demonstrated (Morant *et al.*, 2010). Tryptophan labelling studies performed in *Pisum sativum and Phaseolus vulgaris* had shown that Trp is a major precursor for IAA biosynthesis in legumes (Bialek *et al.*, 1992, Quittenden *et al.*, 2009), suggesting that a tryptophan-dependent pathway such as the IPA pathway is a major source of IAA in legumes. Strong evidence for the role of IPA pathway in regulating nodule auxin homeostasis in soybean came from experiments in this study where YUCCA enzyme activity was inhibitied using yucasin (Nishimura *et al.*, 2014). The rescue of nodule numbers by treatment with 20µM yucasin

suggested that increased auxin accumulation in GmCYP83B1-RNAi roots almost certainly occurred via the IPA pathway. On the other hand, the Arabidopsis Arabidopsis CYP83B1 loss of function *sur2* mutant phenotypes could not be rescued by yucasin treatment (Nishimura *et al.*, 2014). Therefore, it is likely that GmCYP83B1 either directly competes for or acts in a pathway that directly competes for the tryptophan substrate with the IPA pathway unlike in Arabidopsis. Additional biochemical assays are necessary to determine specific substrates and products of GmCYP83B1. We concluded that a tryptophan-dependent auxin biosynthesis pathway (likely the IPA pathway) contributes to nodule auxin output; and that a nodule-specific CYP83B1 acting in a parallel pathway regulates auxin homeostasis in nodules and governs proper soybean nodule development.

There were other phenotypic differences between soybean CYP83B1-RNAi roots and Arabidopsis CYP83B1 loss of function mutants. Arabidopsis *sur2* mutants had reduced root length and increased number of LRs due to increased auxin accumulation (Bak *et al.*, 2001). In contrast, the length and LR density of GmCYP83B1-RNAi roots were not different from those of vector control roots (Figure S2-4). Similarly, differences in Trp and IAA levels between control and CYP83B1-RNAi were limited only to nodules and not observed in adjacent root tissues. The observation that phenotypes were restricted to nodule tissues in CYP83B1-RNAi roots are best explained as resulting from nodule-specific expression of GmCPY83B1 vs. the expression of AtCYP83B1 (*SUR2*) across a number of organs and tissues resulting in pleiotropic phenotypes. The failure to observe a phenotype in mis-expression of GmCYP83B1 could be due to availability

of substrate since this is an enzymatic reaction. Mis-expression of GmCYP83B1 might have caused some unknown changes in the metabolite profile but not sufficient enough to observe a phenotype in nodule development.

Yucasin treatment was able to restore normal nodule numbers, but not proper vasculature branching or nodule size in CYP83B1-RNAi roots. This is likely due to the patterns of IAA distribution manifested by CYP83B1 activity during nodule development. While an initial auxin maximum is observed during nodule initiation and early primordium development, auxin output is diminished in the central tissues of the nodule at later stages(Suzaki *et al.*, 2012b, Turner *et al.*, 2013b). Sustained/increased auxin output throughout the root and particularly in the nodule primordium inhibits nodule development(Turner *et al.*, 2013b, Wang *et al.*, 2015, Hobecker *et al.*, 2017). In agreement, CYP83B1-RNAi roots with increased nodule auxin levels produced fewer nodules. Together with the observation that CYP83B1 is expressed throughout the nodule primordium, this gene might play a role in reducing auxin levels after nodule initiation and early primordium development. Yucasin, being a molecule able to diffuse throughout root tissues, can cause an overall reduction in auxin levels throughout the entire root, complementing CYP83B1 activity to promote nodule primordium development. Indeed, vector control roots treated with yucasin also produced more emerging nodules suggesting that an overall reduction in auxin levels can promote nodule organogenesis. This is in agreement with the observation that reduced sensitivity to auxin increased the number of nodules in soybean and *M. truncatula* (Turner *et al.*, 2013b, Wang *et al.*, 2015, Hobecker *et al.*, 2017). In mature nodules, CYP83B1 is present in the

parenchyma, but specifically absent in vascular bundles. We speculate that such an expression pattern early during vascular development might result in the formation of an auxin differential (e.g. high auxin in low CYP83B1 expressing cells and vice versa) between specific cell types leading to vascular identity during nodule maturation. Auxin is one of the key molecular signals involved in conferring provascular identity through its action on a set of CLASS III HOMEODOMAIN LEUCINE ZIPPER (HD-ZIPIII) transcription factors (reviewed by (Ramachandran *et al.*, 2017)). Co-expression of key auxin signaling components and HD-ZIPIII genes occurs during vascular cell specification e.g. (Muller *et al.*, 2016). While polar auxin transport mechanisms that dictate auxin gradients crucial for vascular cell specification are known (Ilegems *et al.*, 2010), tryptophan-dependent local auxin biosynthesis is also crucial for HD-ZIPIII expression and vascular development (Ursache *et al.*, 2014). *L. japonicus* plants treated with auxin transport inhibitors produced nodules with defective vasculatures that had attenuated auxin-response marker gene expression suggesting that auxin transport machinery is crucial for proper nodule vascular development (Takanashi *et al.*, 2011). Therefore, absence of / reduced expression of CYP83B1 in vascular bundles during nodule maturation, is likely to result in increased auxin accumulation in these cell types. We speculate that this pattern of CYP83B1 expression might act in concert with the auxin transport machinery to generate the auxin maxima required for vascular cell specification. While both yucasin and GmCYP83B1 can reduce auxin levels, it is unlikely that an exogenously supplied chemical such as yucasin can achieve a specific spatial distribution of auxin similar to the distinct spatio-temporal

expression patterns of CYP83B1. Therefore, the partial rescue of nodule development in yucasin treated GmCYP83B1-RNAi roots might be due to the relatively tight spatio-temporal GmCYP83B1 activity patterns required for nodule maturity compared to nodule initiation. However, we cannot rule out the possibility that another metabolite produced directly or downstream of GmCYP83B1 activity being crucial for nodule maturity; *i.e.* GmCYP83B1 might regulate auxin homeostasis for proper nodule numbers and might produce another yet unknown compound to regulate proper nodule maturity. In conclusion, we have discovered a key role for GmCYP83B1-regulated auxin metabolism in determining spatio-temporal auxin output during soybean nodule development.

2.5. Conclusion

The complementary spatio-temporal expression patterns of GmCYP83B1 and auxin-response markers indicated a potential role for this gene in regulating auxin levels in nodules. The elevated levels of auxin and Trp in GmCYP83B1-RNAi roots suggested such a role for GmCYP83B1. CYP83B1-RNAi roots produced fewer nodules that were smaller and had impaired nodule vascular branching. Some of these defects were rescued when auxin biosynthesis was chemically inhibited suggesting that the defects were indeed due to increased auxin levels. Overall this suggested that active local auxin biosynthesis regulation occurs during nodule development, and that GmCYP83B1 plays a key role in regulating the levels and likely the distribution of auxin during soybean nodule development.

2.6. Materials and Methods:

2.6.1. RNA Sequencing

To develop a global transcriptome atlas for soybean in Subramanian lab two different root lateral organs at two development stages were harvested from wild type soybean plants: a) emerging lateral root (ELR) b) young lateral root (YLR) c) emerging nodule (EN), and d) mature nodule (MN). As a control to determine organ-enriched gene expression, root segments of about 1 cm above and below (AB) the root lateral organs were harvested as age- and inoculation- appropriate controls. The nodule tissues were harvested from *B. japonicum* inoculated plants at 7 and 14 dpi (days post inoculation) for EN and MN respectively. RNA was isolated from the tissues; and sequencing library construction and high throughput sequencing were performed at University of Missouri, Columbia. A ScriptSeq v2 RNA-Seq Library preparation kit (Epicenter Biotechnologies) was used for strand specific cDNA synthesis and library construction. The synthesized libraries were used for sequencing using a Highseq2000 instrument (1x50nt). Data analysis was performed by a colleague Dr. Sajag Adhikari and Dr. Senthil Subramanian using a set of tools to quality check and trim the sequences; and map reads to the genome sequence of soybean. Fragments Per Kilobase of transcript per Million mapped reads (FPKM) and the $\log_2$ fold change of gene expression in the respective tissue to their corresponding control root segments were determined using the tuxedo pipeline (Trapnell *et al.*, 2012). The absolute expression levels (FPKM) and tissue enrichment ($\log_2$ fold change) values of GmCYP83B1 was obtained from this data.

2.6.2. Phylogenetic and peptide domain identification

Full length Peptide sequences coding for CYP83B1 gene were obtained from *Arabidopsis thaliana, Medicago truncatula, Populus trichocarpa, Brachypodium distachyon, Solanum lycopersicum, Vitis vinifera and Lotus japonicus* using the peptide sequence of GmCYP83B1 as follows. The peptide sequence of GmCYP83B1 was used in the BLAST P search tool in www.phytozome.net and using the BLOSUM62 matrix the peptide orthologs of GmCYP83B1 was obtained with an extension value of -1. A phylogenetic tree was built using the neighbor joining method using the MEGA V tool after performing a multiple sequence alignment. The signal peptides in the CYP83B1 sequences were determined using signalP tool (http://www.cbs.dtu.dk/services/SignalP/) with D-Cutoff value of 0.50.

2.6.3. Plant material

Soybean cultivar Williams 82, was used for the experiments since the genome sequence is available. Seeds were surface sterilized using 8% bleach and 70% ethanol for 4min each and thoroughly rinsed with water to remove any residual ethanol before sowing in a soil mixture made of vermiculite and perlite (3:1). The plants were grown in a 4" pot and watered regularly using Hoagland nutrient solution (Appendix A. Table A1). The plants were grown in a vertical growth chamber with a cycle of 16hr light/day and 25˚C followed by a night cycle of 8hr at 20 ˚C (Conviron, Manitoba, CA). Two weeks old germinated plants with first set of trifoliate leaves were used for composite hairy root plant transformation as described in (Collier *et al.*, 2005a).

2.6.4. Composite hairy root transformation

The vectors used in the study were transformed in to *Agrobacterium rhizogenes* AK599. Composite hairy root plant transformation was performed using 14 days old soybean plant with the first trifoliate leaves. To prepare the *A. rhizogenes* culture harboring desired vector, the bacterial culture was inoculated in LB (supplemented with the appropriate antibiotic) and incubated overnight at 28°C on a rotary shaker at 200rpm. To prepare the culture for transformation it was centrifuged at 3500xg for 8 min and re-suspended in N^- PNS to a final concentration of OD_{600}= 0.3. Sterile rock wool plug cubes (Hummert International, MO) were placed on petridishes and it was flooded with the respective culture (about 5-7 ml). Soybean plants were cut below the trifoliate leaves in a slanting manner to increase the surface area of infection with bacteria and it is placed in to the rock wool plug. The transformed plants in petridishes were placed in a plant growth tray and covered with a transparent lid. The plants were placed in a growth shelf with 16h light and 8h dark for 2-3 weeks until the appearance of adventious root.

2.6.5. Nodulation assays

For nodulation assays the plants were inoculated with *Bradyrhizobium japonicum,* USDA110 culture, grown in Vincents rich media supplemented with chloramphenicol (0.02mg/ml) and incubated in a shaker set at 28˚C and 200 rpm. At the time of inoculation, the culture was centrifuged at 3500xG for 8min and the pellet was resuspended to a final concentration of OD_{600nm}=0.08 in nitrogen free plant nutrient solution (N^- PNS) (Appendix A. Table A2). For nodulation

assay the nodules were counted at 14-17dpi and the emerging nodules were classified to be a bump on the root surface and mature nodules are classified as protruded structure on root surface. The nodule count data was collected from three biological replicates and the count data was compared to respective control and data was analyzed using zero inflated poisson distribution package available in R.

2.6.6. Yucasin treatment

The plants were treated with different concentrations of yucasin 0, 10, 20, 50µM prepared as described in (Nishimura *et al*. 2014). The plants were watered alternatively between yucasin mixed with N^- PNS and with N^- PNS. For root length, lateral root density and gene expression assays, wild type soybean plants were treated with the corresponding concentration of yucasin at 3 and 7 days post germination (Figure S2-5). Assays were performed at 10days post germination. The normality of the data was determined using Shapiro wilk test and the statistical significance was determined using Wilcoxon-mann-Whitney test in R version 3.3.0. For studying the effect of nodulation with yucasin treatment the plants were inoculated 3days post germination or three days after transfer of composite plants in vermiculite:perlite and inoculated with *B. japonicum* and the next day (1dpi) they were treated with the corresponding yucasin solution and again at 5 and 10dpi (for detailed plan, Fig S5). For the co-treatment of yucasin and 2,4-D a similar treatment approach was used by mixing 20 µM yucasin with 0.2 µM 2,4-D. The concentration of 2,4-D was chosen based on (Nizampatnam *et*

al., 2015) of the Nodulation assays were performed at 14dpi and nodules harvested at this timepoint were used for morphological analysis.

2.6.7. Vector Construction

A ~1900bp upstream region of GmCYP83B1 was amplified from soybean genomic DNA using Platinum PCR supermix High fidelity (Thermofisher Scientific, Waltham, MA). The PCR product was cloned in to pCR8/GW/TOPO-TA vector (Thermofisher Scientific, Waltham, MA) and its sequence was verified. The promoter fragment was cloned in to destination vector, pCAMGFP-GW:GUS using Gateway LR clonase II enzyme mix following the manufacturer's protocol (Thermofisher Scientific, Waltham, MA) to obtain pCAMGFP-GmCYP83B1p:GUS.

To generate the GmCYP83B1-RNAi construct, a 130bp region of the GmCYP83B1 coding sequence was amplified and cloned in to pCR8/GW/TOPO-TA (Thermofisher Scientific, Waltham, MA). The sequence verified RNAi region was cloned in to pCAMGFPCsVMV:GWi using Gateway LR clonase II enzyme mix (Thermofisher Scientific, Waltham, MA) to obtain pCAMGFP-GmCYP83B1-RNAi binary vector. To generate pCAMGFP-CsVMV:GWi vector the FMV-driven RNAi vector (Govindarajulu et al., 2009) was used and the FMV promoter was replaced with the CsVMV promoter (Govindarajulu et al., 2008).

To generate the pCAMGFP-CsVMV:CYP83B1-DR5:GUS construct, the coding sequence (1506bp) was amplified and cloned in to the destination vector following the same procedure as GmCYP83B1promoter:GUS construct. The same CDS sequence cloned in to the pCR8GWTOPOTA construct was used in

generating the mis-expression vectors pCAMGFP-ENOD40:CYP83B1 and pCAMGFP-FWL1:CYP83B1.

2.6.8. Staining, Microscopy and Image Analysis

The transgenic roots were screened for the expression of GFP fluorescent protein marker using the FITC filter in an epi-fluoresence microscope (Olympus SZX16 Epi-Fluorescent Stereo Microscope) and used for different microscopy staining procedures.

2.6.9. GUS staining assay

The transgenic root of mock (N^- PNS) or *B. japonicum* inoculated plants were incubated in GUS staining buffer (Appendix B, TABLE B1) to which X-GLUC (substrate) was added at a concentration of 0.5mg/ml. The roots were stained overnight (16hrs) or until the appearance of blue coloration of substrate indicating end product of GUS activity at 22˚C. The stained roots were dehydrated by a series of ethanol dilution from (10% to 70%) to arrest the enzyme activity and stain diffusion. Before microscopy the roots were rehydrated by a series of ethanol dilution (70% to 10%) and roots were mounted directly or after hand sectioning with 10% glycerol (v/v) on a glass slide. The staining in the transgenic roots or nodule sections were imaged using an Olympus SZX16 Epi –fluorescent microscope under white light trans-illumination or with BX-53 upright microscope.

2.6.10. Pholoroglucinol staining

The transgenic roots inoculated with *B. japonicum* was collected at 14-17dpi and the mature nodules were hand sectioned horizontally with the root for transverse

section and used for staining. To visualize the nodule area, infection zone and vasculature, the phloroglucinol dye was used. A saturated solution of phloroglucinol was prepared freshly before staining by dissolving the dye in 20% HCl and added to the mature nodule cross section. The images were obtained under white light trans-illumination in BX-53 upright microscope. ImageJ tool was used in measuring the nodule area by drawing a border around the nodule area using free hand tool and the area was measured (Figure S2-6). Normality of the data distribution was determined using shapiro-wilk test and the statistical significance was determined using Wilcoxon mann whitney test package available on R version 3.3.0. The vasculature branches are identified by inspection of lignified nodule vascular endodermis and xylem vessels in the transverse sections. The statistical significance was evaluated by student *t*-test in Microsoft Excel.

2.6.11. Gene expression Analysis

The transgenic roots expressing GFP were screened using epifluorescence stereomicroscope and harvested in dry ice or Liquid nitrogen. In case of nodule tissues, a segment of the tissue is dissected under microscope and collected in cold TRI reagent. The tissue is stored in -70˚C until it is used for further processing.

2.6.12. RNA Extraction

The harvested plant tissues were weighed and about 500mg of tissue was used for RNA extraction using the TRI reagent. The whole root tissues were grounded using liquid nitrogen in a pre-cold pestle and mortar until a fine powder is obtained. About 10ml of TRI reagent was added to the mixture and mixed

completely. The mixture was centrifuged at 7000xg for 15min at 4˚C and the supernatant was collected in a fresh tube and 1/5vol of Chloroform was added and thoroughly mixed. The mixture is centrifuged and the clear supernatant was collected and the step was repeated until a clear aqueous layer is obtained. To precipitate the RNA, isopropanol (0.7x volume of supernatant) was added and incubated in -20˚C for overnight. The mixture is centrifuged and the supernatant was discarded. To the pellet added 3ml of 70% ethanol and centrifuged to remove residual salt and contaminants. The supernatant was removed after centrifugation and pellet was dissolved in DEPC (Diethyl pyrocarbonate) treated water. The samples were quantified using NanoDrop ND-1000 spectrophotometer and integrity of RNA was verified using agarose gel electrophoresis.

2.6.13. DNA contamination Test

To check the purity of RNA from any detectable DNA contamination before proceeding with quantitiative RT-PCR, the RNA is subjected to DNA contamination test. A qRT-PCR was performed as explained in the section below with the respective RNA itself as template and using a constitutively expressed marker/housekeeping gene such as ACTIN. Absence or very minimal amplification would indicate the absence of any contaminating DNA.

2.6.14. cDNA Synthesis

The complementary strand for the mRNA was synthesized using M-MuLV reverse transcriptase. Total RNA of about 2µg was used as a template and added a combination of 1µL of 10mM dNTP mix and 1µL of 10µM oligodT primer in a 200µL PCR tube. The final volume was made up to 17.5µL with DEPC treated

water and the sample was incubated at 75˚C in a thermocycler. After incubation the samples were snap cooled in ice for 5min. For synthesizing cDNA 2µL of 10x Reverse transcriptase was added along with 0.5µL of 200,000U/ml reverse transcriptase. The sample was incubated in the thermocycler at 42˚C for 60min and deactivated for 5min at 90˚C.

2.6.15. Reverse Transcription – quantitative Polymerase Chain Reaction (RT-qPCR)

To determine the expression levels of mRNA in the cDNA synthesized from the above-mentioned protocol using the ABI, quantstudio 3 qPCR system. The reaction is set up in a 20µL final reaction volume with 10µL of 2X SYBR premix (Catalogue# 639676, Clontech, CA), 1.6µL of cDNA as template, 0.4µL of each 10µM forward and reverse primers, 0.4µL of 50X ROX reference dye and made up the rest of the volume with DEPC water. The reactions were setup in a 96 well plate and using the thermal cycle of 95°C for 10sec, then 40 Cycles of amplification at 95°C for 5 secs, 58°C - 64°C for 20sec during which the fluorescence emission from each well was collected through FAM/SYBR GREEN 1 filter. The dissociation curve was determined using the thermal cycle at 55°C for 30sec followed by heating at 0.1°C/sec to 95°C for 1min; while collecting fluorescence emission continuously. The data was collected from the quant studio 3 software and the gene expression levels were calculated using the dC_t method. The gene expression was normalized to the house keeping gene GmACTIN and to ensure reproducibility it was also normalized to GmCONS6, GmCONS7 or GmCONS15. The statistical significance of gene expression was

determined using Wilcoxon Mann Whitney test with ***-P<0.001, **- P<0.01, *-P<0.05 using R version 3.3.0. Primers used in this study is listed in Appendix C.

2.6.16. Metabolite quantification

To determine the quantity of IAA and Trp in root tissues like EN, MN and its corresponding control root segments were harvested from CYPi and vector control roots and stored in -80˚C. The levels of IAA and Trp were quantified following the method outlined in (Blakeslee and Murphy, 2016). To extract the metabolites, the samples were weighed and grounded to fine powder using liquid nitrogen. To the grounded sample, 1ml of 50mM sodium-phosphate buffer (pH7.0 and containing 1%DETC) was added immediately. 12.5ng of [$^2H_5$] Indole 3-acetic acid (d5-IAA, OlChemlm, ltd, Olomouc, Czech Republic, Part# 0311532), 25ng [$^2H_3$] tryptophan (d3- Trp, CDN isotopes, Qubec, Canada, part#D-7419) were added to each sample as internal standard. The samples were vortexed, extracted at 4˚C on a lab nutator and then centrifuged at 12000xG for 15min at 4 ˚C. The supernatant was collected and the pH was adjusted to 3 using 1N HCl. Further concentration and purification of samples were performed by passing the supernatant over an HLB column (conditioned using 1ml methanol) followed by 1ml of water and 0.5ml of 50mM sodium-phosphate buffer (pH 2.7). After loading the sample, HLB columns were washed with 2ml of 5% methanol and final extraction with 2ml of 80% methanol. The eluates were dried under nitrogen gas and reconstituted in 200µL methanol. This was filtered through 4mm 0.2µM PTFE filters (Phenomenex Inc, Torrance, CA, Part# AF0-3202-52). To analyze the metabolite levels the eluates were injected for LC-MS/MS analyses. The

quantity of IAA and Trp levels were measured from five technical replicates and the change in metabolite concentration between CYPi and vector control were determined statistically using Wilcoxon Mann whitney test using R version 3.3.0 with ***-$P<0.001$, **- $P<0.01$, *-$P<0.05$.

2.7. References

Abel, S. and Theologis, A. (2010) Odyssey of Auxin. *Cold Spring Harbor Perspectives in Biology*, 2.

Bak, S. and Feyereisen, R. (2001) The Involvement of Two P450 Enzymes, CYP83B1 and CYP83A1, in Auxin Homeostasis and Glucosinolate Biosynthesis. *Plant Physiology*, 127, 108-118.

Bak, S., Tax, F.E., Feldmann, K.A., Galbraith, D.W. and Feyereisen, R. (2001) CYP83B1, a cytochrome P450 at the metabolic branch point in auxin and indole glucosinolate biosynthesis in Arabidopsis. *Plant Cell*, 13, 101-111.

Barlier, I., Kowalczyk, M., Marchant, A., Ljung, K., Bhalerao, R., Bennett, M., Sandberg, G. and Bellini, C. (2000) The SUR2 gene of Arabidopsis thaliana encodes the cytochrome P450 CYP83B1, a modulator of auxin homeostasis. *Proc Natl Acad Sci U S A*, 97, 14819-14824.

Bialek, K., Michalczuk, L. and Cohen, J.D. (1992) Auxin Biosynthesis during Seed Germination in Phaseolus vulgaris. *Plant Physiology*, 100, 509-517.

Blakeslee, J.J. and Murphy, A.S. (2016) Microscopic and Biochemical Visualization of Auxins in Plant Tissues. *Methods in molecular biology (Clifton, N.J.)*, 1398, 37-53.

Böttcher, C., Keyzers, R.A., Boss, P.K. and Davies, C. (2010) Sequestration of auxin by the indole-3-acetic acid-amido synthetase GH3-1 in grape berry (Vitis vinifera L.) and the proposed role of auxin conjugation during ripening. *Journal of Experimental Botany*, 61, 3615-3625.

Brechenmacher, L., Lei, Z., Libault, M., Findley, S., Sugawara, M., Sadowsky, M.J., Sumner, L.W. and Stacey, G. (2010) Soybean Metabolites Regulated in Root Hairs in Response to the Symbiotic Bacterium Bradyrhizobium japonicum. *Plant Physiology*, 153, 1808-1822.

Calvert, H.E., Pence, M.K., Pierce, M., Malik, N.S.A. and Bauer, W.D. (1984) Anatomical analysis of the development and distribution of Rhizobium infections in soybean roots. *Canadian Journal of Botany*, 62, 2375-2384.

Chandler, J.W. (2009) Local auxin production: a small contribution to a big field. *BioEssays : news and reviews in molecular, cellular and developmental biology*, 31, 60-70.

Cheng, Y., Dai, X. and Zhao, Y. (2006) Auxin biosynthesis by the YUCCA flavin monooxygenases controls the formation of floral organs and vascular tissues in Arabidopsis. *Genes Dev*, 20, 1790-1799.

Collier, R., Fuchs, B., Walter, N., Kevin Lutke, W. and Taylor, C.G. (2005) Ex vitro composite plants: an inexpensive, rapid method for root biology. *The Plant Journal*, 43, 449-457.

Delarue, M., Prinsen, E., Onckelen, H.V., Caboche, M. and Bellini, C. (1998) Sur2 mutations of Arabidopsis thaliana define a new locus involved in the control of auxin homeostasis. *The Plant journal : for cell and molecular biology*, 14, 603-611.

Desbrosses, Guilhem J. and Stougaard, J. (2011) Root Nodulation: A Paradigm for How Plant-Microbe Symbiosis Influences Host Developmental Pathways. *Cell Host & Microbe*, 10, 348-358.

Eckardt, N.A. (2006) The Role of Flavonoids in Root Nodule Development and Auxin Transport in Medicago truncatula. *The Plant Cell*, 18, 1539-1540.

Enders, T.A. and Strader, L.C. (2015) Auxin activity: Past, present, and future. *American journal of botany*, 102, 180-196.

F Sanchez, J E Padilla, H Perez, a. and Lara, M. (1991) Control of Nodulin Genes in Root-Nodule Development and Metabolism. *Annual review of plant physiology and plant molecular biology*, 42, 507-528.

Ferguson, B.J., Indrasumunar, A., Hayashi, S., Lin, M.H., Lin, Y.H., Reid, D.E. and Gresshoff, P.M. (2010) Molecular analysis of legume nodule development and autoregulation. *Journal of integrative plant biology*, 52, 61-76.

Ferguson, B.J. and Mathesius, U. (2014) Phytohormone regulation of legume-rhizobia interactions. *Journal of chemical ecology*, 40, 770-790.

Geurts, R. and Bisseling, T. (2002) Rhizobium Nod Factor Perception and Signalling. *The Plant Cell*, 14, s239-s249.

Guo, J., Wei, J., Xu, J. and Sun, M.-X. (2014) Inducible knock-down of GNOM during root formation reveals tissue-specific response to auxin transport and its modulation of local auxin biosynthesis. *Journal of Experimental Botany*.

Gutierrez, L., Mongelard, G., Floková, K., Păcurar, D.I., Novák, O., Staswick, P., Kowalczyk, M., Păcurar, M., Demailly, H., Geiss, G. and Bellini, C. (2012) Auxin Controls Arabidopsis Adventitious Root Initiation by Regulating Jasmonic Acid Homeostasis. *The Plant Cell*, 24, 2515-2527.

Hagen, G., Kleinschmidt, A. and Guilfoyle, T. (1984) Auxin-regulated gene expression in intact soybean hypocotyl and excised hypocotyl sections. *Planta*, 162, 147-153.

Harper, J.E. (1974) Soil and Symbiotic Nitrogen Requirements for Optimum Soybean Production1. *Crop Science*, 14, 255-260.

Hirsch, A.M. (1992) Developmental biology of legume nodulation. *New Phytologist*, 122, 211-237.

Hirsch, A.M., Bhuvaneswari, T.V., Torrey, J.G. and Bisseling, T. (1989) Early nodulin genes are induced in alfalfa root outgrowths elicited by auxin transport inhibitors. *Proc Natl Acad Sci U S A*, 86, 1244-1248.

Huo, X., Schnabel, E., Hughes, K. and Frugoli, J. (2006) RNAi Phenotypes and the Localization of a Protein::GUS Fusion Imply a Role for Medicago truncatula PIN Genes in Nodulation. *Journal of Plant Growth Regulation*, 25, 156-165.

Jackson, R.G., Lim, E.K., Li, Y., Kowalczyk, M., Sandberg, G., Hoggett, J., Ashford, D.A. and Bowles, D.J. (2001) Identification and biochemical characterization of an Arabidopsis indole-3-acetic acid glucosyltransferase. *J Biol Chem*, 276, 4350-4356.

Johnson, C.F. and Morris, D.A. (1987) Regulation of auxin transport in pea (Pisum sativum L.) by phenylacetic acid: effects on the components of transmembrane transport of indol-3yl-acetic acid. *Planta*, 172, 400-407.

Khan, S. and Stone, J.M. (2007) Arabidopsis thaliana GH3.9 influences primary root growth. *Planta*, 226, 21-34.

Kim, J.I., Dolan, W.L., Anderson, N.A. and Chapple, C. (2015) Indole Glucosinolate Biosynthesis Limits Phenylpropanoid Accumulation in Arabidopsis thaliana. *Plant Cell*.

Kim, J.I., Sharkhuu, A., Jin, J.B., Li, P., Jeong, J.C., Baek, D., Lee, S.Y., Blakeslee, J.J., Murphy, A.S., Bohnert, H.J., Hasegawa, P.M., Yun, D.J. and Bressan, R.A. (2007) yucca6, a dominant mutation in Arabidopsis, affects auxin accumulation and auxin-related phenotypes. *Plant Physiol*, 145, 722-735.

Korasick, D.A., Enders, T.A. and Strader, L.C. (2013) Auxin biosynthesis and storage forms. *Journal of Experimental Botany*, 64, 2541-2555.

Kramer, E.M. and Ackelsberg, E.M. (2015) Auxin metabolism rates and implications for plant development. *Frontiers in Plant Science*, 6, 150.

Larrainzar, E., Riely, B.K., Kim, S.C., Carrasquilla-Garcia, N., Yu, H.-J., Hwang, H.-J., Oh, M., Kim, G.B., Surendrarao, A.K., Chasman, D., Siahpirani, A.F., Penmetsa, R.V., Lee, G.-S., Kim, N., Roy, S., Mun, J.-H. and Cook, D.R. (2015) Deep Sequencing of the Medicago truncatula Root Transcriptome Reveals a Massive and Early Interaction between Nodulation Factor and Ethylene Signals. *Plant Physiology*, 169, 233-265.

LeClere, S., Tellez, R., Rampey, R.A., Matsuda, S.P. and Bartel, B. (2002) Characterization of a family of IAA-amino acid conjugate hydrolases from Arabidopsis. *J Biol Chem*, 277, 20446-20452.

Libault, M., Farmer, A., Joshi, T., Takahashi, K., Langley, R.J., Franklin, L.D., He, J., Xu, D., May, G. and Stacey, G. (2010) An integrated transcriptome atlas of the crop model Glycine max, and its use in comparative analyses in plants. *The Plant journal : for cell and molecular biology*, 63, 86-99.

Liu, Z.B., Ulmasov, T., Shi, X., Hagen, G. and Guilfoyle, T.J. (1994) Soybean GH3 promoter contains multiple auxin-inducible elements. *The Plant Cell*, 6, 645-657.

Ljung, K. (2013a) Auxin metabolism and homeostasis during plant development. *Development*, 140, 943-950.

Ljung, K. (2013b) Auxin metabolism and homeostasis during plant development. *Development (Cambridge, England)*, 140, 943-950.

Ljung, K., Hull, A.K., Celenza, J., Yamada, M., Estelle, M., Normanly, J. and Sandberg, G. (2005) Sites and regulation of auxin biosynthesis in Arabidopsis roots. *Plant Cell*, 17, 1090-1104.

Ljung, K., Hull, A.K., Kowalczyk, M., Marchant, A., Celenza, J., Cohen, J.D. and Sandberg, G. (2002) Biosynthesis, conjugation, catabolism and homeostasis of indole-3-acetic acid in Arabidopsis thaliana. *Plant Mol Biol*, 50, 309-332.

Ludwig-Muller, J. (2011) Auxin conjugates: their role for plant development and in the evolution of land plants. *J Exp Bot*, 62, 1757-1773.

Ludwig-Müller, J. (2011) Auxin conjugates: their role for plant development and in the evolution of land plants. *Journal of Experimental Botany*, 62, 1757-1773.

Maharjan, P.M., Dilkes, B.P., Fujioka, S., Pencik, A., Ljung, K., Burow, M., Halkier, B.A. and Choe, S. (2014) Arabidopsis gulliver1/SUPERROOT2-7 identifies a metabolic basis for auxin and brassinosteroid synergy. *The Plant journal : for cell and molecular biology*, 80, 797-808.

Mallory, A.C., Bartel, D.P. and Bartel, B. (2005) MicroRNA-Directed Regulation of Arabidopsis AUXIN RESPONSE FACTOR17 Is Essential for Proper Development and Modulates Expression of Early Auxin Response Genes. *The Plant Cell*, 17, 1360-1375.

Marhavy, P., Vanstraelen, M., De Rybel, B., Zhaojun, D., Bennett, M.J., Beeckman, T. and Benkova, E. (2013) Auxin reflux between the endodermis and pericycle promotes lateral root initiation. *Embo j*, 32, 149-158.

Mathesius, U. (2008) Goldacre paper: Auxin: at the root of nodule development? *Functional Plant Biology*, 35, 651-668.

Mathesius, U., Schlaman, H.R., Spaink, H.P., Of Sautter, C., Rolfe, B.G. and Djordjevic, M.A. (1998) Auxin transport inhibition precedes root nodule formation in white clover roots and is regulated by flavonoids and derivatives of chitin oligosaccharides. *The Plant journal : for cell and molecular biology*, 14, 23-34.

McKhann, H.I., Paiva, N.L., Dixon, R.A. and Hirsch, A.M. (1998) Expression of Genes for Enzymes of the Flavonoid Biosynthetic Pathway in the Early Stages of the Rhizobium-Legume Symbiosis. In *Flavonoids in the Living System* (Manthey, J.A. and Buslig, B.S. eds). Boston, MA: Springer US, pp. 45-54.

Morant, M., Ekstrom, C., Ulvskov, P., Kristensen, C., Rudemo, M., Olsen, C.E., Hansen, J., Jorgensen, K., Jorgensen, B., Moller, B.L. and Bak, S. (2010) Metabolomic, transcriptional, hormonal, and signaling cross-talk in superroot2. *Molecular plant*, 3, 192-211.

Mus, F., Crook, M.B., Garcia, K., Garcia Costas, A., Geddes, B.A., Kouri, E.D., Paramasivan, P., Ryu, M.H., Oldroyd, G.E., Poole, P.S., Udvardi, M.K., Voigt, C.A., Ane, J.M. and Peters, J.W. (2016) Symbiotic Nitrogen Fixation and the Challenges to Its Extension to Nonlegumes. *Applied and environmental microbiology*, 82, 3698-3710.

Mutava, R.N., Prince, S.J., Syed, N.H., Song, L., Valliyodan, B., Chen, W. and Nguyen, H.T. (2015) Understanding abiotic stress tolerance mechanisms in soybean:

a comparative evaluation of soybean response to drought and flooding stress. *Plant physiology and biochemistry : PPB*, 86, 109-120.

Nakazawa, M., Yabe, N., Ichikawa, T., Yamamoto, Y.Y., Yoshizumi, T., Hasunuma, K. and Matsui, M. (2001) DFL1, an auxin-responsive GH3 gene homologue, negatively regulates shoot cell elongation and lateral root formation, and positively regulates the light response of hypocotyl length. *The Plant journal : for cell and molecular biology*, 25, 213-221.

Naur, P., Petersen, B.L., Mikkelsen, M.D., Bak, S., Rasmussen, H., Olsen, C.E. and Halkier, B.A. (2003) CYP83A1 and CYP83B1, two nonredundant cytochrome P450 enzymes metabolizing oximes in the biosynthesis of glucosinolates in Arabidopsis. *Plant Physiol*, 133, 63-72.

Newcomb, W., Sippell, D. and Peterson, R.L. (1979) The early morphogenesis of Glycine max and Pisum sativum root nodules. *Canadian Journal of Botany*, 57, 2603-2616.

Nishimura, T., Hayashi, K., Suzuki, H., Gyohda, A., Takaoka, C., Sakaguchi, Y., Matsumoto, S., Kasahara, H., Sakai, T., Kato, J., Kamiya, Y. and Koshiba, T. (2014) Yucasin is a potent inhibitor of YUCCA, a key enzyme in auxin biosynthesis. *The Plant journal : for cell and molecular biology*, 77, 352-366.

Nizampatnam, N.R., Schreier, S.J., Damodaran, S., Adhikari, S. and Subramanian, S. (2015) microRNA160 dictates stage-specific auxin and cytokinin sensitivities and

directs soybean nodule development. *The Plant journal : for cell and* molecular *biology*, 84, 140-153.

Overvoorde, P., Fukaki, H. and Beeckman, T. (2010a) Auxin Control of Root Development. *Cold Spring Harbor Perspectives in Biology*, 2, a001537.

Overvoorde, P., Fukaki, H. and Beeckman, T. (2010b) Auxin Control of Root Development. *Cold Spring Harbor Perspectives in Biology*, 2.

Pacios-Bras, C., Schlaman, H.R.M., Boot, K., Admiraal, P., Mateos Langerak, J., Stougaard, J. and Spaink, H.P. (2003) Auxin distribution in Lotus japonicus during root nodule development. *Plant Mol Biol*, 52, 1169-1180.

Park, J.E., Park, J.Y., Kim, Y.S., Staswick, P.E., Jeon, J., Yun, J., Kim, S.Y., Kim, J., Lee, Y.H. and Park, C.M. (2007) GH3-mediated auxin homeostasis links growth regulation with stress adaptation response in Arabidopsis. *J Biol Chem*, 282, 10036-10046.

Peat, T.S., Bottcher, C., Newman, J., Lucent, D., Cowieson, N. and Davies, C. (2012) Crystal structure of an indole-3-acetic acid amido synthetase from grapevine involved in auxin homeostasis. *Plant Cell*, 24, 4525-4538.

Peer, W.A. and Murphy, A.S. (2007) Flavonoids and auxin transport: modulators or regulators? *Trends in plant science*, 12, 556-563.

Peoples, M.B., Brockwell, J., Herridge, D.F., Rochester, I.J., Alves, B.J.R., Urquiaga, S., Boddey, R.M., Dakora, F.D., Bhattarai, S., Maskey, S.L., Sampet, C.,

Rerkasem, B., Khan, D.F., Hauggaard-Nielsen, H. and Jensen, E.S. (2009) The contributions of nitrogen-fixing crop legumes to the productivity of agricultural systems. *Symbiosis*, 48, 1-17.

Quittenden, L.J., Davies, N.W., Smith, J.A., Molesworth, P.P., Tivendale, N.D. and Ross, J.J. (2009) Auxin Biosynthesis in Pea: Characterization of the Tryptamine Pathway. *Plant Physiology*, 151, 1130-1138.

Rampey, R.A., LeClere, S., Kowalczyk, M., Ljung, K., Sandberg, G. and Bartel, B. (2004) A family of auxin-conjugate hydrolases that contributes to free indole-3-acetic acid levels during Arabidopsis germination. *Plant Physiol*, 135, 978-988.

Santi, C., Bogusz, D. and Franche, C. (2013) Biological nitrogen fixation in non-legume plants. *Annals of botany*, 111, 743-767.

Schultze, M. and Kondorosi, A. (1998) Regulation of symbiotic root nodule development. *Annual review of genetics*, 32, 33-57.

Simon, S. and Petrasek, J. (2011) Why plants need more than one type of auxin. *Plant science : an international journal of experimental plant biology*, 180, 454-460.

Staswick, P.E. (2009) The Tryptophan Conjugates of Jasmonic and Indole-3-Acetic Acids Are Endogenous Auxin Inhibitors. *Plant Physiology*, 150, 1310-1321.

Staswick, P.E., Serban, B., Rowe, M., Tiryaki, I., Maldonado, M.T., Maldonado, M.C. and Suza, W. (2005) Characterization of an Arabidopsis Enzyme Family That Conjugates Amino Acids to Indole-3-Acetic Acid. *The Plant Cell*, 17, 616-627.

Stepanova, A.N., Robertson-Hoyt, J., Yun, J., Benavente, L.M., Xie, D.Y., Dolezal, K., Schlereth, A., Jurgens, G. and Alonso, J.M. (2008) TAA1-mediated auxin biosynthesis is essential for hormone crosstalk and plant development. *Cell*, 133, 177-191.

Subramanian, S., Stacey, G. and Yu, O. (2006) Endogenous isoflavones are essential for the establishment of symbiosis between soybean and Bradyrhizobium japonicum. *The Plant journal : for cell and molecular biology*, 48, 261-273.

Suzaki, T., Ito, M. and Kawaguchi, M. (2013) Genetic basis of cytokinin and auxin functions during root nodule development. *Frontiers in plant science*, 4, 42.

Suzaki, T., Yano, K., Ito, M., Umehara, Y., Suganuma, N. and Kawaguchi, M. (2012) Positive and negative regulation of cortical cell division during root nodule development in Lotus japonicus is accompanied by auxin response. *Development*, 139, 3997-4006.

Takanashi, K., Sugiyama, A. and Yazaki, K. (2011) Involvement of auxin distribution in root nodule development of Lotus japonicus. *Planta*, 234, 73-81.

Takase, T., Nakazawa, M., Ishikawa, A., Kawashima, M., Ichikawa, T., Takahashi, N., Shimada, H., Manabe, K. and Matsui, M. (2004) ydk1-D, an auxin-responsive GH3 mutant that is involved in hypocotyl and root elongation. *The Plant journal : for cell and molecular biology*, 37, 471-483.

Tao, Y., Ferrer, J.L., Ljung, K., Pojer, F., Hong, F., Long, J.A., Li, L., Moreno, J.E., Bowman, M.E., Ivans, L.J., Cheng, Y., Lim, J., Zhao, Y., Ballare, C.L., Sandberg,

G., Noel, J.P. and Chory, J. (2008) Rapid synthesis of auxin via a new tryptophan-dependent pathway is required for shade avoidance in plants. *Cell*, 133, 164-176.

Tobena-Santamaria, R., Bliek, M., Ljung, K., Sandberg, G., Mol, J.N., Souer, E. and Koes, R. (2002) FLOOZY of petunia is a flavin mono-oxygenase-like protein required for the specification of leaf and flower architecture. *Genes & development*, 16, 753-763.

Trapnell, C., Roberts, A., Goff, L., Pertea, G., Kim, D., Kelley, D.R., Pimentel, H., Salzberg, S.L., Rinn, J.L. and Pachter, L. (2012) Differential gene and transcript expression analysis of RNA-seq experiments with TopHat and Cufflinks. *Nat. Protocols*, 7, 562-578.

Turner, M., Adhikari, S. and Subramanian, S. (2013a) Optimizing stem-loop qPCR assays through multiplexed cDNA synthesis of U6 and miRNAs. *Plant signaling & behavior*, 8.

Turner, M., Nizampatnam, N.R., Baron, M., Coppin, S., Damodaran, S., Adhikari, S., Arunachalam, S.P., Yu, O. and Subramanian, S. (2013b) Ectopic expression of miR160 results in auxin hypersensitivity, cytokinin hyposensitivity, and inhibition of symbiotic nodule development in soybean. *Plant Physiol*, 162, 2042-2055.

Udvardi, M.K. and Day, D.A. (1997) METABOLITE TRANSPORT ACROSS SYMBIOTIC MEMBRANES OF LEGUME NODULES. *Annual review of plant physiology and plant molecular biology*, 48, 493-523.

van de Wiel, C., Scheres, B., Franssen, H., van Lierop, M.J., van Lammeren, A., van Kammen, A. and Bisseling, T. (1990) The early nodulin transcript ENOD2 is located in the nodule parenchyma (inner cortex) of pea and soybean root nodules. *Embo j*, 9, 1-7.

Wasson, A.P., Pellerone, F.I. and Mathesius, U. (2006) Silencing the flavonoid pathway in Medicago truncatula inhibits root nodule formation and prevents auxin transport regulation by rhizobia. *Plant Cell*, 18, 1617-1629.

Westfall, C.S., Herrmann, J., Chen, Q., Wang, S. and Jez, J.M. (2010) Modulating plant hormones by enzyme action: the GH3 family of acyl acid amido synthetases. *Plant signaling & behavior*, 5, 1607-1612.

Westfall, C.S., Sherp, A.M., Zubieta, C., Alvarez, S., Schraft, E., Marcellin, R., Ramirez, L. and Jez, J.M. (2016) Arabidopsis thaliana GH3.5 acyl acid amido synthetase mediates metabolic crosstalk in auxin and salicylic acid homeostasis. *Proceedings of the National Academy of Sciences*, 113, 13917-13922.

Westfall, C.S., Zubieta, C., Herrmann, J., Kapp, U., Nanao, M.H. and Jez, J.M. (2012) Structural basis for prereceptor modulation of plant hormones by GH3 proteins. *Science (New York, N.Y.)*, 336, 1708-1711.

Woodward, A.W. and Bartel, B. (2005) Auxin: regulation, action, and interaction. *Annals of botany*, 95, 707-735.

Yang, W.C., Katinakis, P., Hendriks, P., Smolders, A., de Vries, F., Spee, J., van Kammen, A., Bisseling, T. and Franssen, H. (1993) Characterization of

GmENOD40, a gene showing novel patterns of cell-specific expression during soybean nodule development. *The Plant journal : for cell and molecular biology*, 3, 573-585.

Yang, Y., Yue, R., Sun, T., Zhang, L., Chen, W., Zeng, H., Wang, H. and Shen, C. (2015) Genome-wide identification, expression analysis of GH3 family genes in Medicago truncatula under stress-related hormones and Sinorhizobium meliloti infection. *Applied microbiology and biotechnology*, 99, 841-854.

Zhang, J., Lin, J.E., Harris, C., Campos Mastrotti Pereira, F., Wu, F., Blakeslee, J.J. and Peer, W.A. (2016) DAO1 catalyzes temporal and tissue-specific oxidative inactivation of auxin in Arabidopsis thaliana. *Proceedings of the National Academy of Sciences*, 113, 11010-11015.

Zhang, S.-W., Li, C.-H., Cao, J., Zhang, Y.-C., Zhang, S.-Q., Xia, Y.-F., Sun, D.-Y. and Sun, Y. (2009) Altered Architecture and Enhanced Drought Tolerance in Rice via the Down-Regulation of Indole-3-Acetic Acid by TLD1/OsGH3.13 Activation. *Plant Physiology*, 151, 1889-1901.

Zhao, Y. (2010) Auxin biosynthesis and its role in plant development. *Annual review of plant biology*, 61, 49-64.

Zhao, Y. (2012a) Auxin biosynthesis: a simple two-step pathway converts tryptophan to indole-3-acetic acid in plants. *Molecular plant*, 5, 334-338.

Zhao, Y. (2012b) Auxin Biosynthesis: A Simple Two-Step Pathway Converts Tryptophan to Indole-3-Acetic Acid in Plants. *Molecular plant*, 5, 334-338.

Zhao, Y. (2014) Auxin Biosynthesis. *The Arabidopsis Book*, e0173.

Zhao, Y., Christensen, S.K., Fankhauser, C., Cashman, J.R., Cohen, J.D., Weigel, D. and Chory, J. (2001) A role for flavin monooxygenase-like enzymes in auxin biosynthesis. *Science (New York, N.Y.)*, 291, 306-309.

2.8. Supplementary information

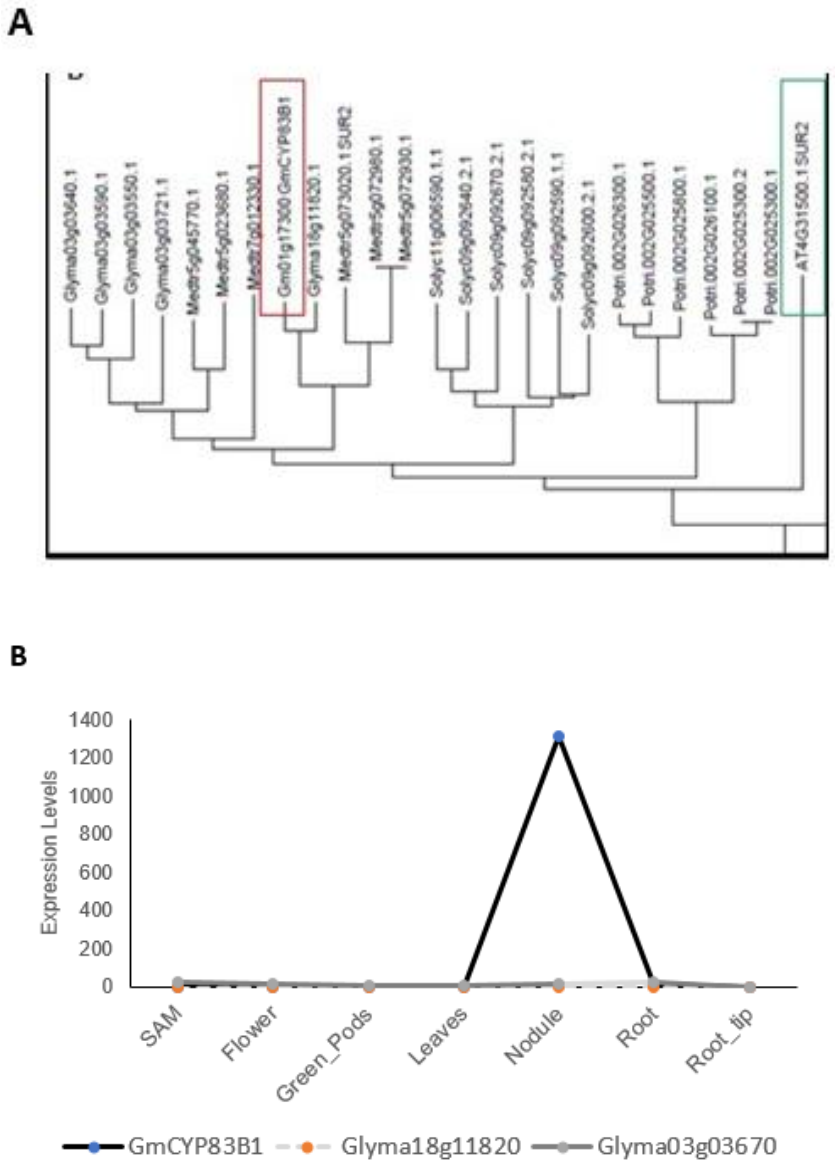

Figure S2-1 . **Nodule enriched GmCYP83B1 is a close ortholog of AtCYP83B1**.

A) Part of the phylogenetic tree of cytochrome P450 oxidase peptide sequence from multiple species showing the close homology of GmCYP83B1/Glyma01g17330 and AtCYP83B1/AtSUR2 highlighted in red and green box respectively.

B) Gene expression data of GmCYP83B1 and its close homologs. Nodule enriched expression of GmCYP83B1(Glyma 01g17330) and its two close homologs in soybean genome atlas (Libault et al., 2010).

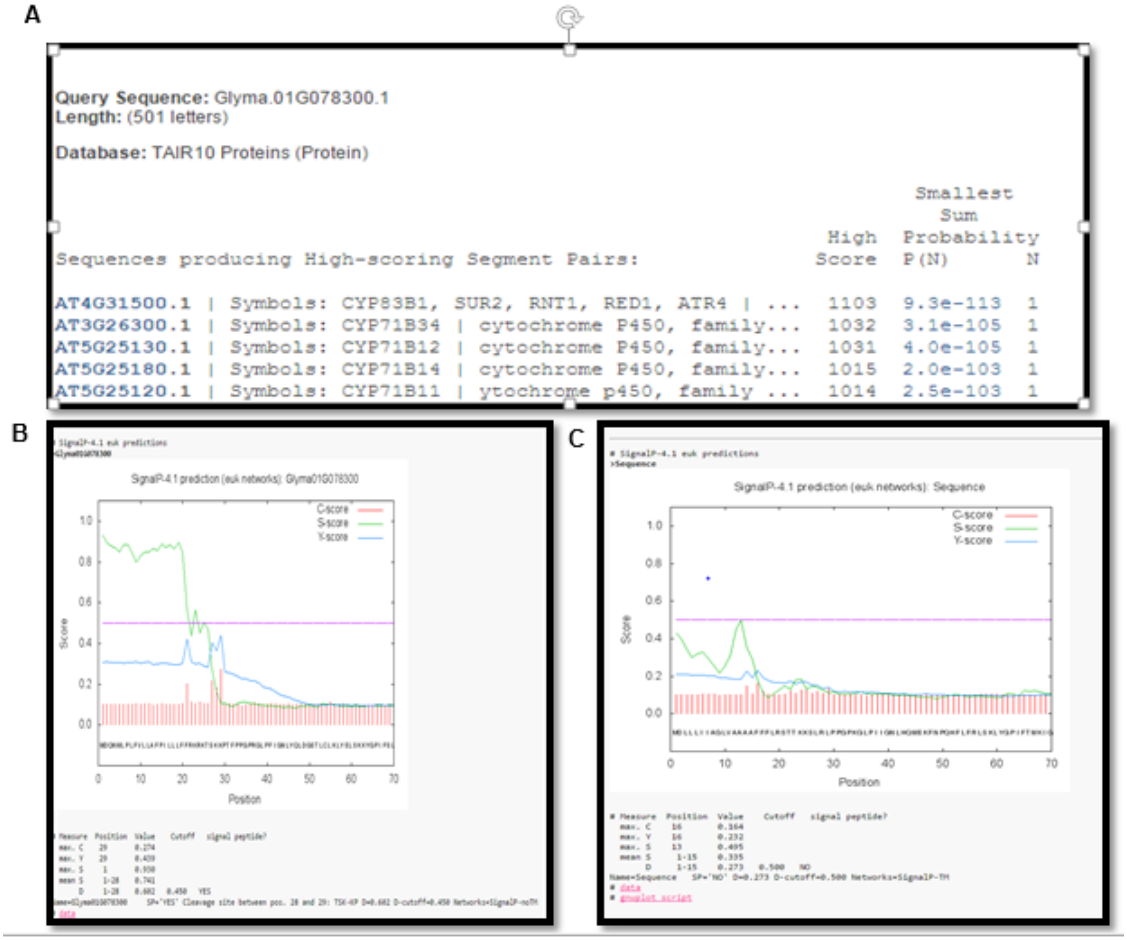

Figure S2-2: **GmCYP83B1 peptides sequence analysis.**

A) BLAST search of soybean CYP83B1 peptide sequence in Arabidopsis sequence database showing AtSUR2 as top hit. B) Membrane localization signal of GmCYP83B1 peptide sequence detected using signalP. C) Absence of membrane localization signal in arabidopsis CYP83B1 peptide sequence analyzed using signalP tool.

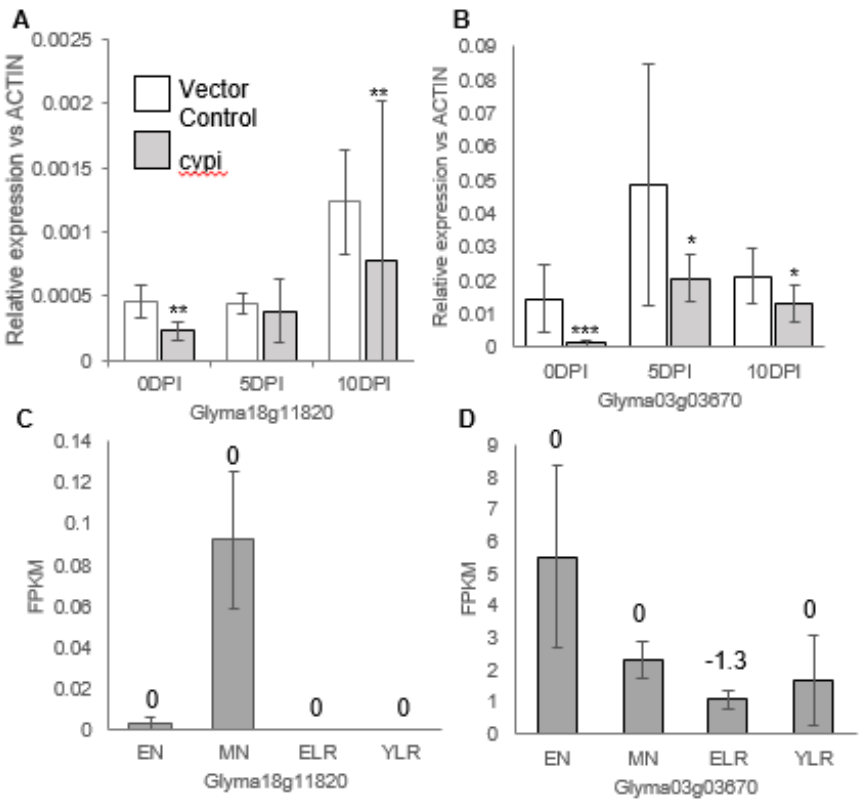

Figure S2-3: **Non-target expression levels in GmCYP83B1-RNAi.**

Fig A & B shows the expression of close homologs of GmCYP83B1, namely Glyma18g11820 & Glyma03g03670 in GmCYP83B1-RNAi roots time course of 0, 5 and 10dpi. The data shown in A and B are average of expression levels in three biological replicates and error bars indicate the range of possible expression values based on SD. * - P<0.05, ** -P<0.01, *** -P<0.001 Statistical significance based on Wilcoxon Mann whitney test. Fig C & D Expression levels of non-targets of GmCYP83B1 in EN, MN, ELR, YLR presented as average FPKM across three biological replicates. Statistically significant fold change vs. respective control root segments are indicated above the bars and error bars indicate SD.

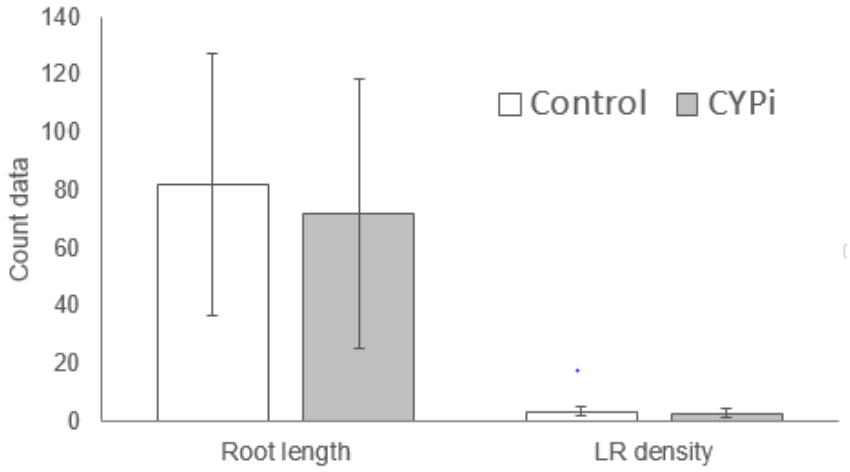

Figure S2-4: **Root length and lateral root density measurement in CYPi compared to vector control.**

The data represents average and error bars indicate SEM, n=30 independent transgenic root each.

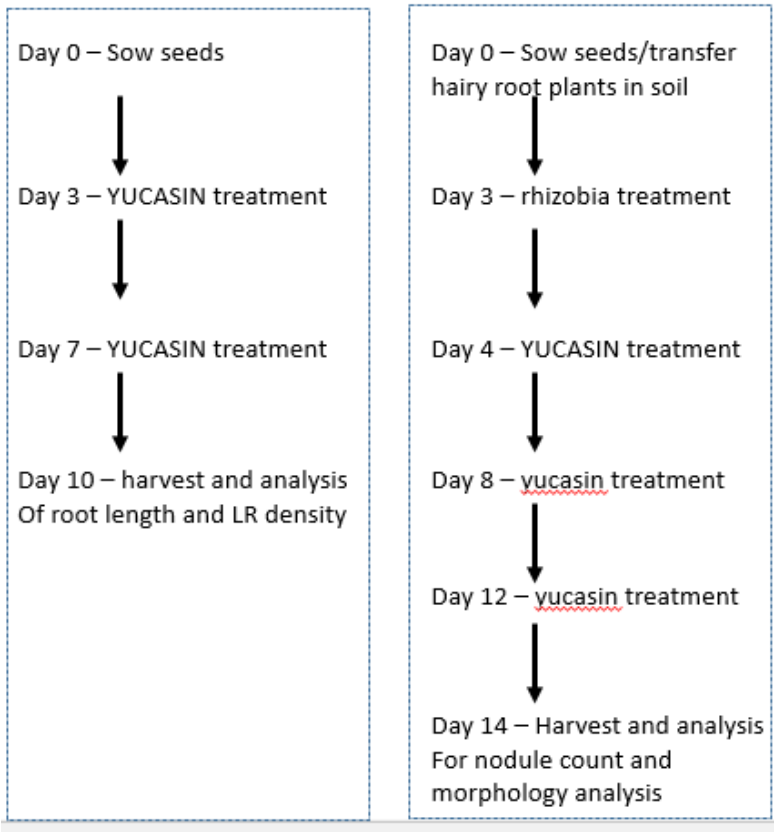

Figure S2-5: **A flow Chart depicting the treatment plan for yucasin on WT and composite hairy root system.**

The left panel shows treatment plan for root length and LR density measurement and right panel shows treatment plan for rhizobia inoculation and nodulation assay.

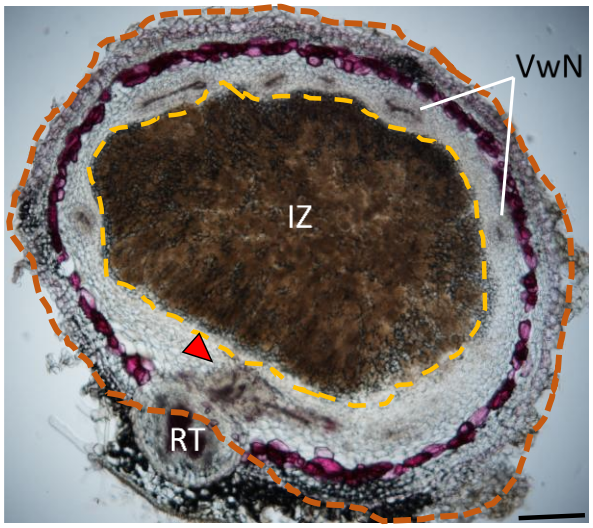

Figure S2-6: **Mature nodule transverse section stained with phloroglucinol.**

The vasculature branches at root- nodule junction (red arrow head) and within nodule (VwN) is shown. The area of infection zone and area of nodule are highlighted by green and yellow borders respectively. RT- root, IZ- infection zone and VwN – vasculature within nodule.

Chapter 3

3. NODULE-ENRICHED GRETCHEN *HAGEN 3* ENZYMES HAVE DISTINCT SUBSTRATE SPECIFICITIES AND ARE IMPORTANT FOR PROPER SOYBEAN NODULE DEVELOPMENT

3.1. Abstract

Legume root nodules develop as a result of symbiotic relationship between the plant and nitrogen-fixing rhizobia bacteria in soil. Auxin activity is detected in different cell types at different stages of nodule development; and enhanced sensitivity to auxin inhibits nodule development. While some transport and signaling mechanisms that achieve precise spatiotemporal auxin output are known, the role of auxin metabolism during nodule development is unclear. Using a soybean root lateral organ transcriptome data set, we identified distinct nodule enrichment of three auxin-deactivating *Gretchen Hagen 3* (GH3) indole-3-acetic acid (IAA) amido transferase genes: *GmGH3-11/12*, *GmGH3-14* and *GmGH3-15*. In vitro enzymatic assays showed that each of these GH3 proteins preferred IAA and aspartate as acyl and amino acid substrates, respectively. *GmGH3-15* showed a broad substrate preference, especially with different forms of auxin. Promoter:GUS expression analysis indicated that *GmGH3-14* acts primarily in the root epidermis and the nodule primordium where as *GmGH3-15* might act in the vasculature. Silencing the expression of these GH3 genes in soybean composite plants led to altered nodule numbers, maturity, and size. Our results indicate that these GH3s are needed for proper nodule maturation in soybean, but the precise mechanism by which they regulate nodule development remains to be explained.

3.2. Introduction

Spatiotemporal auxin output is a combination of tightly regulated biosynthesis, catabolism, inactivation, activation, transport, and signaling (Westfall *et al.*, 2010, Ljung, 2013a). The major form of auxin in plants, indole-3-acetic acid (IAA), is primarily synthesized via the two-step Indole pyruvic acid (IPA) pathway (Zhao, 2012b). In this pathway, tryptophan is converted to IPA by *TRYPTOPHAN AMINO TRANSFERASE OF ARABIDOPSIS (*TAA*)* and IPA is metabolized to IAA by YUCCA flavin monoxygenases (Zhao *et al.*, 2001, Stepanova *et al.*, 2008). It was recently revealed that 2-oxoindole-3-acetic acid (oxIAA) is the major catabolite of IAA in Arabidopsis and rice (Peer *et al.*, 2013, Pencik *et al.*, 2013). A dioxygenase enzyme that catabolizes IAA to oxIAA has also been identified (Pencik *et al.*, 2013, Zhao *et al.*, 2013, Porco *et al.*, 2016, Zhang *et al.*, 2016b). Different biologically inactive forms of IAA including amide-linked peptide conjugates, amide-linked amino acid conjugates, and ester-linked sugar (carbohydrate) conjugates have been identified in plant tissues (Woodward and Bartel, 2005a, Ludwig-Muller, 2011, Korasick *et al.*, 2013). Conjugation of different amino acids leads to different downstream fates for IAA. For example, IAA-alanine and IAA-leucine conjugates can be hydrolyzed to release free IAA in specific cell types for proper embryo development in Arabidopsis (LeClere *et al.*, 2002, Rampey *et al.*, 2004). IAA conjugates of aspartate (IAA-Asp) and glutamate appear to be catabolic forms that typically cannot be hydrolyzed back to IAA (Westfall *et al.*, 2010). The fate of conjugated forms of IAA varies from species to species (Westfall *et al.*, 2010).

Therefore, conjugation of IAA is a key regulatory step that dictates the levels of free (active) IAA pools and thus spatiotemporal auxin output during plant development. Members of the GRETCHEN HAGEN3 (GH3) family of acyl amido transferase enzymes can conjugate IAA to amino acids (Westfall *et al.*, 2010). The first GH3 gene was identified in soybean through a screen for auxin responsive gene expression (Hagen and Guilfoyle, 1985). Subsequently, GH3 family members were identified in other plant species including Arabidopsis, and found to play critical roles in plant development through the conjugation of various plant hormones [2]. For example, a change in local auxin pool is achieved at the site of organ development or in response to biotic/abiotic interaction through conjugation of IAA by GH3 proteins (Park *et al.*, 2007b, Zhang *et al.*, 2009, Böttcher *et al.*, 2010, Zheng *et al.*, 2016). A gain of function mutation in an Arabidopsis GH3 gene, *wes1-D* conferred resistance against multiple factors and a loss of function mutation in the same gene led to reduced resistance (Park *et al.*, 2007a). A gain-of-function mutation in another Arabidopsis GH3 gene, *ydk1-D* led to reduced root length and lateral root density because of altered auxin activity (Takase *et al.*, 2004). An activation-tagged Arabidopsis line with increased expression of GH3.9 exhibited increased sensitivity to IAA, resulting in reduced root growth (Khan and Stone, 2007). Recently, the X-ray crystal structures of IAA- and jasmonate-conjugating GH3 proteins were determined. This has revealed key features of substrate recognition and to the re-classification of the GH3 enzyme family into different groups based on the preference of the acyl acid substrate (Peat *et al.*, 2012, Westfall *et al.*, 2012). Group II GH3 proteins catalyze IAA-amino acid

conjugation and alter the free IAA pool to regulate various plant developmental programs in Arabidopsis and other plant species (Staswick *et al.*, 2005b). Symbiotic nodule development in legumes such as soybean is also influenced by auxin. Nodule development results from a symbiotic relationship between the plant and nitrogen-fixing rhizobia bacteria. Rhizobia colonize plant root hairs, and after initial signal exchange to ensure host-symbiont compatibility, plant developmental pathways are activated to enable nodule organogenesis in the root cortex. Auxin signaling has been implicated in both root hair as well as cortical responses during nodule development (Turner *et al.*, 2013b, Breakspear *et al.*, 2014a, Nizampatnam *et al.*, 2015, Wang *et al.*, 2015, Cai *et al.*, 2017, Hobecker *et al.*, 2017); however, distinct mechanisms might contribute to overall auxin output in these cell types. The distribution and levels of auxin in the root cortex may be distinct in different legumes (reviewed by (Kohlen *et al.*, 2017)). There are two major classes of legume nodules (reviewed by (Hirsch, 1992, Sprent and James, 2007)). Indeterminate nodules characterized by the presence of a persistent meristem with an oblong mature nodule are produced by *Medicago truncatula* (barrelclover), *Pisum sativum* (peas), and *Trifolium repens* (white clover). Determinate nodules that lack a persistent meristem with a spherical mature nodule are produced by *Lotus japonicus, Glycine max* (soybean), and *Phaseolus vulgaris* (common bean). Altered auxin signaling is reported to affect root hair responses to rhizobium inoculation in soybean and *M. truncatula* (Breakspear *et al.*, 2014a, Cai *et al.*, 2017). A local auxin maximum occurs in the root cortex at the site of initiation of both determinate and indeterminate nodules. Evidence for this comes primarily from auxin-responsive marker gene

expression, and at least one study where auxin levels were measured at the site of nodule initiation (Mathesius *et al.*, 1998, Pacios-Bras *et al.*, 2003, Takanashi *et al.*, 2011, Suzaki *et al.*, 2012a). The type of mechanism involved and the degree of auxin accumulation or output required appear to differ between these two types of nodules (Kohlen *et al.*, 2017). Inhibition of rootward auxin transport at the site of nodule initiation by flavonoids is crucial for indeterminate nodule formation (Wasson *et al.*, 2006, Zhang *et al.*, 2009). Expression patterns of genes encoding PIN auxin efflux transporters, and phenotypes of PIN-RNAi plants in *M. truncatula* also indicate a key role for the auxin transport machinery during indeterminate nodule development (Huo *et al.*, 2006, Sanko-Sawczenko *et al.*, 2016). On the other hand, inhibition of auxin transport does not appear to be crucial for determinate nodule formation (Pacios-Bras *et al.*, 2003, Subramanian *et al.*, 2006). While an auxin maximum appears to be crucial for nodule initiation, enhanced sensitivity to auxin inhibits both determinate and indeterminate nodule formation (Turner *et al.*, 2013b, Breakspear *et al.*, 2014a, Nizampatnam *et al.*, 2015, Wang *et al.*, 2015, Hobecker *et al.*, 2017).

Determinate and indeterminate nodules also display similarities and differences in the overall distribution of auxin activity during nodule development. As mentioned above, local auxin activity indicated by marker gene expression occurs in the nodule initials and nodule primordia of determinate nodules (soybean and *L. japonicus),* as well as indeterminate nodules (white clover and *M. truncatula*) (Mathesius *et al.*, 1998, Wasson *et al.*, 2006, Takanashi *et al.*, 2011, Turner *et al.*, 2013b). Auxin responsive gene expression is significantly diminished/absent in the infection zone of determinate nodules; however, the nodule meristem and invasion zone of

indeterminate nodules continue to display auxin response gene expression. In mature nodules, auxin activity is detectable in the vasculatures of both determinate and indeterminate nodules (e.g., (Mathesius *et al.*, 1998, Turner *et al.*, 2013b)). Therefore, precise regulation of auxin activity appears to occur during nodule development. While auxin transport appears to dictate auxin distribution during initiation of indeterminate nodules, it is unclear what mechanisms contribute to it during determinate nodule initiation. Multiple microRNA-regulated AUXIN RESPONSE FACTORs (ARFs) that might act in concert to dictate precise spatiotemporal auxin sensitivity during nodule development are also known (Turner *et al.*, 2013b, Breakspear *et al.*, 2014a, Nizampatnam *et al.*, 2015, Wang *et al.*, 2015, Hobecker *et al.*, 2017). However, the role of auxin metabolism in regulating auxin homeostasis during nodule development remains unclear. Flavonoids that accumulate at the sites of nodule initiation can inhibit peroxidases capable of degrading auxin and this has been suggested as a possible mechanism for auxin accumulation in these tissues (Mathesius, 2001a). Transient induction of *TRYPTOPHAN AMINOTRANSFERASE RELATED1*, a paralog of TAA, occurs in response to rhizobium inoculation in *L. japonicus* (Suzaki *et al.*, 2012a). In soybean, we have shown enrichment of *YUCCA*, *GH3*, and IAA oxidase gene expression in emerging nodules (Damodaran et al. unpublished data (Damodaran *et al.*, In review)). In *M. truncatula*, the expression of several GH3 genes is induced in *Sinorhizobium meliloti* treated roots (Yang *et al.*, 2015). Similarly, rhizobium-responsive expression of auxin conjugate hydrolases capable of hydrolyzing the ester bonds of IAA-glucose and thus releasing free IAA have also been reported (Campanella *et al.*, 2008). Rhizobia are also capable of

synthesizing auxin (Fukuhara *et al.*, 1994, Perrine *et al.*, 2004). Therefore, expression of auxin-modifying enzymes during nodule development is likely to enable the plant to efficiently regulate rhizobia-derived auxin as well. While these observations suggested that local auxin metabolism might contribute to auxin output during nodule initiation and development, no functional evidence existed for this hypothesis. We sought to identify the roles of auxin-conjugating GH3 proteins in soybean nodule development.

Here, we identified three GH3s with preferential expression during nodule development and characterized their enzymatic activity through in vitro assays. We also evaluated their expression patterns in roots and nodules of soybean, and their functional significance during nodule development by knocking down their expression using artificial microRNAs. We show that these GH3 proteins have distinct expression patterns in soybean, and show highest activity towards IAA-Asp conjugation, but have distinct specificities especially for other acyl substrates. Suppression of GH3 protein activity led to alterations in nodule number and nodule size indicating that these enzymes play important roles in soybean nodule development likely via their effect on auxin homeostasis.

3.3. Results

3.3.1. Identification of nodule-enriched GmGH3 genes

Nodule-enriched GH3 genes in soybean were identified from our RNA-seq dataset on emerging nodules (EN), mature nodules (MN), emerging lateral roots (ELR), and young lateral roots (YLR) *(Damodaran et al., In review)*; Table 3.3-A. Adjacent root

segments above and below these organs were used as age- and rhizobium inoculation-appropriate controls to determine GH3 genes specifically enriched in nodules versus lateral roots at two different stages of development (Table 3.3-A). We identified three nodule-enriched GH3 proteins with high expression and enrichment in either emerging or mature nodule tissues (highlighted in Table 3.3-A; Figure 3.3-1A). Among a total of five GH3 genes that showed enrichment in nodule tissues, these three showed the highest expression values with two of the three GH3s showing nodule-specific enrichment. The three genes were named as *GmGH3-11/12* (Glyma11g05510 (a1. v1.1), Glyma.11g051600 (a2. v1.1)), *GmGH3-14* (Glyma01g39780 (a1. v1.1), Glyma.01g190600 (a2. v1.1)), and *GmGH3-15* (Glyma12g17510 (a1. v1.1), Glyma.12g141000 (a2. v1.1)) based on the nomenclature/classification of the 25 soybean GH3 genes previously *(Westfall et al., 2012)*. Gene IDs in parenthesis correspond to those of soybean genome assembly release a1.v1.1 and a2.v1.1 (www.phytozome.net). The three GmGH3 genes used in this study were classified under group II GH3s that catalyze IAA conjugation.

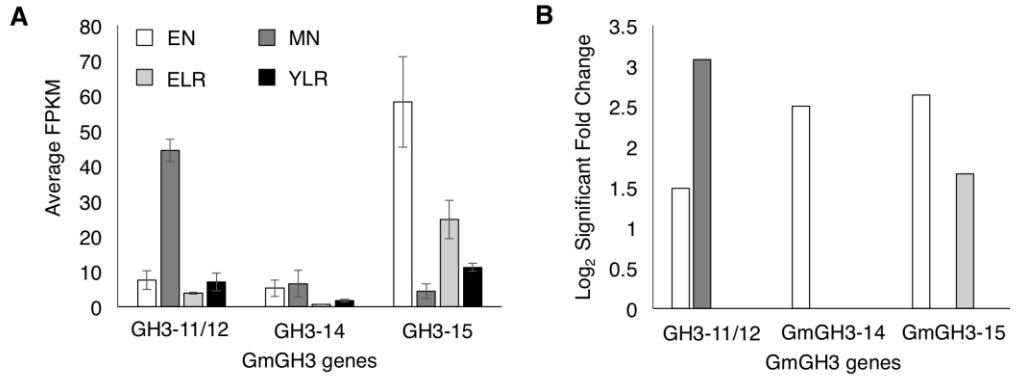

Figure 3.3-1: **Expression of GmGH3s in soybean root lateral organs.**

(**A**) Expression levels of GmGH3s in emerging nodule (EN), mature nodule (MN), emerging lateral root (ELR), and young lateral root (YLR) tissues. Data shown are average expression values from three biological replicates obtained using RNA-seq. Normalized gene expression levels based on RNA-seq read counts are shown in FPKM (fragments per kilobase of transcript per million mapped reads). Error bars indicate SD; (**B**) Enrichment of GmGH3s in the same four tissue types relative to adjacent root tissues. Data shown are statistically significant $\log_2$ fold change values vs. the respective control root segments from three biological replicates. See Table S1 for additional details.

GmGH3-11/12 was expressed in all four lateral organ tissues examined with highest expression in mature nodule tissues (Figure 3.3-1A). It showed enrichment only in nodule tissues with a 3.1-fold $\log_2$ fold change in MN followed by 1.5 in EN (Figure 3.3-1B). Expression of *GmGH3-14* and *GmGH3-15* was detected in all four lateral organ tissues. Despite near equal expression in EN and MN tissues, GH3-14 expression was enriched only in EN tissues (Figure 3.3-1A and B). *GmGH3-15* was expressed at relatively higher levels than *GmGH3-14* in general, and was enriched in both EN and ELR with $\log_2$ fold change values of 2.6 and 1.7, respectively (Figure 3.3-1A and B).

	Average FPKM				log_2 Fold Change				
Gene ID	**EN**	**MN**	**ELR**	**LR**	**EN**	**MN**	**ELR**	**LR**	
Glyma01g39780.1	**5.35**	**6.45**	**0.69**	**1.79**	**2.50**	**0.00**	**0.00**	**0.00**	**Gm-14**
Glyma02g13910.1	109.18	37.23	35.60	26.96	0.00	-2.75	0.00	0.00	Gm-9
Glyma05g21680.1	4.35	6.04	1.28	13.71	0.00	0.00	0.00	0.00	Gm-21/22
Glyma06g40860.1	21.28	4.43	27.90	10.67	0.00	-2.31	0.93	0.00	Gm-17
Glyma06g45640.1	0.01	0.04	0.01	0.01	0.00	0.00	0.00	0.00	Gm-23
Glyma11g05510.1	**7.62**	**43.93**	**3.63**	**7.24**	**1.49**	**3.08**	**0.00**	**0.00**	**Gm-11/12**
Glyma12g11200.1	0.20	0.16	1.82	0.55	0.00	0.00	2.16	0.00	Gm-16
Glyma12g17510.1	**57.49**	**4.49**	**23.18**	**11.17**	**2.64**	**0.00**	**1.67**	**0.00**	**Gm-15**
Glyma12g32410.1	0.18	0.35	4.45	1.11	0.00	0.00	2.37	4.71	Gm-18
Glyma12g34480.2	0.08	0.02	0.04	0.04	0.00	0.00	0.00	0.00	Gm-23
Glyma13g36030.1	2.51	0.46	2.91	2.20	3.06	0.00	1.13	0.00	Gm-13
Glyma13g38000.1	0.06	0.03	5.16	1.35	0.00	0.00	2.75	6.71	Gm-10
Glyma17g18040.1	2.60	1.06	1.44	0.84	2.27	0.00	1.55	0.00	Gm-24
Glyma17g18080.1	0.35	0.06	1.13	0.17	0.00	0.00	2.01	0.00	Gm-25
Glyma02g17360	0.01	0.00	0.14	0.06	0.00	0.00	0.00	0.00	Gm-19
Glyma10g02440.1	0.10	0.01	0.02	0.03	0.00	0.00	0.00	0.00	Gm-20
Glyma07g06370.1	2.82	1.76	3.02	1.66	0.00	0.00	0.00	0.00	Gm-1
Glyma03g41700.1	41.10	29.59	32.00	21.08	0.00	-1.77	-1.40	-2.05	Gm-2
Glyma19g44310.1	14.68	10.59	10.54	8.13	0.00	0.00	-1.01	-1.51	Gm-3
Glyma16g03011.1	3.22	4.71	2.80	3.79	0.00	0.00	0.00	0.00	Gm-4
Glyma12g32910.1	0.00	0.01	0.03	0.04	0.00	0.00	0.00	0.00	Gm-5
Glyma12g11890.1	0.14	0.03	0.06	0.03	0.00	0.00	0.00	0.00	Gm-6
Glyma13g37550.1	0.01	0.02	0.00	0.00	0.00	0.00	0.00	0.00	Gm-7
Glyma06g45120.1	0.05	0.00	0.09	0.39	0.00	0.00	0.00	0.00	Gm-8

Table 3.3-A: **GmGH3 expression data from RNA-seq data**.

3.3.2. Nodule –Enriched GmGH3s show Distinct Acyl Substrate specificities

Enzymatic activities of the nodule enriched GH3 proteins were evaluated using in vitro enzyme kinetics assays. Full-length proteins were expressed in bacterial cells, and purified for biochemical assays in which the conjugation of the 20 amino acids to IAA were evaluated. *GmGH3-11/12*, *GmGH3-14*, and *GmGH3-15* all displayed a clear preference for conjugation of IAA to aspartate (Figure 3.3-2). *GmGH3-11/12* had a specific activity of 296.2 nmol min^{-1} mg $protein^{-1}$ with aspartate and much lower specific activities with tryptophan (51.12 nmol min^{-1} mg $protein^{-1}$) and methionine (26.05 nmol min^{-1} mg $protein^{-1}$) (Figure 3.3-2A). *GmGH3-14* had a specific activity of 305.9 nmol min^{-1} mg $protein^{-1}$ with aspartate, and much lower rates with methionine (51.8 nmol min^{-1} mg $protein^{-1}$) and tryptophan (44.4 nmol min^{-1} mg $protein^{-1}$) (Figure 3.3-2B). The specific activity profile of *GmGH3-15* was similar with conjugation of IAA to aspartate (377.8 nmol min^{-1} mg $protein^{-1}$) as the primary function, although methionine (26.1 nmol min^{-1} mg $protein^{-1}$), cysteine (24.4 nmol min^{-1} mg $protein^{-1}$), and tryptophan (24.9 nmol min^{-1} mg $protein^{-1}$) were accepted as amino acid substrates (Figure 3.3-2C).

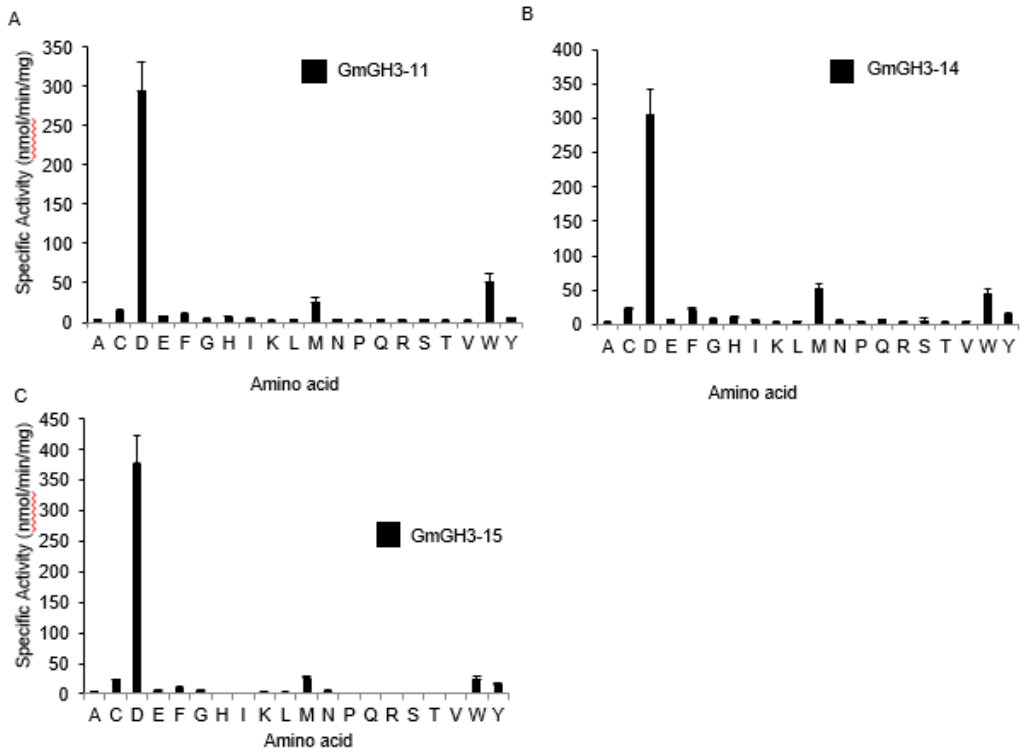

Figure 3.3-2: **Amino acid substrate preference of nodule enriched GmGH3s**.

Specific activities of (**A**) GmGH3-11/12; (**B**) GmGH3-14, and (**C**) GmGH3-15 (**C**) with IAA as acyl substrate with each of the 20 different amino acids denoted by single letter IUPAC codes. Data shown are the average specific activities from three replicate assays and error bars indicate SD.

GH3 proteins are capable of generating conjugates of different plant hormones including jasmonic acid, IAA and other auxins, and benzoate-derived compounds *(Westfall et al., 2012)*. Therefore, steady-state kinetic assays were performed using IAA, the ethylene precursor 1-aminocyclopropane carboxylic acid (ACC), abscisic acid (ABA), jasmonic acid (JA), and salicylic acid (SA) to further examine substrate preference (Figure 3.3-3A). *GmGH3-11/12*, *GmGH3-14*, and *GmGH3-15* exhibited little to no activity with ACC, ABA, JA, and SA (Figure 3.3-3A).

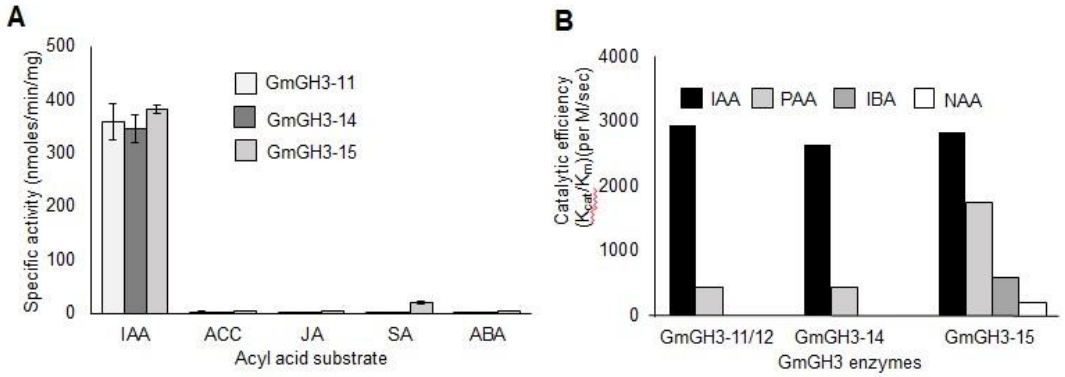

Figure 3.3-3: **Acyl substrate preference of nodule-enriched GmGH3s.**

(**A**) Specific activity of GmGH3-11/12, GmGH3-14, and GmGH3-15 with aspartate as aminoacid substrate, and the plant hormones indole-3-acetic acid (IAA), aminocyclopropane carboxylic acid (ACC), jasmonic acid (JA), salicylic acid (SA), and abscisic acid (ABA) as acyl substrate. Data shown are averages of three replicate assays and error bars indicate SD; (**B**) Catalytic efficiency of GmGH3-11/12, GmGH3-14, and GmGH3-15 with aspartate as amino acid substrate, and different forms of auxin: IAA, phenyl acetic acid (PAA), indole butyric acid (IBA), and naphthalene acetic acid (NAA) as acyl substrate. See Table S1 for additional details.

Although IAA is the primary auxin in many plants, several different forms of auxin are present in plant tissues and the levels of auxin analogs vary between species and between different tissues *(Simon and Petrasek, 2011, Korasick et al., 2013)*. To determine the substrate preference of the three GmGH3 proteins with different auxins, kinetic assays were performed using most abundant natural forms of auxin, IAA, phenyl acetic acid (PAA), and indole butyric acid (IBA), and the synthetic auxin, naphthalene acetic acid (NAA). As mentioned above, all three GmGH3s showed high catalytic efficiency towards IAA (Figure 3.3-3B; Table S1). The catalytic efficiencies (k_{cat}/K_m) of *GmGH3-11/12*, *GmGH3-14*, and *GmGH3-15* with IAA were 2950 M^{-1} s^{-1}, 2640 M^{-1} s^{-1}, and 2840 M^{-1} s^{-1}, respectively. Each of the

soybean GH3 proteins were also capable of using PAA as substrate, although not as efficiently as IAA. Of the three proteins, *GmGH3-15* displayed a 3-fold higher k_{cat}/K_m for PAA compared to the other two enzymes (Figure 3.3-3B; Table S1). *GmGH3-15* also used IBA (k_{cat}/K_m = 592 M^{-1} s^{-1}) and NAA (k_{cat}/K_m = 207 M^{-1} s^{-1}) as substrates, whereas the other two GH3s did not show any activity with these auxins (Figure 3.3-3B; Table S1). These results suggest that all these GH3 proteins likely conjugate IAA with aspartate to mark IAA for degradation in soybean. While *GmGH3-11/12* and *GmGH3-14* had comparable substrate preferences, *GmGH3-15* showed a broader auxin substrate preference.

3.3.3. Distinct Spatio-temporal expression pattern of GmGH3-14 and GmGH3-15 in Soybean roots and nodules

We characterized in detail the expression patterns and functional roles of *GmGH3-14* and *GmGH3-15* genes in soybean roots and nodules. Technical difficulties in cloning the promoter region precluded the characterization of *GmGH3-11/12* expression patterns. The promoter region upstream (~1900 bp) of the coding sequences of both *GmGH3-14* and *GmGH3-15* were fused to bacterial uidA gene encoding a beta-glucuronidase (GUS) and the transcriptional fusions were expressed in soybean hairy root composite plants. The expression patterns of GmGH3-14p:GUS and GmGH3-15p:GUS were monitored at 0, 10, and 14 days post rhizobium inoculation (dpi) through histochemical staining for GUS activity.

At 0 dpi, GmGH3-14p:GUS was expressed primarily in the root epidermis above the meristematic region (Figure 3.3-4A). There was no detectable gene expression in the root tip, including the root cap, quiescent center, and the root meristem, until the differentiation zone. In mature regions of the root, the expression of the construct was

primarily in the root epidermis and was more prominent in the lateral root primordia (Figure 3.3-4B). As the lateral root emerges, the expression of GmGH3-14p:GUS is not detectable in the ELR at the root tip similar to that of the primary root tips (Figure 3.3-4C). The epidermal expression of GmGH3-14p:GUS made it difficult to clearly image the early cortical cell division during nodule development, but in emerging nodules, GUS expression was observed in the nodule primordia (Figure 3.3-4D). As the nodule matures the expression of GmGH3-14p:GUS was localized to the nodule parenchyma including the nodule vasculature (Figure 3.3-4E).

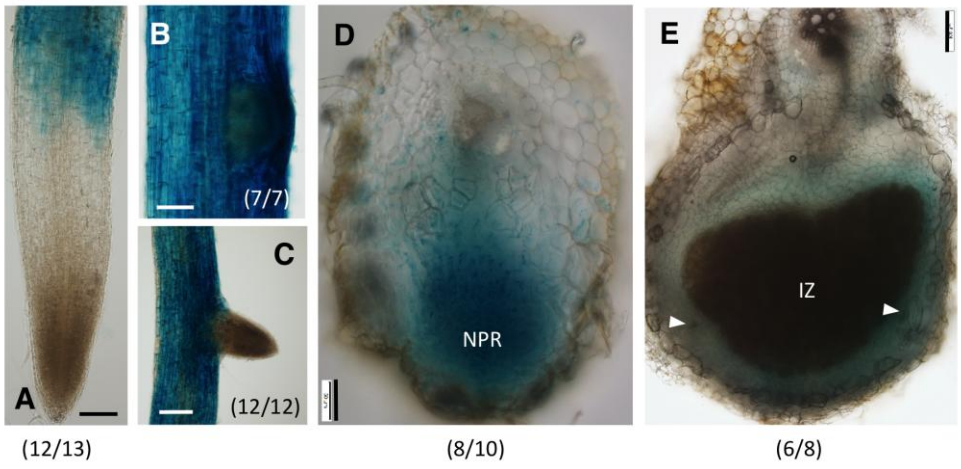

Figure 3.3-4: **Expression patterns of GmGH3-14p:GUS in soybean roots and nodules.**

(**A**–**C**) Expression of GmGH3-14p:GUS in (**A**) root tips, (**B**) mature root region with a lateral root primordium, and (**C**) mature root region with a young lateral root; (**D**,**E**) Expression of GmGH3-14p:GUS in (**D**) emerging nodule (transverse section at 10 dpi), and (**E**) mature nodule (transverse section at 17 dpi). NPR-nodule primordium; IZ–infection zone; Arrowheads indicate nodule vascular bundles. The number of independent transgenic roots/nodules showing the representative staining pattern out of the number of roots/nodules examined is indicated in each panel. Scale bars: (**A**,**B**,**E**) −100 μm; (**C**) −200 μm; (**D**) −50 μm.

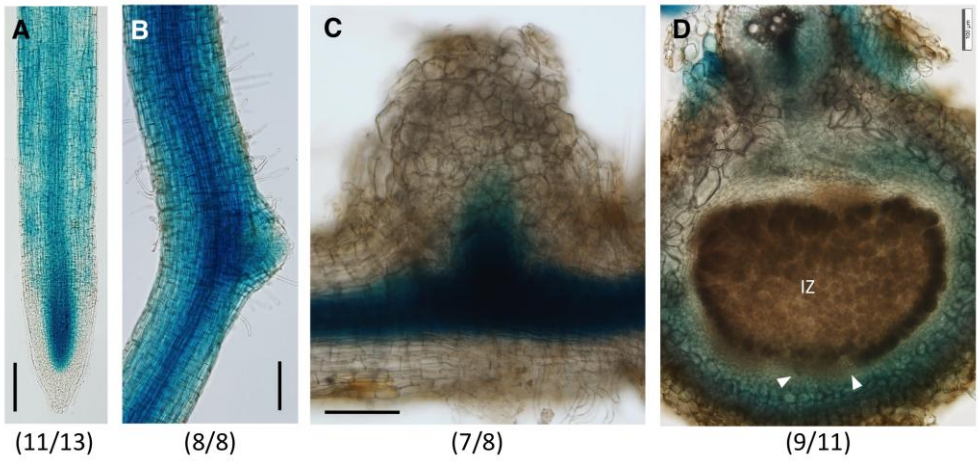

Figure 3.3-5: **Expression patterns of GmGH3-15p:GUS in soybean roots and nodules.** (**A**,**B**) Expression of GmGH3-14p:GUS in (**A**) root tips, and (**B**) mature root region with an emerging lateral root; (**C**,**D**) Expression of GmGH3-15p:GUS in (**C**) emerging nodule at 10 dpi and (**E**) mature nodule (transverse section at 17 dpi). IZ–infection zone; Arrowheads indicate nodule vascular bundles. The number of independent transgenic roots/nodules showing the representative staining pattern out of the number of roots/nodules examined is indicated in each panel. Scale bars: 100 μm.

GmGH3-15 was expressed in the root meristematic region, specifically above the quiescent center cells and in the elongating cells of the root vasculature (Figure 3.3-5A). GUS staining was absent in the root cap, as well as young epidermal and cortex cells of the root meristem. In the mature regions of the root, GmGH3-15p:GUS expression was detectable in the root epidermis and was prominent in the vasculature (Figure 3.3-5B). Similar to *GmGH3-14*, the promoter of *GmGH3-15* was also active in the lateral root primordia (Figure 3.3-5B). In emerging nodules, GmGH3-15p:GUS expression was observed at the junction of root and nodule where initiation of nodule vasculature development occurs (Figure 3.3-5C). There was no detectable expression in the nodule primordium or other nodule tissues. As the nodule matured, the expression was primarily localized in the parenchyma region and tissues surrounding the sclerid layer (Figure 3.3-5D). Expression was largely absent in parenchyma cells

closest to the infection zone, unlike that of GmGH3-14p:GUS, which was expressed throughout the parenchyma. Overall, *GmGH3-14* and *GmGH3-15* have distinct spatiotemporal expression patterns in root tips and emerging nodules. Both genes were generally expressed in the nodule parenchyma of mature nodules with subtle differences.

3.3.4. GmGH3-14 and GmGH3-15 are important for proper nodule numbers in soybean

To evaluate the role of GmGH3 proteins in soybean nodule development, we sought to knock down their expression in soybean composite plants. High sequence similarity among family members precluded the use of RNAi; therefore, artificial miRNAs to independently silence *GmGH3-14* and *GmGH3-15* were designed (*(Schwab et al., 2006)*; Figure S3-1). The high sequence similarity between *GmGH3-14* and *GmGH3-11/12* made it difficult to design a specific artificial miRNA construct against *GmGH3-14*. Therefore, the amiRNA against *GmGH3-14* was expected to silence both *GmGH3-11/12* and *GmGH3-14* and was named GH3-amiR12n14. The amiRNA targeting GH3-15 was named GH3-amiR15. The amiRNA sequences were synthesized using gma-miR164 pri-miRNA as backbone (Figure S3-1) and expressed using the constitutive CsVMV promoter *(Govindarajulu et al., 2008)* in soybean hairy root composite plants. The "empty vector", pCAMGFP-CsVMV:GW was used to generate vector control hairy root composite plants. To evalute amiRNA-mediated gene silencing, the expression of GmGH3 genes were quantified using RT-qPCR (Figure 3.3-6). The expression levels of the corresponding targets were significantly reduced in roots expressing GH3-amiR12n14 and GH3-amiR15 compared to the vector control roots (Figure 3.3-6A,B). However, the amiRNAs also led to the reduction in expression

levels of non-target GH3s (Figure 3.3-6A,B). GH3-amiR12n14 led to reduction in the levels of *GmGH3-15*; and GH3-amiR15 led to a significant reduction in the expression levels of *GmGH3-11/12* and *GmGH3-14* (Figure 3.3-6A,B). GH3-amiR15 led to >95% reduction in GmGH3-12 and *GmGH3-14* expression where as GH3-amiR12n14 led to ~60–70% reduction of these genes. Despite the silencing of non-target GH3s, we expected that suppression of GH3 expression in these roots might lead to a reduction in IAA-Asp formation, resulting in an increased active auxin pool. As a proxy for increased active auxin levels, we measured root length and lateral root density (number of lateral roots/cm of primary root) in these roots. There was no significant differences in these phenotypes in either of the GH3-amiR expressing roots relative to the vector control roots (Figure 3.3-6C,D). We also assayed the expression of auxin response marker GH3 (not targeted by the amiRNA) and INDOLE ACETIC ACID1 (IAA1) as a proxy for increased auxin levels. We observed 2.4-fold and 72-fold increases in expression of auxin-responsive GH3 in GH3-amiR12n14 roots and GH3-amiR15 roots, respectively. However, The differences were not statistically significant due to high variation between biological replicates (Figure 3.3-6E,F). IAA1 showed a statistically significant 2-fold higher expression in GH3-amiR12n14 roots, but no change in GH3-amiR15 roots compared to vector control roots. While physiological assays such as root length and lateral root density are likely to indicate cumulative effects of potential changes in auxin levels, gene expression markers are typically indicative of responses at the time of tissue harvest. This is likely the reason for inconsistency between markers, and large variation among replicates.

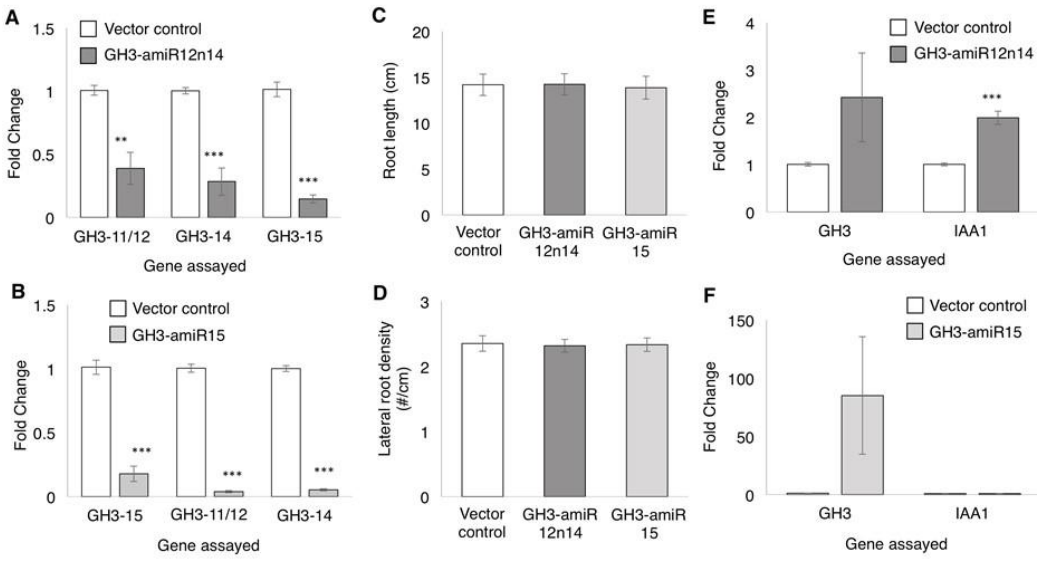

Figure 3.3-6: **Suppression of GmGH3 expression by artificial microRNAs.**

(**A**,**B**) Expression of target GmGH3 genes in roots expressing (**A**) GH3-amiR12n14 and (**B**) GH3-amiR15 relative to vector control roots; (**C**) Root length and (**D**) lateral root density of vector control roots and roots expressing GH3-amiRs. Data shown are averages (n = 21) and error bars indicate SEM. No significant difference observed using Student's t-test; (**E**,**F**) Expression of auxin response marker genes GH3 and IAA1 in roots expressing (**E**) GH3-amiR12n14, and (**F**) GH3-amiR15, relative to vector control roots. Expression levels shown in (**A**,**B**,**E**,**F**) were assayed by RT-qPCR and normalized to that of Actin in each sample. Data shown are average relative expression values (fold change vs. vector control) from three biological replicates and error bars indicate the range of possible value based on SD between replicates. ** —$p < 0.01$, *** —$p < 0.001$, Wilcoxon-Mann-Whitney test.

To determine the role of the amiRNA in nodule development, composite plants over-expressing GH3-amiRNAs were inoculated with *B. japonicum* and the numbers of emerging and mature nodules were counted at 14–17 dpi (Figure 3.3-7A). In roots over-expressing GH3-amiR12n14, there was a significant increase in the number of emerging nodules and a significant reduction in the number of mature nodules compared to the vector control. Roots expressing GH3-amiR15 also displayed a significant increase in the number of emerging nodules and a reduction in the number of mature nodules. The effects on the two amiRNAs on total nodule numbers were

distinct from each other. While GH3-12n14amiRNA caused a reduction in total nodule numbers, GH3-15amiRNA caused an increase in total nodule number (Figure 3.3-7A). This was due to the difference in magnitude of increase in emerging nodules and decrease in mature nodules between the two amiRNAs. GH3-amiR12n14 caused a relatively lower magnitude of increase in emerging nodule numbers, but a much higher reduction in mature nodule numbers versus GH3-amiR15. This data suggested that the expression of GmGH3 genes during nodule development is crucial for proper nodule organogenesis and maturation.

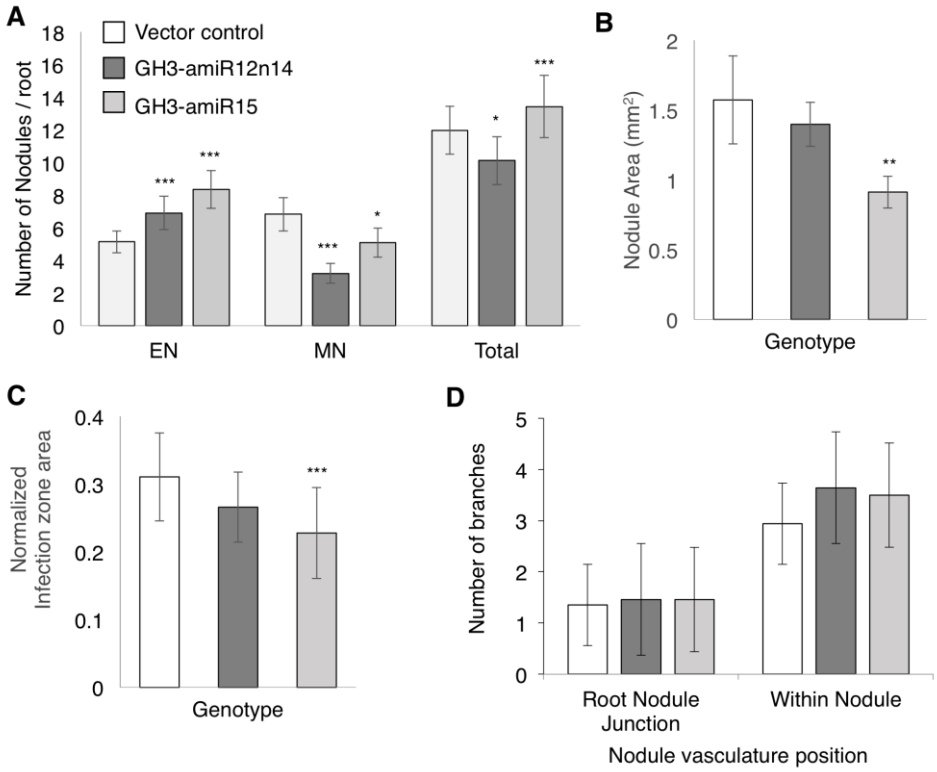

Figure 3.3-7: **Nodule numbers and morphology in GH3-amiR expressing soybean roots.**

(**A**) Numbers of emerging, mature, and total nodules in vector control, GH3-amiR12n14, and GH3-amiR15 expressing roots at 17 dpi. Data shown are the averages of at least 68 roots for each construct from three independent experiments. Error bars indicate SE. * —$p < 0.05$, *** —$p < 0.001$, Poisson distribution test; (**B**) Nodule area, and (**C**) normalized infection zone size of mature nodules from vector control, GH3-amiR12n14, and GH3-amiR15 expressing roots. Data shown are averages of at least 15 nodules each from three biological replicates. Error bars indicate SE. ** —$p < 0.01$, *** —$p < 0.001$, Wilcoxon-Mann-Whitney test; (**D**) Number of vasculature branches detectable at the root-nodule junction and within the nodule in transverse sections of mature nodules from vector control, GH3-amiR12n14, and GH3-amiR15 expressing roots. Data shown in C are averages of at least 15 nodules each from three biological replicates. Error bars indicate SE. Student's t-test.

3.3.5. GmGH3s influence nodule size in soybean

To evaluate the effect of suppressing GmGH3 genes on nodule morphology, median cross sections of mature nodules perpendicular to the root were imaged, and nodule and infection zone area were measured using ImageJ (Figure 3.3-7B–D). In roots over-expressing GH3-amiR12n14, there was no significant change in either the nodule area or the infection zone area compared to the nodules from vector control roots (Figure 3.3-7B). In roots overexpressing GH3-amiR15, there was a significant reduction in both the nodule and infection zone area (Figure 3.3-7C). The nodule sections were also stained with phloroglucinol and evaluated for nodule vasculature development by counting the number of visible vasculature branches at the nodule-root junction and in the nodule parenchyma (Figure 3.3-7D). Typically, 1–2 vascular strands are visible at the nodule-root junction, and 3–5 strands are visible in the parenchyma indicating branching of the vasculature in nodule tissues. There was no significant difference in the number of vasculature branches at either position in GH3-amiR12n14 or GH3-amiR15 over-expressing roots. Overall, our results suggest that GmGH3 proteins regulate nodule number, infection zone size, and nodule size.

3.4. Discussion

Auxin appears to play both positive and negative roles during nodule development depending on the level of auxin output, developmental stage, and type of legume nodule. Auxin perception by TIR/AFB family of F-box proteins appears to be crucial for root hair curling during determinate nodule development in soybean (Cai *et al.*, 2017). On the other hand, in *M. truncatula* (that produced indeterminate nodules) *arf16-1* mutants and lines over-expressing miR390, both of which had enhanced sensitivity to auxin had impaired root hair responses (Breakspear *et al.*, 2014a, Hobecker *et al.*, 2017). Enhanced response to auxin due to suppression of repressor auxin response factor transcription factors (ARF10/16/17) inhibits nodule development in soybean, although root hair responses and nodule initial cell division were unaffected (Turner *et al.*, 2013b). Similar conclusions on the relationship between auxin sensitivity and nodule formation were suggested by other studies in soybean (ARF8, (Wang *et al.*, 2015)) and *M. truncatula* (ARF3/4, (Hobecker *et al.*, 2017)). In particular, suppression of repressor ARF transcription factors in the nodule primordium tissues using an *ENOD40:miR160* construct inhibited nodule formation suggesting that enhanced auxin response in the primordium might inhibit formation of additional nodules in soybean (Turner *et al.*, 2013b). We observed increased numbers of emerging nodules and reduced numbers of mature nodules in soybean composite plants over-expressing GH3amiR constructs. This was unexpected, as one would have expected reduced nodulation resulting from an increase in free auxin levels due to reduced IAA-Asp conjugation in these roots. While we did observe an

overall reduction in nodulation in GH3-amiR12n14 plants, we observed an increased number of total nodules in GH3-amiR15 plants.

Two issues made it difficult for us to clearly interpret these results: non-specific silencing of GH3s by the amiRNAs, and broad-substrate specificity of *GmGH3-15*. Despite bioinformatics predictions and careful design, both amiRNAs significantly reduced the expression of all three GH3 proteins. GH3-amiR15 plants had a >95% reduction in expression levels of *GmGH3-11/12* and *GmGH3-14* where as it was ~60–70% in GH3-amiR12n14 plants; however, the level of suppression of *GmGH3-15* was comparable between GH3-amiR12n14 and GH3-amiR15 plants. Therefore, the phenotypic difference between GH3-amiR12n14 and GH3-amiR15 plants is likely to have resulted from difference in suppression of *GmGH3-11/12* and *GmGH3-14*. Promoter:GUS assays showed that *GmGH3-14* is highly expressed in the root epidermis, and soybean gene expression atlas showed that the expression of both *GmGH3-11/12* and GmGH13-14 are induced in root hairs upon rhizobium inoculation (Figure S10). Reduced expression of these genes is likely to have resulted in an increase in free auxin levels in root hairs upon rhizobium inoculation. We speculate that this would have resulted in increased infection and nodule formation because increased auxin response appears to promote rhizobial infection at least in soybean (Cai *et al.*, 2017). *GmGH3-14* is also expressed in the nodule primordium, and its suppression in these cells should have led to more free auxin and suppression of nodule development. The apparent contradiction might have resulted from suppression of more than one GH3 with distinct expression patterns by the amiRNA constructs. For example, the construct also silenced *GmGH3-12* which is highly

expressed and enriched in mature nodules. Nevertheless, we observed a reduction in number of mature nodules in both GH3-amiR expressing roots. In GH3-amiR15 roots where the expression levels of all three GH3s were strongly reduced, we also observed reduction in nodule size. Together these data indicate that the GmGH3s evaluated in this study play a key role in nodule maturation and contribute to nodule size. It was also interesting to note that these *GH3-14* and *GH3-15* were expressed in vascular tissues where typically high auxin activity is observed. It is possible that these genes act to establish threshold auxin levels for vascular differentiation. Generation of specific knock-outs in each GH3 through CRISPR/Cas-mediated gene editing might offer a more clear answer to the role of each of these GH3s in nodule development.

Secondly, *GmGH3-15* displayed a broad substrate specificity and much higher catalytic efficiency than other characterized GH3s. Since *GmGH3-15* showed substantial activity towards PAA, and IBA, it is possible that the activity of more than one auxin and even other hormones might have been affected in the GH3-amiR roots (see below). The ability of *GmGH3-15* to utilize different forms of auxin such as IAA, PAA, IBA, and NAA was reminiscent of the broad substrate specificity of the Arabidopsis GH3.5 (AtGH3.5) protein (Westfall *et al.*, 2016). Indeed, phylogenetic analyses indicate that both *GmGH3-15* and AtGH3.5 belong to the same orthoclade (Li *et al.*, 2012). *GmGH3-15* had a much higher catalytic efficiency on IAA (Figure 3B) compared to AtGH3.5 (Westfall *et al.*, 2016). Similarly, while AtGH3.5 had near equal catalytic efficiencies between IAA and PAA, *GmGH3-15* was about 3-fold more efficient with IAA over PAA. The abundance of PAA in plants is near equal or

even higher than that of IAA, although the former is relatively less active than IAA (Sugawara *et al.*, 2015). In Arabidopsis, over-expression of *AtGH3.5* or gain of function mutations resulted in reduced free IAA and PAA levels and increased IAA-Asp and PAA-Asp levels (Park *et al.*, 2007a, Zhang *et al.*, 2007, Westfall *et al.*, 2016), but the relative ratio of PAA-Asp vs. PAA was much higher than that of IAA-Asp vs. IAA. It was suggested that PAA-Asp might be more stable or a storage form (Westfall *et al.*, 2016). Therefore, we speculate that silencing of *GmGH3-15* might have resulted in altered PAA accumulation as well in GH3-amiR roots. It is possible that PAA in addition to IAA might play a role in soybean nodule development. *GmGH3-15* also displayed high catalytic efficiency towards benzoic acid (BA), and 4-hydroxy benzoic acid (4-HBA), and low, but detectable activity towards SA (Table S3). Arabidopsis GH3.5 gain of functions mutants (*wes1-D* and *gh3.5-1D*) accumulate higher levels of SA during pathogen challenge, and over-expression of *AtGH3.5* also led to increase in SA and SA-Asp (Park *et al.*, 2007a, Zhang *et al.*, 2007, Westfall *et al.*, 2016). It has been suggested that at least part of this SA might have been derived through conversion of BA or BA-Asp to SA (Westfall *et al.*, 2016). Therefore, we speculate that *GmGH3-15* might regulate SA levels in soybean. SA inhibits nodule development, but its site of action is unclear. Exogenous SA clearly inhibited both rhizobial association with root hairs and nodule primordium formation in indeterminate nodule forming legumes, but not in determinate nodule forming legumes (van Spronsen *et al.*, 2003). However, reduction in endogenous SA levels by expressing *nahG* (a bacterial SA hydroxylase gene) increased rhizobial infection as well as nodule formation in both determinate and indeterminate nodule

forming legumes. When plants were co-treated with nod factors and SA, root hair deformation responses were unaffected, but primordium initiation was significantly reduced (van Spronsen *et al.*, 2003, Stacey *et al.*, 2006) suggesting that SA might primarily inhibit cortical cell responses during nodule development. Given that gain of GH3.5 function in Arabidopsis led to increased SA accumulation in Arabidopsis, one might expect reduced SA and BA accumulation in GH3-15-silenced soybean roots. This is also plausible explanation for increased emerging nodule formation in these roots. While PAA has not been directly implicated in legume nodule development, a balance between positive effect of PAA and negative effect of SA has been suggested during actinorhizal nodule development (Hammad *et al.*, 2003). It is possible that *GmGH3-15* influences nodule development through its action on more than one plant hormone. Precise tissue-specific assays of the target hormones and conjugates are expected to clarify the specific role of *GmGH3-15* in soybean nodule development. In conclusion, our results clearly show that these GH3 proteins are important for proper nodulation in soybean while the precise mechanism by which they regulate nodule development remains to be explained.

3.5. Conclusion

In this study we identified a regulator of auxin metabolism essential for root nodule development in soybean. Through global gene expression analysis, we were able to identify three GH3 enzymes to be expressed in a nodule enriched pattern and were referred to as GmGH3-11, GmGH3-14 and GmGH3-15. Functional analysis of the GmGH3 revealed the possible role of GH3 in maintaining proper auxin homeostasis and its influence on nodule development. Gene specific knock outs of the each GH3 could help in understanding clearly their function and tissue specific metabolic analysis could provide more insight in the auxin metabolism during nodule organogenesis and maturation.

3.6. Materials and Methods

3.6.1. Plant Material

Glycine max cv. Williams -82, was the genotype used in this study since this has been used for genome sequencing project. Before sowing the seeds were surface sterilized by rinsing with 8% Clorox for 4min and 70% ethanol for 4min. Later the seeds are thoroughly rinsed with distilled water for 8-12 times to remove any residual bleach or ethanol. Seeds were germinated in 4" pots filled with vermiculite and perlite in the ratio 3:1 (Hummert International, MO). It was watered with Hoagland plant nutrient solution (refer Appendix A, Table A1). The plants were grown in a vertical growth chamber with controlled environmental condition (Conviron Growth Chamber, Manitoba, Canada) with settings as follows: 16h light and 8h dark with a day and night temperature of 25˚C and 20˚C respectively.

3.6.2. Protein expression, purification and enzyme assays

The coding sequences of *GmGH3-12*, *GmGH3-14*, and *GmGH3-15* were amplified by PCR using high fidelity polymerase enzymes from soybean (*Glycine max* cv. Williams82) root cDNA as template. Amplicons were cloned into a pET-28a bacterial expression vector and verified by sequencing. The coding sequence of *GmGH3-15* had a silent mutation (T101T caused by ACT > ACC) and *GmGH3-11* had a S492P mutation (TCT > CCT) compared to the reference sequence in multiple independent clones suggesting that these were not PCR artifacts. The N-terminally His-tagged fusion proteins of the GH3s were expressed in *Escherichia coli* BL21-CodonPlus-RP cells (Stratagene/Agilent, Santa Clara, CA, USA). The fusion protein was purified following cell lysis by sonication using nickel-based affinity purification, and size-exclusion chromatography, as described for other GH3 proteins (Chen *et al.*, 2010, Westfall *et al.*, 2016). The enzymatic activity of the three purified GH3 enzymes were assayed spectrophotometrically as previously described (Chen *et al.*, 2010, Westfall *et al.*, 2016).

3.6.3. Cloning for Promoter:GUS and Artificial miRNA

The promoter region upstream (~1900 bp) of the coding sequences of *GmGH3-14* and *GmGH3-15* were amplified by PCR using high fidelity polymerase enzymes, cloned into the pCR8-GWTOPOTA vector (Thermofisher Scientific, Waltham, MA, USA), and verified by sequencing. The promoter fragments were cloned in to the destination vector, pCAMGFP-GW:GUS using Gateway LR clonase II enzyme mix following the manufacturer's protocol (Thermofisher Scientific, Waltham, MA, USA) to obtain pCAMGFP-GmGH3-14p:GUS and pCAMGFP-GmGH3-15p:GUS.

Artificial miRNAs (amiRNAs) were designed by submitting the sequences of target and non-target GH3 genes to the artificial miRNA designer web tool available at (http://wmd3.weigelworld.org/cgi-bin/webapp.cgi) (Schwab *et al.*, 2006). The top most amiRNA from the resulting output was selected for silencing *GmGH3-15*. Only a common artificial miRNA was available for both *GmGH3-11/12* and *GmGH3-14*. The mature artificial miRNA sequences were inserted in to the pri-miRNA sequence of gma-miR164a using gene synthesis (Figure S1; Table S4). The resulting artificial miRNA precursors were amplified by PCR using high fidelity polymerase enzymes, cloned into pCR8GWTOPOTA vector (Thermofisher Scientific, Waltham, MA, USA), and verified by sequencing. The amiRNA precursors were cloned in to the destination vector, pCAMGFP-CsvMV:GW using Gateway LR clonase II enzyme mix following the manufacturer's protocol (Thermofisher Scientific, Waltham, MA, USA) to obtain pCAMGFP-CsVMV:GH3-amiRNA vectors. The artificial miRNAs were driven by the constitutively active Cassava vein mosaic virus CVP2 promoter (CsVMV) in these constructs.

The vectors were transformed in to *Agrobacterium rhizogenes* (K599) through electroporation using a Bio-Rad Gene pulser (Bio-Rad Laboratories, Hercules, CA, USA) with settings 25 μF, 400 Ω and 1.8 kV in a 0.1 cm gap cuvette..

3.6.4. Plant transformation and nodulation assay

Hairy root composite plant transformation was performed following the protocol described previously (Collier *et al.*, 2005b) using 12–14 days old soybean seedlings as explants and infecting them with *A. rhizogenes* cells transformed with constructs of interest. Twenty-one days after transformation, the plants produced adventitious roots

and *A. rhizogenes*-induced transgenic roots. GFP positive roots carrying the transgene of interest were selected by screening for epifluorescence using the FITC filter in an Olympus SZX16 microscope (Olympus Corporation, Shinjuku, Tokyo, Japan).

For nodulation assays, the screened plants were transferred to 4" pots filled with sterilized 3:1 vermiculite: perlite mix. Five days post transfer, the plants were inoculated with *B. japonicum USDA110* cells re-suspended in nitrogen free plant nutrient solution (N^- PNS) to $OD_{600\ nm}$ of 0.08 (Bhuvaneswari *et al.*, 1980, Turner *et al.*, 2013b). About 25 mL of this suspension was added uniformly to each pot. For mock-inoculated plants, the same quantity of N^- PNS was applied. Transgenic roots were harvested under an epifluorescence microscope at 14–17 dpi and the nodules were counted. Nodules were classified as "emerging" if they appeared as a bump on root surface and "mature" if they were completely protruded out of the root surface. The statistical significance of difference in nodule numbers if any between amiRNA and vector control roots was determined using zero inflated Poisson distribution package available in R statistical software.

3.6.5. Staining and Microscopy

3.6.5.1. GUS staining

For evaluation of spatiotemporal promoter:GUS expression, GFP-positive transgenic roots were subjected to GUS histochemical staining at 0, 7, 10 and 14 dpi. Roots were incubated in GUS staining buffer (Jefferson *et al.*, 1987) containing the chromogenic substrate X-Gluc (concentration of 0.5 mg/mL) overnight or until blue staining was visible on the roots, at room temperature. To avoid diffusion of GUS signal, and to arrest the enzymatic reaction the roots were subjected to dehydration with a series of ethanol dilutions from 10% to 70%. Before imaging the GUS-stained roots, they were

rehydrated through a series of ethanol in the reverse from 70% to 10% and finally collected in water. For evaluation of GUS expression in nodules, free hand transverse sections of nodules were made using a fresh, sharp razor blade where needed. Whole mounts or sections were mounted on a glass slide in sterile water and covered with a thin cover slip for imaging. The samples were imaged using an Olympus SZX16 microscope under white light trans-illumination or with an Olympus BX-53 upright microscope (Olympus Corporation, Shinjuku, Tokyo, Japan).

3.6.5.2. Pholoroglucinol staining

To determine nodule morphology, mature nodules from transgenic roots harvested at 14–17 dpi were used. Free hand transverse sections of mature nodules along with the root were stained with a saturated solution of phloroglucinol (Sigma-Aldrich, St. Louis, MO, USA) prepared freshly before staining by dissolving the dye in 20% HCl. The dyes enable visualization of lignified tissues such as vascular bundles which stain bright red in color. The nodule vasculature within the nodule and at the junction of root and nodule was manually counted from these images and the statistical significance of any differences was evaluated using Student's *t*-test in Microsoft Excel. Measurement of nodule area was performed in *Image J* (Schneider *et al.*, 2012) by manually drawing a border around the nodule area and infection zone using the free hand tool (Figure S2). Statistical significance of any differences was determined using Mann-Whitney-Wilcox test package in R.

3.6.6. Gene expression Analysis

To determine the of target GH3s by artificial miRNAs and to measure the expression of auxin response genes, GH3 and IAA1, root tips were collected from un-inoculated

roots of vector control and artificial miRNA-expressing roots in triplicate, and frozen in liquid nitrogen. Total RNA was isolated from these tissues, and gene expression was assayed using RT-qPCR as previously described (Turner *et al.*, 2013b, Nizampatnam *et al.*, 2015). Gene expression levels were normalized to that of house-keeping genes CONS7, CONS15, Actin, or CONS6 independently (Libault *et al.*, 2008). Data shown are relative to that of Actin. Results obtained using other house-keeping genes yielded similar conclusions. The statistical significance of any difference in gene expression was determined using Mann-Whitney-Wilcox test. The primers used in this study are mentioned in Appendix C.

3.7. References

Abel, S. and Theologis, A. (2010) Odyssey of Auxin. *Cold Spring Harbor Perspectives in Biology*, 2.

Bak, S. and Feyereisen, R. (2001) The Involvement of Two P450 Enzymes, CYP83B1 and CYP83A1, in Auxin Homeostasis and Glucosinolate Biosynthesis. *Plant Physiology*, 127, 108-118.

Bak, S., Tax, F.E., Feldmann, K.A., Galbraith, D.W. and Feyereisen, R. (2001) CYP83B1, a cytochrome P450 at the metabolic branch point in auxin and indole glucosinolate biosynthesis in Arabidopsis. *Plant Cell*, 13, 101-111.

Barlier, I., Kowalczyk, M., Marchant, A., Ljung, K., Bhalerao, R., Bennett, M., Sandberg, G. and Bellini, C. (2000) The SUR2 gene of Arabidopsis thaliana encodes the cytochrome P450 CYP83B1, a modulator of auxin homeostasis. *Proceedings of the National Academy of Sciences of the United States of America*, 97, 14819-14824.

Bevan, M.W. and Chilton, M.D. (1982) T-DNA of the Agrobacterium Ti and Ri plasmids. *Annual review of genetics*, 16, 357-384.

Bhuvaneswari, T.V., Turgeon, B.G. and Bauer, W.D. (1980) Early Events in the Infection of Soybean (Glycine max L. Merr) by Rhizobium japonicum: I. LOCALIZATION OF INFECTIBLE ROOT CELLS. *Plant Physiology*, 66, 1027-1031.

Bialek, K., Michalczuk, L. and Cohen, J.D. (1992) Auxin Biosynthesis during Seed Germination in Phaseolus vulgaris. *Plant Physiology*, 100, 509-517.

Blakeslee, J.J. and Murphy, A.S. (2016) Microscopic and Biochemical Visualization of Auxins in Plant Tissues. *Methods in molecular biology (Clifton, N.J.)*, 1398, 37-53.

Bond, L. (1948) Origin and Development Morphology of Root Nodules of Pisum sativum. *Botanical Gazette*, 109, 411-434.

Böttcher, C., Keyzers, R.A., Boss, P.K. and Davies, C. (2010) Sequestration of auxin by the indole-3-acetic acid-amido synthetase GH3-1 in grape berry (Vitis vinifera L.) and the proposed role of auxin conjugation during ripening. *Journal of Experimental Botany*, 61, 3615-3625.

Breakspear, A., Liu, C., Roy, S., Stacey, N., Rogers, C., Trick, M., Morieri, G., Mysore, K.S., Wen, J., Oldroyd, G.E., Downie, J.A. and Murray, J.D. (2014a) The root hair "infectome" of Medicago truncatula uncovers changes in cell cycle genes and reveals a requirement for Auxin signaling in rhizobial infection. *Plant Cell*, 26, 4680-4701.

Breakspear, A., Liu, C., Roy, S., Stacey, N., Rogers, C., Trick, M., Morieri, G., Mysore, K.S., Wen, J., Oldroyd, G.E.D., Downie, J.A. and Murray, J.D. (2014b) The Root Hair “Infectome” of Medicago truncatula Uncovers Changes in Cell Cycle Genes and Reveals a Requirement for Auxin Signaling in Rhizobial Infection. *The Plant Cell*, 26, 4680-4701.

Brechenmacher, L., Lei, Z., Libault, M., Findley, S., Sugawara, M., Sadowsky, M.J., Sumner, L.W. and Stacey, G. (2010) Soybean Metabolites Regulated in Root Hairs

in Response to the Symbiotic Bacterium Bradyrhizobium japonicum. *Plant Physiology*, 153, 1808-1822.

Brewin, N.J. (1991) Development of the Legume Root Nodule. *Annual Review of Cell Biology*, 7, 191-226.

Brown, S. and Walsh, K. (1994) Anatomy of the Legume Nodule Cortex With Respect to Nodule Permeability. *Functional Plant Biology*, 21, 49-68.

Caba, J.M., Centeno, M.L., Fernandez, B., Gresshoff, P.M. and Ligero, F. (2000) Inoculation and nitrate alter phytohormone levels in soybean roots: differences between a supernodulating mutant and the wild type. *Planta*, 211, 98-104.

Cai, Z., Wang, Y., Zhu, L., Tian, Y., Chen, L., Sun, Z., Ullah, I. and Li, X. (2017) GmTIR1/GmAFB3-based auxin perception regulated by miR393 modulates soybean nodulation. *The New phytologist*, 215, 672-686.

Calvert, H.E., Pence, M.K., Pierce, M., Malik, N.S.A. and Bauer, W.D. (1984) Anatomical analysis of the development and distribution of Rhizobium infections in soybean roots. *Canadian Journal of Botany*, 62, 2375-2384.

Campanella, J.J., Smith, S.M., Leibu, D., Wexler, S. and Ludwig-Müller, J. (2008) The Auxin Conjugate Hydrolase Family of Medicago truncatula and Their Expression During the Interaction with Two Symbionts. *Journal of Plant Growth Regulation*, 27, 26-38.

Champion, A., Lucas, M., Tromas, A., Vaissayre, V., Crabos, A., Diedhiou, I., Prodjinoto, H., Moukouanga, D., Pirolles, E., Cissoko, M., Bonneau, J., Gherbi, H., Franche, C., Hocher, V., Svistoonoff, S. and Laplaze, L. (2015) Inhibition of auxin signaling in Frankia species-infected cells in Casuarina glauca nodules leads to increased nodulation. *Plant Physiol*, 167, 1149-1157.

Chandler, J.W. (2009) Local auxin production: a small contribution to a big field. *BioEssays : news and reviews in molecular, cellular and developmental biology*, 31, 60-70.

Chen, Q., Westfall, C.S., Hicks, L.M., Wang, S. and Jez, J.M. (2010) Kinetic Basis for the Conjugation of Auxin by a GH3 Family Indole-acetic Acid-Amido Synthetase. *J Biol Chem*, 285, 29780-29786.

Cheng, Y., Dai, X. and Zhao, Y. (2006) Auxin biosynthesis by the YUCCA flavin monooxygenases controls the formation of floral organs and vascular tissues in Arabidopsis. *Genes & development*, 20, 1790-1799.

Clough, S.J. and Bent, A.F. (1998) Floral dip: a simplified method for Agrobacterium-mediated transformation of Arabidopsis thaliana. *The Plant journal : for cell and molecular biology*, 16, 735-743.

Collier, R., Fuchs, B., Walter, N., Kevin Lutke, W. and Taylor, C.G. (2005a) Ex vitro composite plants: an inexpensive, rapid method for root biology. *The Plant Journal*, 43, 449-457.

Collier, R., Fuchs, B., Walter, N., Kevin Lutke, W. and Taylor, C.G. (2005b) Ex vitro composite plants: an inexpensive, rapid method for root biology. *The Plant journal : for cell and molecular biology*, 43, 449-457.

Crespi, M. and Frugier, F. (2008) De novo organ formation from differentiated cells: root nodule organogenesis. *Sci Signal*, 1, re11.

Dai, X., Mashiguchi, K., Chen, Q., Kasahara, H., Kamiya, Y., Ojha, S., Dubois, J., Ballou, D. and Zhao, Y. (2013) The Biochemical Mechanism of Auxin Biosynthesis by an Arabidopsis YUCCA Flavin-containing Monooxygenase. *J Biol Chem*, 288, 1448-1457.

Damodaran, S., Adhikari, S., Lin, J., Pathak, S., Ge X., Blakeslee, L., , and Subramanian, S. (In review) Comparative transcriptomics reveals a role for GmCYP83B1 in regulating auxin homeostasis during soybean nodule development. *Plant Physiol*.

Delarue, M., Prinsen, E., Onckelen, H.V., Caboche, M. and Bellini, C. (1998) Sur2 mutations of Arabidopsis thaliana define a new locus involved in the control of auxin homeostasis. *The Plant journal : for cell and molecular biology*, 14, 603-611.

Desbrosses, Guilhem J. and Stougaard, J. (2011) Root Nodulation: A Paradigm for How Plant-Microbe Symbiosis Influences Host Developmental Pathways. *Cell Host & Microbe*, 10, 348-358.

Ding, Y. and Oldroyd, G.E. (2009) Positioning the nodule, the hormone dictum. *Plant signaling & behavior*, 4, 89-93.

Enders, T.A. and Strader, L.C. (2015) Auxin activity: Past, present, and future. *American journal of botany*, 102, 180-196.

F Sanchez, J E Padilla, H Perez, a. and Lara, M. (1991) Control of Nodulin Genes in Root-Nodule Development and Metabolism. *Annual Review of Plant Physiology and Plant Molecular Biology*, 42, 507-528.

Ferguson, B.J., Indrasumunar, A., Hayashi, S., Lin, M.H., Lin, Y.H., Reid, D.E. and Gresshoff, P.M. (2010) Molecular analysis of legume nodule development and autoregulation. *Journal of integrative plant biology*, 52, 61-76.

Ferguson, B.J. and Mathesius, U. (2014a) Phytohormone regulation of legume-rhizobia interactions. *Journal of chemical ecology*, 40, 770-790.

Ferguson, B.J. and Mathesius, U. (2014b) Phytohormone Regulation of Legume-Rhizobia Interactions. *J Chem Ecol*.

Fukuhara, H., Minakawa, Y., Akao, S. and Minamisawa, K. (1994) The Involvement of Indole-3-Acetic Acid Produced by Bradyrhizobium elkanii in Nodule Formation. *Plant and Cell Physiology*, 35, 1261-1265.

Gage, D.J. (2004) Infection and invasion of roots by symbiotic, nitrogen-fixing rhizobia during nodulation of temperate legumes. *Microbiology and molecular biology reviews : MMBR*, 68, 280-300.

Geurts, R. and Bisseling, T. (2002) Rhizobium Nod Factor Perception and Signalling. *The Plant Cell*, 14, s239-s249.

Govindarajulu, M., Elmore, J.M., Fester, T. and Taylor, C.G. (2008) Evaluation of constitutive viral promoters in transgenic soybean roots and nodules. *Molecular plant-microbe interactions : MPMI*, 21, 1027-1035.

Gronlund, M., Roussis, A., Flemetakis, E., Quaedvlieg, N.E., Schlaman, H.R., Umehara, Y., Katinakis, P., Stougaard, J. and Spaink, H.P. (2005) Analysis of promoter activity of the early nodulin Enod40 in Lotus japonicus. *Molecular plant-microbe interactions : MPMI*, 18, 414-427.

Guan, D., Stacey, N., Liu, C., Wen, J., Mysore, K.S., Torres-Jerez, I., Vernié, T., Tadege, M., Zhou, C., Wang, Z.-y., Udvardi, M.K., Oldroyd, G.E.D. and Murray, J.D. (2013) Rhizobial Infection Is Associated with the Development of Peripheral Vasculature in Nodules of Medicago truncatula. *Plant Physiology*, 162, 107-115.

Guo, J., Wei, J., Xu, J. and Sun, M.-X. (2014) Inducible knock-down of GNOM during root formation reveals tissue-specific response to auxin transport and its modulation of local auxin biosynthesis. *Journal of Experimental Botany*.

Hagen, G. and Guilfoyle, T.J. (1985) Rapid induction of selective transcription by auxins. *Molecular and Cellular Biology*, 5, 1197-1203.

Hammad, Y., Nalin, R., Marechal, J., Fiasson, K., Pepin, R., Berry, A.M., Normand, P. and Domenach, A.-M. (2003) A possible role for phenyl acetic acid (PAA) on Alnus glutinosa nodulation by Frankia. *Plant and Soil*, 254, 193-205.

Harper, J.E. (1974) Soil and Symbiotic Nitrogen Requirements for Optimum Soybean Production1. *Crop Science*, 14, 255-260.

Hirsch, A.M. (1992) Developmental Biology of Legume Nodulation. *New Phytologist*, 122, 211-237.

Hirsch, A.M., Bhuvaneswari, T.V., Torrey, J.G. and Bisseling, T. (1989) Early nodulin genes are induced in alfalfa root outgrowths elicited by auxin transport inhibitors. *Proceedings of the National Academy of Sciences of the United States of America*, 86, 1244-1248.

Hobecker, K.V., Reynoso, M.A., Bustos Sanmamed, P., Wen, J., Mysore, K.S., Crespi, M., Blanco, F.A. and Zanetti, M.E. (2017) The microRNA390/TAS3 pathway mediates in symbiotic nodulation and lateral root growth. *Plant Physiology*.

Huo, X., Schnabel, E., Hughes, K. and Frugoli, J. (2006) RNAi Phenotypes and the Localization of a Protein::GUS Fusion Imply a Role for Medicago truncatula PIN Genes in Nodulation. *J Plant Growth Regul*, 25, 156-165.

Ilegems, M., Douet, V., Meylan-Bettex, M., Uyttewaal, M., Brand, L., Bowman, J.L. and Stieger, P.A. (2010) Interplay of auxin, KANADI and Class III HD-ZIP transcription factors in vascular tissue formation. *Development*, 137, 975-984.

Jefferson, R.A., Kavanagh, T.A. and Bevan, M.W. (1987) GUS fusions: beta-glucuronidase as a sensitive and versatile gene fusion marker in higher plants. *The EMBO journal*, 6, 3901-3907.

Khan, S. and Stone, J.M. (2007) Arabidopsis thaliana GH3.9 influences primary root growth. *Planta*, 226, 21-34.

Kim, J.I., Dolan, W.L., Anderson, N.A. and Chapple, C. (2015) Indole Glucosinolate Biosynthesis Limits Phenylpropanoid Accumulation in Arabidopsis thaliana. *Plant Cell*.

Kim, J.I., Sharkhuu, A., Jin, J.B., Li, P., Jeong, J.C., Baek, D., Lee, S.Y., Blakeslee, J.J., Murphy, A.S., Bohnert, H.J., Hasegawa, P.M., Yun, D.J. and Bressan, R.A. (2007) yucca6, a dominant mutation in Arabidopsis, affects auxin accumulation and auxin-related phenotypes. *Plant Physiol*, 145, 722-735.

Kohlen, W., Ng, J.L.P., Deinum, E.E. and Mathesius, U. (2017) Auxin transport, metabolism, and signalling during nodule initiation: indeterminate and determinate nodules. *Journal of Experimental Botany*, erx308-erx308.

Korasick, D.A., Enders, T.A. and Strader, L.C. (2013) Auxin biosynthesis and storage forms. *Journal of Experimental Botany*, 64, 2541-2555.

Kouchi, H., Imaizumi-Anraku, H., Hayashi, M., Hakoyama, T., Nakagawa, T., Umehara, Y., Suganuma, N. and Kawaguchi, M. (2010) How Many Peas in a Pod? Legume Genes Responsible for Mutualistic Symbioses Underground. *Plant and Cell Physiology*, 51, 1381-1397.

Kowalczyk, M. and Sandberg, G. (2001) Quantitative Analysis of Indole-3-Acetic Acid Metabolites in Arabidopsis. *Plant Physiology*, 127, 1845-1853.

Kramer, E.M. and Ackelsberg, E.M. (2015) Auxin metabolism rates and implications for plant development. *Frontiers in Plant Science*, 6, 150.

Larrainzar, E., Riely, B.K., Kim, S.C., Carrasquilla-Garcia, N., Yu, H.-J., Hwang, H.-J., Oh, M., Kim, G.B., Surendrarao, A.K., Chasman, D., Siahpirani, A.F., Penmetsa, R.V., Lee, G.-S., Kim, N., Roy, S., Mun, J.-H. and Cook, D.R. (2015) Deep Sequencing of the Medicago truncatula Root Transcriptome Reveals a Massive and Early Interaction between Nodulation Factor and Ethylene Signals. *Plant Physiology*, 169, 233-265.

LeClere, S., Tellez, R., Rampey, R.A., Matsuda, S.P. and Bartel, B. (2002) Characterization of a family of IAA-amino acid conjugate hydrolases from Arabidopsis. *J Biol Chem*, 277, 20446-20452.

Li, J., Dai, X., Liu, T. and Zhao, P.X. (2012) LegumeIP: an integrative database for comparative genomics and transcriptomics of model legumes. *Nucleic Acids Research*, 40, D1221-D1229.

Li, X., Lei, M., Yan, Z., Wang, Q., Chen, A., Sun, J., Luo, D. and Wang, Y. (2014) The REL3-mediated TAS3 ta-siRNA pathway integrates auxin and ethylene signaling to regulate nodulation in Lotus japonicus. *The New phytologist*, 201, 531-544.

Libault, M., Farmer, A., Joshi, T., Takahashi, K., Langley, R.J., Franklin, L.D., He, J., Xu, D., May, G. and Stacey, G. (2010a) An integrated transcriptome atlas of the crop model Glycine max, and its use in comparative analyses in plants. *The Plant journal : for cell and molecular biology*, 63, 86-99.

Libault, M., Thibivilliers, S., Bilgin, D.D., Radwan, O., Benitez, M., Clough, S.J. and Stacey, G. (2008) Identification of Four Soybean Reference Genes for Gene Expression Normalization. *The Plant Genome*, 1, 44-54.

Libault, M., Zhang, X.C., Govindarajulu, M., Qiu, J., Ong, Y.T., Brechenmacher, L., Berg, R.H., Hurley-Sommer, A., Taylor, C.G. and Stacey, G. (2010b) A member of the highly conserved FWL (tomato FW2.2-like) gene family is essential for soybean nodule organogenesis. *The Plant journal : for cell and molecular biology*, 62, 852-864.

Liu, Z.B., Ulmasov, T., Shi, X., Hagen, G. and Guilfoyle, T.J. (1994) Soybean GH3 promoter contains multiple auxin-inducible elements. *The Plant Cell*, 6, 645-657.

Ljung, K. (2013a) Auxin metabolism and homeostasis during plant development. *Development*, 140, 943-950.

Ljung, K. (2013b) Auxin metabolism and homeostasis during plant development. *Development*, 140, 943-950.

Ljung, K., Hull, A.K., Celenza, J., Yamada, M., Estelle, M., Normanly, J. and Sandberg, G. (2005) Sites and regulation of auxin biosynthesis in Arabidopsis roots. *Plant Cell*, 17, 1090-1104.

Ludwig-Muller, J. (2011) Auxin conjugates: their role for plant development and in the evolution of land plants. *J Exp Bot*, 62, 1757-1773.

Ludwig-Müller, J. (2011) Auxin conjugates: their role for plant development and in the evolution of land plants. *Journal of Experimental Botany*, 62, 1757-1773.

Maharjan, P.M., Dilkes, B.P., Fujioka, S., Pencik, A., Ljung, K., Burow, M., Halkier, B.A. and Choe, S. (2014) Arabidopsis gulliver1/SUPERROOT2-7 identifies a metabolic basis for auxin and brassinosteroid synergy. *The Plant journal : for cell and molecular biology*, 80, 797-808.

Marhavy, P., Vanstraelen, M., De Rybel, B., Zhaojun, D., Bennett, M.J., Beeckman, T. and Benkova, E. (2013) Auxin reflux between the endodermis and pericycle promotes lateral root initiation. *The EMBO journal*, 32, 149-158.

Mashiguchi, K., Tanaka, K., Sakai, T., Sugawara, S., Kawaide, H., Natsume, M., Hanada, A., Yaeno, T., Shirasu, K., Yao, H., McSteen, P., Zhao, Y., Hayashi, K., Kamiya, Y. and Kasahara, H. (2011) The main auxin biosynthesis pathway in Arabidopsis. *Proceedings of the National Academy of Sciences of the United States of America*, 108, 18512-18517.

Mathesius, U. (2001a) Flavonoids induced in cells undergoing nodule organogenesis in white clover are regulators of auxin breakdown by peroxidase. *J Exp Bot*, 52, 419-426.

Mathesius, U. (2001b) Flavonoids induced in cells undergoing nodule organogenesis in white clover are regulators of auxin breakdown by peroxidase. *Journal of Experimental Botany*, 52, 419-426.

Mathesius, U. (2003) Conservation and divergence of signalling pathways between roots and soil microbes – the Rhizobium-legume symbiosis compared to the development of lateral roots, mycorrhizal interactions and nematode-induced galls. *Plant and Soil*, 255, 105-119.

Mathesius, U. (2008) Goldacre paper: Auxin: at the root of nodule development? *Functional Plant Biology*, 35, 651-668.

Mathesius, U., Schlaman, H.R., Spaink, H.P., Of Sautter, C., Rolfe, B.G. and Djordjevic, M.A. (1998) Auxin transport inhibition precedes root nodule formation in white clover roots and is regulated by flavonoids and derivatives of chitin oligosaccharides. *The Plant journal : for cell and molecular biology*, 14, 23-34.

Morant, M., Ekstrom, C., Ulvskov, P., Kristensen, C., Rudemo, M., Olsen, C.E., Hansen, J., Jorgensen, K., Jorgensen, B., Moller, B.L. and Bak, S. (2010) Metabolomic, transcriptional, hormonal, and signaling cross-talk in superroot2. *Mol Plant*, 3, 192-211.

Muller, C.J., Valdes, A.E., Wang, G., Ramachandran, P., Beste, L., Uddenberg, D. and Carlsbecker, A. (2016) PHABULOSA Mediates an Auxin Signaling Loop to Regulate Vascular Patterning in Arabidopsis. *Plant Physiol*, 170, 956-970.

Mus, F., Crook, M.B., Garcia, K., Garcia Costas, A., Geddes, B.A., Kouri, E.D., Paramasivan, P., Ryu, M.H., Oldroyd, G.E., Poole, P.S., Udvardi, M.K., Voigt, C.A., Ane, J.M. and Peters, J.W. (2016) Symbiotic Nitrogen Fixation and the Challenges to

Its Extension to Nonlegumes. *Applied and environmental microbiology*, 82, 3698-3710.

Mutava, R.N., Prince, S.J., Syed, N.H., Song, L., Valliyodan, B., Chen, W. and Nguyen, H.T. (2015) Understanding abiotic stress tolerance mechanisms in soybean: a comparative evaluation of soybean response to drought and flooding stress. *Plant physiology and biochemistry : PPB*, 86, 109-120.

Nakazawa, M., Yabe, N., Ichikawa, T., Yamamoto, Y.Y., Yoshizumi, T., Hasunuma, K. and Matsui, M. (2001) DFL1, an auxin-responsive GH3 gene homologue, negatively regulates shoot cell elongation and lateral root formation, and positively regulates the light response of hypocotyl length. *The Plant journal : for cell and molecular biology*, 25, 213-221.

Naur, P., Petersen, B.L., Mikkelsen, M.D., Bak, S., Rasmussen, H., Olsen, C.E. and Halkier, B.A. (2003) CYP83A1 and CYP83B1, two nonredundant cytochrome P450 enzymes metabolizing oximes in the biosynthesis of glucosinolates in Arabidopsis. *Plant Physiol*, 133, 63-72.

Newcomb, W. (1976) A correlated light and electron microscopic study of symbiotic growth and differentiation in Pisum sativum root nodules. *Canadian Journal of Botany*, 54, 2163-2186.

Newcomb, W., Sippell, D. and Peterson, R.L. (1979) The early morphogenesis of Glycine max and Pisum sativum root nodules. *Canadian Journal of Botany*, 57, 2603-2616.

Nishimura, R., Hayashi, M., Wu, G.J., Kouchi, H., Imaizumi-Anraku, H., Murakami, Y., Kawasaki, S., Akao, S., Ohmori, M., Nagasawa, M., Harada, K. and Kawaguchi, M. (2002) HAR1 mediates systemic regulation of symbiotic organ development. *Nature*, 420, 426-429.

Nishimura, T., Hayashi, K., Suzuki, H., Gyohda, A., Takaoka, C., Sakaguchi, Y., Matsumoto, S., Kasahara, H., Sakai, T., Kato, J., Kamiya, Y. and Koshiba, T. (2014) Yucasin is a potent inhibitor of YUCCA, a key enzyme in auxin biosynthesis. *The Plant journal : for cell and molecular biology*, 77, 352-366.

Nizampatnam, N.R., Schreier, S.J., Damodaran, S., Adhikari, S. and Subramanian, S. (2015) microRNA160 dictates stage-specific auxin and cytokinin sensitivities and directs soybean nodule development. *The Plant journal : for cell and molecular biology*, 84, 140-153.

Oldroyd, G.E., Murray, J.D., Poole, P.S. and Downie, J.A. (2011) The rules of engagement in the legume-rhizobial symbiosis. *Annual review of genetics*, 45, 119-144.

Overvoorde, P., Fukaki, H. and Beeckman, T. (2010a) Auxin Control of Root Development. *Cold Spring Harbor Perspectives in Biology*, 2, a001537.

Overvoorde, P., Fukaki, H. and Beeckman, T. (2010b) Auxin Control of Root Development. *Cold Spring Harbor Perspectives in Biology*, 2.

Pacios-Bras, C., Schlaman, H.R.M., Boot, K., Admiraal, P., Mateos Langerak, J., Stougaard, J. and Spaink, H.P. (2003) Auxin distribution in Lotus japonicus during root nodule development. *Plant Molecular Biology*, 52, 1169-1180.

Park, J.-E., Park, J.-Y., Kim, Y.-S., Staswick, P.E., Jeon, J., Yun, J., Kim, S.-Y., Kim, J., Lee, Y.-H. and Park, C.-M. (2007a) GH3-mediated Auxin Homeostasis Links Growth Regulation with Stress Adaptation Response in Arabidopsis. *Journal of Biological Chemistry*, 282, 10036-10046.

Park, J.E., Park, J.Y., Kim, Y.S., Staswick, P.E., Jeon, J., Yun, J., Kim, S.Y., Kim, J., Lee, Y.H. and Park, C.M. (2007b) GH3-mediated auxin homeostasis links growth regulation with stress adaptation response in Arabidopsis. *J Biol Chem*, 282, 10036-10046.

Peat, T.S., Bottcher, C., Newman, J., Lucent, D., Cowieson, N. and Davies, C. (2012) Crystal structure of an indole-3-acetic acid amido synthetase from grapevine involved in auxin homeostasis. *Plant Cell*, 24, 4525-4538.

Peer, W.A., Cheng, Y. and Murphy, A.S. (2013) Evidence of oxidative attenuation of auxin signalling. *Journal of experimental botany*, 64, 2629-2639.

Peer, W.A. and Murphy, A.S. (2007) Flavonoids and auxin transport: modulators or regulators? *Trends in plant science*, 12, 556-563.

Pencik, A., Simonovik, B., Petersson, S.V., Henykova, E., Simon, S., Greenham, K., Zhang, Y., Kowalczyk, M., Estelle, M., Zazimalova, E., Novak, O., Sandberg, G. and Ljung, K. (2013) Regulation of auxin homeostasis and gradients in Arabidopsis roots

through the formation of the indole-3-acetic acid catabolite 2-oxindole-3-acetic acid. *The Plant cell*, 25, 3858-3870.

Pěnčík, A., Simonovik, B., Petersson, S.V., Henyková, E., Simon, S., Greenham, K., Zhang, Y., Kowalczyk, M., Estelle, M., Zažímalová, E., Novák, O., Sandberg, G. and Ljung, K. (2013a) Regulation of Auxin Homeostasis and Gradients in Arabidopsis Roots through the Formation of the Indole-3-Acetic Acid Catabolite 2-Oxindole-3-Acetic Acid. *The Plant Cell*, 25, 3858-3870.

Pěnčík, A., Simonovik, B., Petersson, S.V., Henyková, E., Simon, S., Greenham, K., Zhang, Y., Kowalczyk, M., Estelle, M., Zažímalová, E., Novák, O., Sandberg, G. and Ljung, K. (2013b) Regulation of Auxin Homeostasis and Gradients in Arabidopsis Roots through the Formation of the Indole-3-Acetic Acid Catabolite 2-Oxindole-3-Acetic Acid. *The Plant Cell*, 25, 3858-3870.

Peoples, M.B., Brockwell, J., Herridge, D.F., Rochester, I.J., Alves, B.J.R., Urquiaga, S., Boddey, R.M., Dakora, F.D., Bhattarai, S., Maskey, S.L., Sampet, C., Rerkasem, B., Khan, D.F., Hauggaard-Nielsen, H. and Jensen, E.S. (2009) The contributions of nitrogen-fixing crop legumes to the productivity of agricultural systems. *Symbiosis*, 48, 1-17.

Perrine, F.M., Rolfe, B.G., Hynes, M.F. and Hocart, C.H. (2004) Gas chromatography-mass spectrometry analysis of indoleacetic acid and tryptophan following aqueous chloroformate derivatisation of Rhizobium exudates. *Plant physiology and biochemistry : PPB*, 42, 723-729.

Pii, Y., Crimi, M., Cremonese, G., Spena, A. and Pandolfini, T. (2007) Auxin and nitric oxide control indeterminate nodule formation. *BMC plant biology*, 7, 21.

Porco, S., Pencik, A., Rashed, A., Voss, U., Casanova-Saez, R., Bishopp, A., Golebiowska, A. and Bhosale, R. (2016) Dioxygenase-encoding AtDAO1 gene controls IAA oxidation and homeostasis in Arabidopsis. 113, 11016-11021.

Quittenden, L.J., Davies, N.W., Smith, J.A., Molesworth, P.P., Tivendale, N.D. and Ross, J.J. (2009) Auxin Biosynthesis in Pea: Characterization of the Tryptamine Pathway. *Plant Physiology*, 151, 1130-1138.

Ramachandran, P., Carlsbecker, A. and Etchells, J.P. (2017) Class III HD-ZIPs govern vascular cell fate: an HD view on patterning and differentiation. *J Exp Bot*, 68, 55-69.

Rampey, R.A., LeClere, S., Kowalczyk, M., Ljung, K., Sandberg, G. and Bartel, B. (2004) A family of auxin-conjugate hydrolases that contributes to free indole-3-acetic acid levels during Arabidopsis germination. *Plant Physiol*, 135, 978-988.

Reid, D.E., Ferguson, B.J. and Gresshoff, P.M. (2011) Inoculation- and nitrate-induced CLE peptides of soybean control NARK-dependent nodule formation. *Molecular plant-microbe interactions : MPMI*, 24, 606-618.

Sanko-Sawczenko, I., Lotocka, B. and Czarnocka, W. (2016) Expression Analysis of PIN Genes in Root Tips and Nodules of Medicago truncatula. *International journal of molecular sciences*, 17.

Sasaki, T., Suzaki, T., Soyano, T., Kojima, M., Sakakibara, H. and Kawaguchi, M. (2014) Shoot-derived cytokinins systemically regulate root nodulation. *Nature Communications*, 5, 4983.

Schnabel, E., Journet, E.P., de Carvalho-Niebel, F., Duc, G. and Frugoli, J. (2005) The Medicago truncatula SUNN gene encodes a CLV1-like leucine-rich repeat receptor kinase that regulates nodule number and root length. *Plant Mol Biol*, 58, 809-822.

Schneider, C.A., Rasband, W.S. and Eliceiri, K.W. (2012) NIH Image to ImageJ: 25 years of image analysis. *Nature methods*, 9, 671-675.

Schultze, M. and Kondorosi, A. (1998) Regulation of symbiotic root nodule development. *Annual review of genetics*, 32, 33-57.

Schwab, R., Ossowski, S., Riester, M., Warthmann, N. and Weigel, D. (2006) Highly Specific Gene Silencing by Artificial MicroRNAs in Arabidopsis. *The Plant Cell*, 18, 1121-1133.

Simon, S. and Petrasek, J. (2011) Why plants need more than one type of auxin. *Plant science : an international journal of experimental plant biology*, 180, 454-460.

Sprent, J.I. and James, E.K. (2007) Legume Evolution: Where Do Nodules and Mycorrhizas Fit In? *Plant Physiology*, 144, 575-581.

Stacey, G., McAlvin, C.B., Kim, S.Y., Olivares, J. and Soto, M.J. (2006) Effects of endogenous salicylic acid on nodulation in the model legumes Lotus japonicus and Medicago truncatula. *Plant physiology*, 141, 1473-1481.

Staswick, P.E., Serban, B., Rowe, M., Tiryaki, I., Maldonado, M.T., Maldonado, M.C. and Suza, W. (2005a) Characterization of an Arabidopsis enzyme family that conjugates amino acids to indole-3-acetic acid. *The Plant cell*, 17, 616-627.

Staswick, P.E., Serban, B., Rowe, M., Tiryaki, I., Maldonado, M.T., Maldonado, M.C. and Suza, W. (2005b) Characterization of an Arabidopsis Enzyme Family That Conjugates Amino Acids to Indole-3-Acetic Acid. *The Plant Cell*, 17, 616-627.

Stepanova, A.N., Robertson-Hoyt, J., Yun, J., Benavente, L.M., Xie, D.Y., Dolezal, K., Schlereth, A., Jurgens, G. and Alonso, J.M. (2008) TAA1-mediated auxin biosynthesis is essential for hormone crosstalk and plant development. *Cell*, 133, 177-191.

Subramanian, S., Stacey, G. and Yu, O. (2006) Endogenous isoflavones are essential for the establishment of symbiosis between soybean and Bradyrhizobium japonicum. *The Plant journal : for cell and molecular biology*, 48, 261-273.

Subramanian, S., Stacey, G. and Yu, O. (2007) Distinct, crucial roles of flavonoids during legume nodulation. *Trends in plant science*, 12, 282-285.

Sugawara, S., Hishiyama, S., Jikumaru, Y., Hanada, A., Nishimura, T., Koshiba, T., Zhao, Y., Kamiya, Y. and Kasahara, H. (2009) Biochemical analyses of indole-3-

acetaldoxime-dependent auxin biosynthesis in Arabidopsis. *Proceedings of the National Academy of Sciences of the United States of America*, 106, 5430-5435.

Sugawara, S., Mashiguchi, K., Tanaka, K., Hishiyama, S., Sakai, T., Hanada, K., Kinoshita-Tsujimura, K., Yu, H., Dai, X., Takebayashi, Y., Takeda-Kamiya, N., Kakimoto, T., Kawaide, H., Natsume, M., Estelle, M., Zhao, Y., Hayashi, K.-i., Kamiya, Y. and Kasahara, H. (2015) Distinct Characteristics of Indole-3-Acetic Acid and Phenylacetic Acid, Two Common Auxins in Plants. *Plant and Cell Physiology*, 56, 1641-1654.

Suzaki, T., Ito, M. and Kawaguchi, M. (2013) Genetic basis of cytokinin and auxin functions during root nodule development. *Frontiers in Plant Science*, 4, 42.

Suzaki, T., Yano, K., Ito, M., Umehara, Y., Suganuma, N. and Kawaguchi, M. (2012a) Positive and negative regulation of cortical cell division during root nodule development in Lotus japonicus is accompanied by auxin response. *Development*, 139, 3997-4006.

Suzaki, T., Yano, K., Ito, M., Umehara, Y., Suganuma, N. and Kawaguchi, M. (2012b) Positive and negative regulation of cortical cell division during root nodule development in Lotus japonicus is accompanied by auxin response. *Development*, 139, 3997-4006.

Takanashi, K., Sugiyama, A. and Yazaki, K. (2011) Involvement of auxin distribution in root nodule development of Lotus japonicus. *Planta*, 234, 73-81.

Takase, T., Nakazawa, M., Ishikawa, A., Kawashima, M., Ichikawa, T., Takahashi, N., Shimada, H., Manabe, K. and Matsui, M. (2004) ydk1-D, an auxin-responsive GH3 mutant that is involved in hypocotyl and root elongation. *The Plant journal : for cell and molecular biology*, 37, 471-483.

Tanaka, K., Hayashi, K.-i., Natsume, M., Kamiya, Y., Sakakibara, H., Kawaide, H. and Kasahara, H. (2014) UGT74D1 Catalyzes the Glucosylation of 2-Oxindole-3-Acetic Acid in the Auxin Metabolic Pathway in Arabidopsis. *Plant and Cell Physiology*, 55, 218-228.

Tao, Y., Ferrer, J.L., Ljung, K., Pojer, F., Hong, F., Long, J.A., Li, L., Moreno, J.E., Bowman, M.E., Ivans, L.J., Cheng, Y., Lim, J., Zhao, Y., Ballare, C.L., Sandberg, G., Noel, J.P. and Chory, J. (2008) Rapid synthesis of auxin via a new tryptophan-dependent pathway is required for shade avoidance in plants. *Cell*, 133, 164-176.

Tobena-Santamaria, R., Bliek, M., Ljung, K., Sandberg, G., Mol, J.N., Souer, E. and Koes, R. (2002) FLOOZY of petunia is a flavin mono-oxygenase-like protein required for the specification of leaf and flower architecture. *Genes & development*, 16, 753-763.

Trapnell, C., Roberts, A., Goff, L., Pertea, G., Kim, D., Kelley, D.R., Pimentel, H., Salzberg, S.L., Rinn, J.L. and Pachter, L. (2012) Differential gene and transcript expression analysis of RNA-seq experiments with TopHat and Cufflinks. *Nat. Protocols*, 7, 562-578.

Turner, M., Adhikari, S. and Subramanian, S. (2013a) Optimizing stem-loop qPCR assays through multiplexed cDNA synthesis of U6 and miRNAs. *Plant signaling & behavior*, 8.

Turner, M., Nizampatnam, N.R., Baron, M., Coppin, S., Damodaran, S., Adhikari, S., Arunachalam, S.P., Yu, O. and Subramanian, S. (2013b) Ectopic expression of miR160 results in auxin hypersensitivity, cytokinin hyposensitivity, and inhibition of symbiotic nodule development in soybean. *Plant Physiol*, 162, 2042-2055.

Udvardi, M.K. and Day, D.A. (1997) METABOLITE TRANSPORT ACROSS SYMBIOTIC MEMBRANES OF LEGUME NODULES. *Annu Rev Plant Physiol Plant Mol Biol*, 48, 493-523.

Ursache, R., Miyashima, S., Chen, Q., Vatén, A., Nakajima, K., Carlsbecker, A., Zhao, Y., Helariutta, Y. and Dettmer, J. (2014) Tryptophan-dependent auxin biosynthesis is required for HD-ZIP III-mediated xylem patterning. *Development*, 141, 1250-1259.

van Noorden, G.E., Verbeek, R., Dinh, Q.D., Jin, J., Green, A., Ng, J.L. and Mathesius, U. (2016) Molecular Signals Controlling the Inhibition of Nodulation by Nitrate in Medicago truncatula. *International journal of molecular sciences*, 17.

van Spronsen, P.C., Tak, T., Rood, A.M., van Brussel, A.A., Kijne, J.W. and Boot, K.J. (2003) Salicylic acid inhibits indeterminate-type nodulation but not determinate-type nodulation. *Molecular plant-microbe interactions : MPMI*, 16, 83-91.

Wang, Y., Li, K., Chen, L., Zou, Y., Liu, H., Tian, Y., Li, D., Wang, R., Zhao, F., Ferguson, B.J., Gresshoff, P.M. and Li, X. (2015) MicroRNA167-Directed Regulation of the Auxin Response Factors GmARF8a and GmARF8b Is Required for Soybean Nodulation and Lateral Root Development. *Plant Physiol*, 168, 984-999.

Wasson, A.P., Pellerone, F.I. and Mathesius, U. (2006) Silencing the flavonoid pathway in Medicago truncatula inhibits root nodule formation and prevents auxin transport regulation by rhizobia. *Plant Cell*, 18, 1617-1629.

Westfall, C.S., Herrmann, J., Chen, Q., Wang, S. and Jez, J.M. (2010) Modulating plant hormones by enzyme action: the GH3 family of acyl acid amido synthetases. *Plant signaling & behavior*, 5, 1607-1612.

Westfall, C.S., Sherp, A.M., Zubieta, C., Alvarez, S., Schraft, E., Marcellin, R., Ramirez, L. and Jez, J.M. (2016) Arabidopsis thaliana GH3.5 acyl acid amido synthetase mediates metabolic crosstalk in auxin and salicylic acid homeostasis. *Proceedings of the National Academy of Sciences*, 113, 13917-13922.

Westfall, C.S., Zubieta, C., Herrmann, J., Kapp, U., Nanao, M.H. and Jez, J.M. (2012) Structural basis for prereceptor modulation of plant hormones by GH3 proteins. *Science (New York, N.Y.)*, 336, 1708-1711.

Won, C., Shen, X., Mashiguchi, K., Zheng, Z., Dai, X., Cheng, Y., Kasahara, H., Kamiya, Y., Chory, J. and Zhao, Y. (2011) Conversion of tryptophan to indole-3-acetic acid by TRYPTOPHAN AMINOTRANSFERASES OF ARABIDOPSIS and

YUCCAs in Arabidopsis. *Proceedings of the National Academy of Sciences of the United States of America*, 108, 18518-18523.

Woodward, A.W. and Bartel, B. (2005a) Auxin: regulation, action, and interaction. *Annals of botany*, 95, 707-735.

Woodward, A.W. and Bartel, B. (2005b) Auxin: Regulation, Action, and Interaction. *Ann Bot*, 95, 707-735.

Yang, W.-C., Katinakis, P., Hendriks, P., Smolders, A., de Vries, F., Spee, J., van Kammen, A., Bisseling, T. and Franssen, H. (1993) Characterization of GmENOD40, a gene showing novel patterns of cell-specific expression during soybean nodule development. *The Plant Journal*, 3, 573-585.

Yang, Y., Yue, R., Sun, T., Zhang, L., Chen, W., Zeng, H., Wang, H. and Shen, C. (2015) Genome-wide identification, expression analysis of GH3 family genes in Medicago truncatula under stress-related hormones and Sinorhizobium meliloti infection. *Applied microbiology and biotechnology*, 99, 841-854.

Zhang, J., Lin, J.E., Harris, C., Campos Mastrotti Pereira, F., Wu, F., Blakeslee, J.J. and Peer, W.A. (2016a) DAO1 catalyzes temporal and tissue-specific oxidative inactivation of auxin in Arabidopsis thaliana. *Proceedings of the National Academy of Sciences*, 113, 11010-11015.

Zhang, J., Lin, J.E., Harris, C., Campos Mastrotti Pereira, F., Wu, F., Blakeslee, J.J. and Peer, W.A. (2016b) DAO1 catalyzes temporal and tissue-specific oxidative

inactivation of auxin in Arabidopsis thaliana. *Proceedings of the National Academy of Sciences of the United States of America*, 113, 11010-11015.

Zhang, S.-W., Li, C.-H., Cao, J., Zhang, Y.-C., Zhang, S.-Q., Xia, Y.-F., Sun, D.-Y. and Sun, Y. (2009) Altered Architecture and Enhanced Drought Tolerance in Rice via the Down-Regulation of Indole-3-Acetic Acid by TLD1/OsGH3.13 Activation. *Plant Physiology*, 151, 1889-1901.

Zhang, Z., Li, Q., Li, Z., Staswick, P.E., Wang, M., Zhu, Y. and He, Z. (2007) Dual Regulation Role of GH3.5 in Salicylic Acid and Auxin Signaling during Arabidopsis-Pseudomonas syringae Interaction. *Plant Physiology*, 145, 450-464.

Zhao, Y. (2010) Auxin biosynthesis and its role in plant development. *Annual review of plant biology*, 61, 49-64.

Zhao, Y. (2012a) Auxin biosynthesis: a simple two-step pathway converts tryptophan to indole-3-acetic acid in plants. *Molecular plant*, 5, 334-338.

Zhao, Y. (2012b) Auxin Biosynthesis: A Simple Two-Step Pathway Converts Tryptophan to Indole-3-Acetic Acid in Plants. *Molecular Plant*, 5, 334-338.

Zhao, Y. (2012c) Auxin biosynthesis: a simple two-step pathway converts tryptophan to indole-3-acetic acid in plants. *Mol Plant*, 5, 334-338.

Zhao, Y. (2014) Auxin Biosynthesis. *The Arabidopsis Book*, e0173.

Zhao, Y., Christensen, S.K., Fankhauser, C., Cashman, J.R., Cohen, J.D., Weigel, D. and Chory, J. (2001) A role for flavin monooxygenase-like enzymes in auxin biosynthesis. *Science (New York, N.Y.)*, 291, 306-309.

Zhao, Z., Zhang, Y., Liu, X., Zhang, X., Liu, S., Yu, X., Ren, Y., Zheng, X., Zhou, K., Jiang, L., Guo, X., Gai, Y., Wu, C., Zhai, H., Wang, H. and Wan, J. (2013) A role for a dioxygenase in auxin metabolism and reproductive development in rice. *Developmental cell*, 27, 113-122.

Zheng, Z., Guo, Y., Novák, O., Chen, W., Ljung, K., Noel, J.P. and Chory, J. (2016) Local auxin metabolism regulates environment-induced hypocotyl elongation. *Nature plants*, 2, 16025-16025.

3.8. Supplementary Information

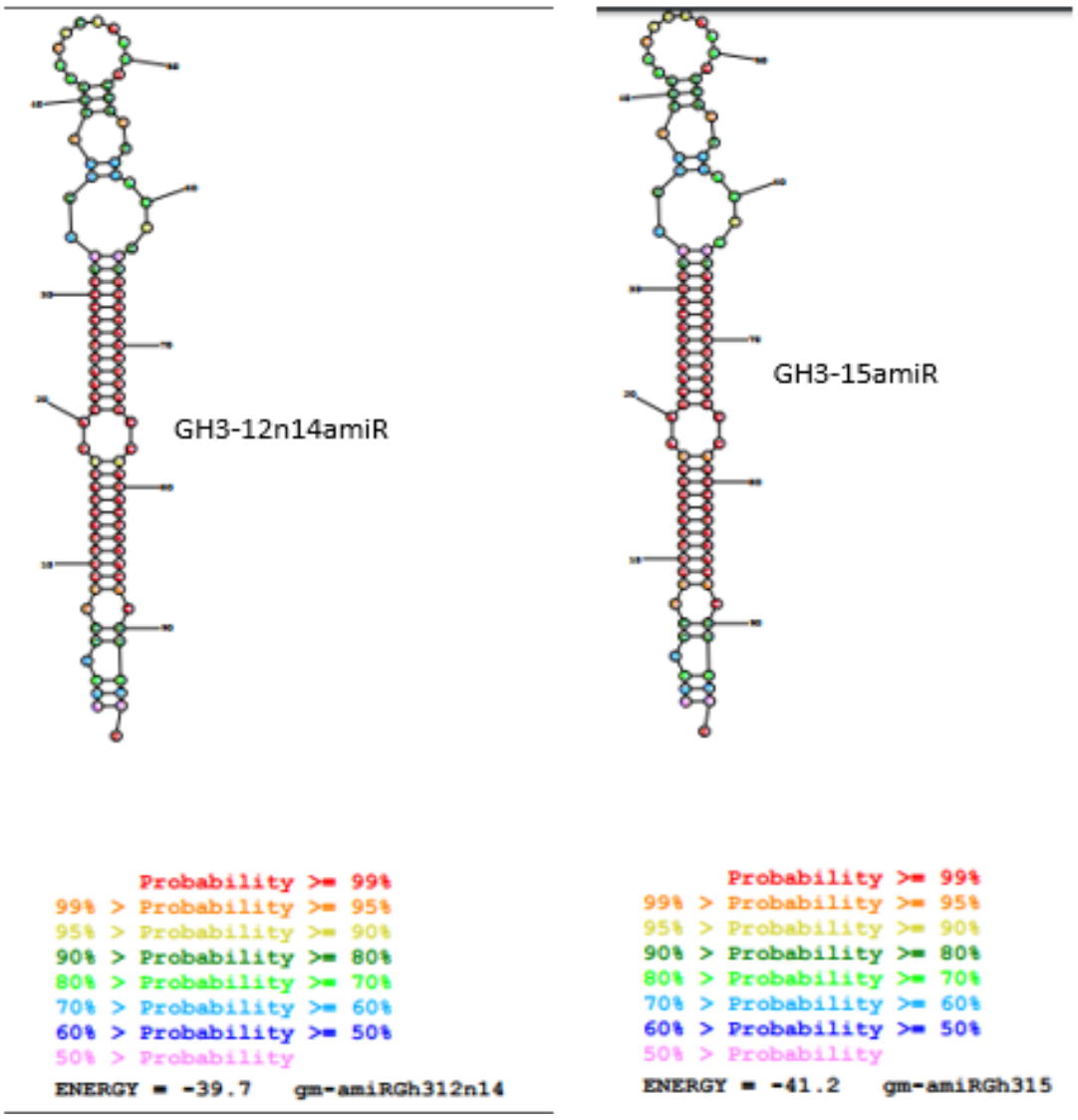

Figure S3-1: **Secondary structure of hairpin loop formed by artificial miRNA (GH3-12n14amiRNA and GH3-15amiRNA) inserted in to the backbone of gma-miR164a backbone.**

Data generated in
https://rna.urmc.rochester.edu/RNAstructureWeb/Servers/Predict1/Predict1.html

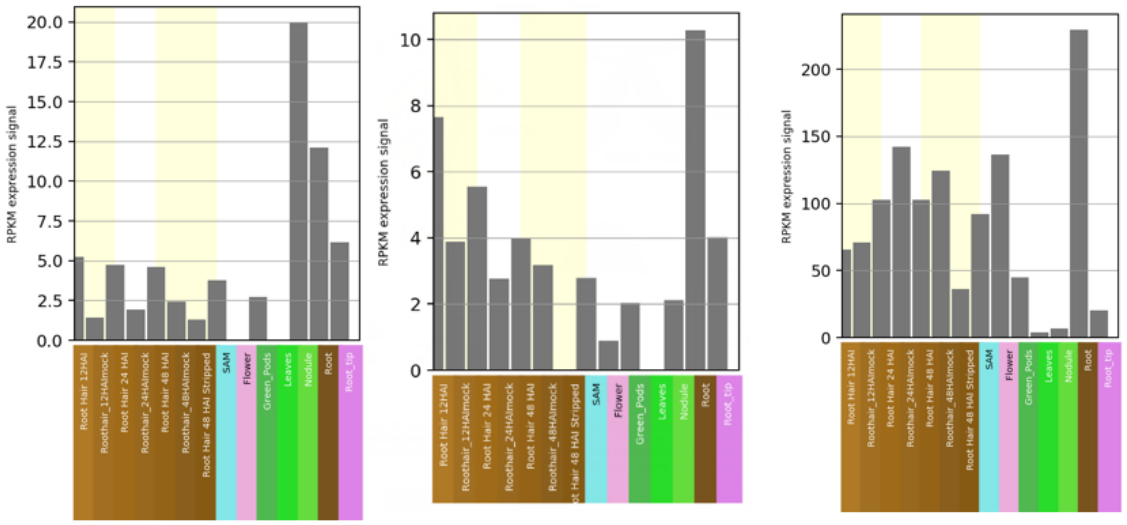

Gene ID	GH3-ID (Westfall et al. 2012 Science)	GH3 Group (Westfall et al. 2012 Science)	Expression levels (FPKM) in other soybean tissues (Soybean gene atlas, Libault et al. 2010 Plant J.)													
			Root Hair 12HAI	Roothair 12HAImock	Root Hair 24 HAI	Roothair 24HAImock	Root Hair 48 HAI	Roothair 48HAImock	Root Hair 48 HAI Stripped	SAM	Flower	Green Pods	Leaves	Nodule	Root	Root tip
Glyma01g39780.	Gm-14	2	7.66	3.88	5.55	2.76	3.99	3.18	0	2.78	0.88	2.04	0	2.12	10.28	4.01
Glyma02g13910.	Gm-9	2	16.94	4.94	7.49	3.87	10.14	6.6	4.14	19.5	7.7	3.41	4.61	1.06	10.28	2.47
Glyma05g21680.	Gm-21/22	2	6.05	5.65	7.77	9.13	11.37	9.54	2.85	1.26	5.04	0	1.06	2.39	1.05	0.61
Glyma06g40860.	Gm-17	2	30.65	31.46	42.76	56.71	66.99	84.88	6.73	56.48	59.59	5.46	0.71	13.56	100.2	14.5
Glyma06g45640.	Gm-23	2	0	0.35	0	0	0	0.48	0.51	0.75	5.33	1.36	1.06	0	0	0.3
Glyma11g05510.	Gm-11/12	2	5.24	1.41	4.72	1.93	4.61	2.44	1.29	3.79	0	2.73	0	19.94	12.13	6.18
Glyma12g11200.	Gm-16	2	1.61	2.47	3.33	4.7	4.61	5.62	3.62	2.53	4.44	0.68	0	0	0.52	0.3
Glyma12g17510.	Gm-15	2	65.74	71.05	102.73	142.21	102.95	124.26	36.01	91.94	136.39	45.09	3.9	6.64	229.4	20.1
Glyma12g32410.	Gm-18	2	0.8	2.82	6.1	10.23	9.52	8.56	0	0.75	0.29	0	0.71	0	0.26	0.92
Glyma12g34480.	Gm-23	2	0	0	0	0	0	0	0	0.25	10.37	2.73	0	0	0	0
Glyma13g36030.	Gm-13	2	2.82	1.41	2.77	1.1	1.53	2.69	4.4	2.53	172.56	17.76	0	0.26	0.52	0.3
Glyma13g38000.	Gm-10	2	2.42	4.24	10.55	10.51	19.36	17.85	0.51	0.5	2.66	0	0	0	0.79	3.39
Glyma17g18040.	Gm-24	2	37.51	15.9	13.6	17.7	15.05	9.05	1.29	2.27	1.48	1.36	0.35	3.45	6.85	1.23
Glyma17g18080.	Gm-25	2	0.8	2.12	0.83	2.21	2.15	0.73	0	0.25	0.59	0.68	0	1.32	0	0
Glyma02g17360	Gm-19	2	0	0	0	0	0	0.24	0	0.5	0.88	0	0	0	0.26	0
Glyma10g02440.	Gm-20	2	0.4	0	0	0	0	0.24	1.29	38.5	19.56	15.71	0	0	0.52	0
Glyma07g06370.	Gm-1	1	22.18	26.86	23.04	34.58	30.11	36.93	13.47	4.05	72.34	29.38	114	60.9	42.45	9.27
Glyma03g41700.	Gm-2	1	17.74	17.32	16.1	16.04	16.59	22.26	40.42	17.98	74.42	10.93	77.77	64.35	38.23	0.61
Glyma19g44310.	Gm-3	1	29.44	20.14	22.76	25.73	20.59	22.74	30.57	9.11	20.16	6.14	29.47	21.27	30.32	4.94
Glyma16g03011.	Gm-4	1	16.94	12.37	15.82	19.92	11.37	15.41	13.47	1.26	14.23	0	18.82	85.36	25.84	9.58
Glyma12g32910.	Gm-5	3	0.4	1.06	0	0.55	0	0	0	2.53	2.07	2.04	2.13	0	0	0.61
Glyma12g11890.	Gm-6	3	2.42	2.82	1.38	3.32	0	0.73	1.81	22.79	4.15	7.51	37.99	0	0.52	0
Glyma13g37550.	Gm-7	3	0.4	0	1.38	0.27	0	0	0.25	1.01	2.07	0	0.35	0	0.26	0
Glyma06g45120.	Gm-8	3	0.4	1.06	0	0	0	0	0.51	4.81	3.26	0	6.03	0	0	0

Figure S3-2: **Gene expression data from soybean transcriptomics atlas.**

Data collected from Libault et al., 2010. http://bar.utoronto.ca/efpsoybean/cgi-bin/efpWeb.cgi. The same data is represented as bar graph (above) and data sheet (below).

A

Substrate	Enzyme	$K_{cat}(min^{-1})$	K_m (μM)	K_{cat}/K_m ($M^{-1}S^{-1}$)
	GmGH3-11/1	23	130	2950
	GmGH3-14	19	120	2640
IAA	GmGH3-15	29	170	2840

Substrate	Enzyme	$K_{cat}(min^{-1})$	K_m (μM)	K_{cat}/K_m ($M^{-1}S^{-1}$)
	GmGH3-11/1	35	1300	448
	GmGH3-14	34	1300	436
PAA	GmGH3-15	21	200	1750

Substrate	Enzyme	$K_{cat}(min^{-1})$	K_m (μM)	K_{cat}/K_m ($M^{-1}S^{-1}$)
	GmGH3-11/1	> 17	>4000	-
	GmGH3-14	>19	>4000	-
IBA	GmGH3-15	27	760	592

Substrate	Enzyme	$K_{cat}(min^{-1})$	K_m (μM)	K_{cat}/K_m ($M^{-1}S^{-1}$)
	GmGH3-11/1	>25	>4000	-
	GmGH3-14	>23	>4000	-
NAA	GmGH3-15	7.7	620	207

B

SA	$K_{cat}(min^{-1})$	K_m (μM)	K_{cat}/K_m ($M^{-1}S^{-1}$)
GmGH3-12	Background		
GmGH3-14	Background		
GmGH3-15	1.1	640	29

BA	$K_{cat}(min^{-1})$	K_m (μM)	K_{cat}/K_m ($M^{-1}S^{-1}$)
GmGH3-12	>6.7	>4000	-
GmGH3-14	>8	>4000	-
GmGH3-15	15	250	1000

4-HBA	$K_{cat}(min^{-1})$	K_m (μM)	K_{cat}/K_m ($M^{-1}S^{-1}$)
GmGH3-12	Background		
GmGH3-14	Background		
GmGH3-15	11	960	191

Table S1: **Catalytic efficiency of GmGH3 enzymes with Asp as substrate and with different plant hormones.**

A) Enzyme Kinetics of nodule enriched GmGH3s using different auxins as acyl substrate and Asp as amino acid. B) Enzyme Kinetics of nodule enriched GmGH3s using different benzoic acids as acyl substrate and Asp as amino acid conjugate.

4. APPENDIX

4.1. Appendix A

Table A1. **Composition of Hoagland nutrient solution**

Chemical	
Macronutrients (Stock concentration)	**Working Concentration(per litre)**
250mM $MgSO_4.7H_2O$	2ml
500mM $CaCl_2.2H_2O$	4ml
150mM $K_2HPO_4.3H_2O$	1ml
300mM K_2SO_4	4ml
10mM $FeCl_3.6H_2O$	2.5ml
Micronutrients g/L (w/v)	**Concentration(g/L) (w/v)**
H_3BO_3	1.42g
$MnSO_4.H_2O$	0.77g
$ZnSO_4.7H_2O$	1.73g
$CuSO_4.5H_2O$	0.37g
$NaMoO_4.2H_2O$	0.24g
$CoCl_2.6H_2O$	0.025g
$NiSO_4$	0.01g

Table A2. **Composition of Nitrogen free plant nutrient solution (N^-PNS)**

Solution	Chemical
Solution -I	0.9MCa(NO$_3$)$_2$.4H$_2$O
Solution-II	0.5MMgSO$_4$.7H$_2$O
Solution-III	a) 1.25MKNO$_3$
	b) 0.2mM KH$_2$PO$_4$
Solution-IV	0.01M NaFeEDTA
Solution -V	a) 0.0035M MnCl$_2$
	b) 0.00035M ZnSO$_4$
	c)0.012M H$_3$BO$_3$
	d) 0.000125M CuSO$_4$
	e) H$_2$MoO$_4$

4.2. Appendix B

Table B1. **GUS buffer composition**

GUS Buffer (1L)
• 0.1M KPO_4 Buffer (pH7.0)
• 0.011M Na_2EDTA
• 0.0006M Potassium ferricyanide ($K_3Fe(CN)_6$)
• 0.00045M Pottasium ferrocyanide ($K_4Fe(CN)_6$)
Staining Buffer (in appropriate volume of GUS buffer)
• 0.1% Triton X-100 (V/V)
• 0.5mg/ml X-GLUC

4.3. Appendix C

Table C1. **Cloning Primers used in the Study**

For cloning		
Primer Name	**Primer Sequence(5'-3')**	**Notes**
Gm-GH312n14amiR	AGCtCCttGtTTAGTATTTACCAAGTTCCCCAGtCtCttGGAtCtCAAAtGCCACtGAACCCttGGGGAACTTGGCCAATACTAAACACGGGttt	
GmGH3-15amiR	AGCtCCttGtTTATGGCTAAGCAACAACCGTAGtCtCttGGAtCtCAAAtGCCACtGAACCCttACGGttGttGCCCAGCCATAAACACGGGttt	amiRNA
GmGH3-12n14amiRF	AGCtCCttGtTTAGTATTTAC	
GmGH3-12n14amiRR	AAACCCGTGTTTAGTATTGGC	
GmGH3-15amiRF	AGCtCCttGtTTATGGCTAAG	
GmGH3-15amiRR	AAACCCGTGTTTATGGCTGGG	
Gm01g17330-RNAiF	TCTCTCTAATCGTTCATGGACCA	
Gm01g17330-RNAiR	AGGCCTCTAGGGCCTGGTGGA	GmCYP83B1_RNAi
Gm01g17330_promoF	ATCAACATCCTCCAATTTGGGAGC	
Gm01g17330_promoR	GAACGATTAGAGAGAGAAAAATGATG	GmCYP83B1_Promoter
GH3-14_PromF	TGTGTATTAACCACATACACCTCTA	GH3-14 promoter
GH3-14_PromR	GATAAGAGAGGGAAGAATTAAGAT	
GH3-15_promF	TGCAGCACACCATTGGAGACAG	GH3-15 promoter
GH3-15_promR	GGTTGTGGTGATGTTAGTGATG	

Table C2. **qPCR primers used in this study**

For qPCR		
Primer Name	**Primer Sequence(5'-3')**	**Notes**
qP_Gm18g11820F	TTCCTTAGCCTCAAGCGTGTGC	
qP_Gm18g11820R	AGCGCTTGTTAGACACGTCAGT	
qP_Gm01g17330F	TTCCTTAGCCTCAAGCGTGTCT	
qP_Gm01g17330R	AGCGCTCGTAAGACACGTGAGC	GmCYP83B1
qP_Gm03g03670F	TCTTTAGTTCCAAGCGTGTCTCT	
qP_Gm03g03670R	GCTTGAGAGAGATATGAGTAACTCACT	
qp_Gm12g17510F	GCACTGGCCCCTCCTTTGCCAC	
qp_Gm12g17510R	GAGATCCCCAAGCCTCGGGTCG	GmGH3-15
qp_Gm01g39780F	CTCCGTCCAGGAGAGAGTCCTTT	
qp_Gm01g39780R	GAGCGAAGCGTTTGAGGTATTCT	GmGH3-14
qp_Gm11g05510F	CTCCGTCCAGGAGAGAGTCCTCA	
qp_Gm11g05510R	AGGCCGAAGCGTTTGAGGTACTCC	GmGH3-12
IAA, GH3	Refer to Turner et al. 2013 & Nizampatnam et al. 2015	